Mechanical
Engineering

Mechanical Engineering
Doctoral Thesis

Individualised Modelling for Preoperative Planning of Total Knee Replacement Surgery

Daniele Ascani

December 2016

Supervisor: Prof Marco Viceconti
CoSupervisor: Dr Claudia Mazzà

Acknowledgments

Firstly, I would like to express my sincere gratitude to my supervisor Prof. Marco Viceconti for the continuous support and related research, for his patience, motivation, and immense knowledge. His guidance always helped me through the personal and professional problems I have encountered during these three years. I could not have imagined having a better guide. I'm very grateful.

I would like to thank my second supervisor Dr. Claudia Mazzá for her insightful comments and encouragement during these years. Thanks for the patience and the presence.

My sincere thanks also goes to Eng. Massimiliano Bernardoni, and Eng. Angelo De Lollis, who provided me the opportunity to join the R&D team in Medacta, and who always gave support during my visiting periods with their professionalism and empathy. Without their precious support this research would have never been possible.

I immensely thank all my office mates for the stimulating discussions and the nonsense conversations during our coffee breaks, and for all the fun we have had in the last three years. I will be missing all of you very much.

Last but not the least, I would like to thank my family: my parents and to my brother for supporting me spiritually throughout writing this thesis and my life in general. Without your love, encouragement and assistance, I would have achieved nothing in my life. Grazie.

In conclusion, I recognize that this research would not have been possible without the financial assistance of Medacta International SA which sponsored and supported this PhD dissertation.

"Life's but a walking shadow, a poor player
that struts and frets his hour upon the stage
and then is heard no more. It is a tale
told by an idiot, full of sound and fury,
signifying nothing."

Macbeth (Act 5, Scene 5, lines 24-28)

Table of Contents

Confidentiality Agreement.....1
Nomenclature.....2
Abstract.....3
List of Tables.....4
List of Figures.....6

Chapter 1 – Introduction.....10

1.1 Background.....10
1.2 Motivational and Rationale.....13
1.3 Specific Aims.....15

Chapter 2 – Literature Review.....22

2.2 Anatomic Reference Terminology.....22

2.2 Knee Joint.....24
2.21 Anatomy and physiology.....24
2.2.2 Structure of the knee joint.....26
2.2.3 Knee osteoarthritis.....31

2.3 Knee Ligaments.....33
2.3.1 Introduction.....33
2.3.2 Mechanical properties.....35
2.3.3 Tensile properties of ligaments.....37
2.3.4 Viscoelastic Properties of Ligaments.....39
2.3.5 Damage threshold in quasi static distraction of human knee ligament.....41

2.4 Total Knee Replacement.....43
2.4.1 Introduction.....43
2.4.2 Surgical Principle.....47
2.4.3 TKR failure.....50
2.4.4 The relevance of Soft Tissue Balancing in TKR.....51
2.4.5 Preoperative planning for TKR.....53

2.5 Computational Knee Models.....63
2.5.1 Overview knee joint model.....63
2.5.2 Computational musculoskeletal model.....69

Chapter 3 **- Estimation of the Origin and Insertion of Knee Ligaments from Computed Tomography Images**.....81

3.1 Introduction.....81
3.2 Material and Methods.....84
3.3 Results.....88
3.4 Discussion.....91

Chapter 4 **– A Subject-Specific Geometric Knee Model to Compute the Soft Tissue Balance in TKR Surgery**.....95

4.1 Introduction.....96
4.2 Material and Methods.....98
4.3 Results.....108
4.4 Discussion.....112

Chapter 5 **– A Subject-Specific Quasi-Static Knee Model to Compute the Soft Tissue Balance in TKR Surgery**.....117

5.1 Introduction.....118
5.2 Material and Methods.....121
5.3 Results.....131
5.4 Discussion.....135

Chapter 6 **– A Subject-Specific Dynamic Musculoskeletal Modelling Framework to Compute the Knee Soft Tissue Balancing for TKR Surgery**.....139

6.1 Introduction.....139
6.2 Material and Methods.....142
6.3 Results.....159
6.4 Discussion.....168

Chapter 7 **– Conclusions**.....177

7.1 Summary.....177
7.2 Novelty and Utility of the work.....179
7.3 Limitatio.....181
7.4 Future Work.....182

Confidentiality Agreement

This dissertation stems from an industrial PhD project founded by Medacta International SA (Castel San Pietro, Switzerland). The University of Sheffield has signed a confidentiality agreement with Medacta International SA and this agreement extends to all people involved in the university. Failure to comply with this restriction may constitute a violation of applicable securities laws.

This dissertation is for informational and for the exclusive use for the recipients to whom it is addressed.

Nomenclature

2D: Two-dimensional
3D: Three-dimensional
A/P: Anterior-Posterior direction/axis
M/L: Medial-Lateral direction/axis
P/D: Proximal-Distal direction/axis
Lg: Longitudinal direction/axis
Fl/Ex: Flexion-Extension angle/rotation
In/Ex: Intra-Extra angle/rotation
Ab/Ad: Abduction-Adduction angle/rotation

MRI: Magnetic Resonance Imaging
CT: Computed Tomography
EMG: Electromyography
GFR: Ground Force Reaction
DICOM: Digital Imaging COmmunications Medicine

ACL: Anterior Cruciate Ligament
PCL: Posterior Cruciate Ligament
MCL: Medial Collateral Ligament
LCL: Lateral Collateral Ligament

MA Mechanical Axis

RBSM: Rigid Body Spring Model
FEM: Finite Element Method
EFM: Elastic Foundation Model
NURBS: Non-uniform rational B-splines

D1 dataset 1
D2 dataset 2
$\mathbf{C_r}$ Reference landmark cloud
$\mathbf{C_s}$ Subject specific landmark cloud
RA Registration Atlas
PD Procrustes Distance
SD Standard deviation

CR Cruciate Retaining
PS Posterior Stabilized

STL Stereolithography
DOFS Degrees of Freedom

TKR TF Quasi static model without patella
TKR PF Quasi static model with patella

CMC Computed muscle control
MSK Musculoskeletal
FDK Force dependant kinematics
KCF Knee contact forces
RMSE Root mean square error
BW Body weight
ICP Iterative closest point
ID Inverse dynamic
IK Inverse kinematics
SO Static Optimization

Abstract

Total knee replacement (TKR) surgery is routinely prescribed for patients with severe knee osteoarthritis to alleviate the pain and restore the kinematics. Although this procedure was proven to be successful in reducing the joint pain, the number of failures and the low patients' satisfaction suggest that while the number of reoperations is small, the surgery frequently fail to restore the function in full. The main cause are surgical techniques which inadequately address the problem of balancing the knee soft tissues.

The preoperative planning technique allows to manufacture subject-specific cutting guides that improves the placement of the prosthesis, however the knee soft tissue is ignored.

The objective of this dissertation was to create an optimized preplanning procedure to compute the soft tissue balance along with the placement of the prosthesis to ensure mechanical stability.

The dissertation comprises the development of CT based static and quasi-static knee models able to estimate the postoperative length of the collateral lateral ligaments using a dataset of seven TKR patients; In addition, a subject-specific dynamic musculoskeletal model of the lower limb was created using *in vivo* knee contact forces to perform the same analysis during walking. The models were evaluated by their ability to predict the postoperative elongation using a threshold based on the 10 % of the preoperative length, through which the model detected whether an elongation was acceptable.

The results showed that the subject-specific static model is the best solution to be included in the optimized, subject-specific, preoperative planning framework; full order musculoskeletal model allowed to estimate the postoperative length of the ligaments during walking, and at least in principle while performing any other activity.

Unlike the current methodology used in clinic this optimized preoperative planning framework might help the surgeon to understand how the position of the TKR affects the knee soft tissue.

List of Tables

2.1 The tests were performed using non-contact strain measurement technique except the Butler et al. (1986) study

2.2 CT scan image settings for MyKnee® workflow

3.1 Information regarding each cadaver knee used in this study to create the Registration Atlas

3.2 The table shows the precision of the landmark positions in terms of Standard Deviation

3.3 Registration Atlas registered on the seven subjects (femur)

3.4 Registration Atlas registered on the seven subjects (tibia)

3.5 Mean Distance between the insertion and the origin of the ligaments predicted and the ones estimated on the MRI images (femur)

3.6 Mean Distance between the insertion and the origin of the ligaments predicted and the ones estimated on the MRI images (tibia). The subject 4 in not included in this comparison because the MRI data was incomplete

3.7 Sensitivity study performed on subject 2, all values are expressed in mm. Each of the 25 simulations corresponds to a combination of the possible different errors on origins and insertions

4.1 Mean distance between the origin and insertion of the ligaments predicted using the CT scan and those estimated on the MRI images

4.2 Soft tissue elements included in the Multifiber model

4.3 Length of sMCL and LCL for the preoperative position; postoperative length of the sMCL and LCL in extended (0 º) and flexed (90 º) position

4.4 Postoperative percentage elongation of the sMCL and LCL in extended (0 º) and flexed (90 º) position

4.5 Results of the sensitivity study

4.6 Results sensitivity study considering a gap between the femoral and tibial bone cuts of 28mm

5.1 Material Properties

5.2 Translation and rotational spring parameters

5.3 Elastic Foundation Model parameters

5.4 Ligaments modelling parameters
5.5 TKR TF Ligaments length in extension position
5.6 TKR TF Ligaments length in flexion position
5.7 TKR TF Ligaments percentage elongation in extension position
5.8 TKR TF Ligaments percentage elongation in flexion position
5.9 TKR PF forward dynamics simulation results of MCL
5.10 TKR PF forward dynamics simulation results of LCL
5.11 Comparison between the forward dynamic simulation results of TKR PF with no muscular activation and the Static model for the sMCL ligament
5.12 Comparison between the forward dynamic simulation results of TKR PF with no muscular activation and the Static model for the LCL ligament
6.1 Body segments' inertial properties (White et al., 1987)
6.2 Knee ligaments' parameters used in the model
6.3 Joint contact forces measurements in a patient with implanted instrumented prosthesis compared to predicted model from a subject specific model of the same patient.

List of Figures

1.1 Current TKR surgery procedure that employs pre-operatively planned, custom-made cutting guides

2.1 The Anatomical references planes

2.2 The knee joint (http://bit.ly/1ojwwwS)

2.3 Frontal view of the knee joint (http://bit.ly/1ojwwwS)

2.4 Posterior view of the knee joint (http://bit.ly/1ojwwwS)

2.5 Medial view of the knee joint (http://bit.ly/1ojwwwS)

2.6 Lateral view of the knee joint (http://bit.ly/1ojwwwS)

2.7 Central compartment of the knee joint (http://bit.ly/1ojwwwS)

2.8 Axial view of the knee menisci cartilage

2.9 Degeneration of knee cartilage (osteoarthritis)

2.10 Human ligament structure. Image modified form Woo et al.,1999

2.11 Ligament Force-elongation curve modified from Benjamin & Ralphs, 1997

2.12 Typical loading (top) and unloading curves (bottom) from tensile testing of knee ligaments. Image modified from Banjamin and Ralphs, 1997.

2.13 The procedure consists of replacing the surface of distal femur and the proximal tibia with high resistant metallic components. The femoral surface is replaced by a femoral metallic component while tibia surface by a tibial metallic baseplate. Between the femoral component and the tibial baseplate, a plastic insert is inserted to replace the cartilage function.

2.14 Proportion of patients achieving optimal and suboptimal outcome (figures from (Baker et al., 2012)).

2.15 Restoration of preoperative varus deformity (left) to correct alignment after TKA (right)

2.16 TKR surgical procedure

2.17 Flexion – Extension gap during Total Knee Replacement Surgery (Griffin et al., 2000)

2.18 CAS system

2.19 Preoperatively planned cutting blocks

2.20 Surgical variables (from left): varus-valgus femur, varus-valgus tibia, ribial slope, external rotation femur

2.21 Medacta® cutting blocks

2.22 MyKnee® workflow - 1) The MRI or CT images upload on the Medacta portal 2) Starting from the 3D reconstruction of the bone morphology, the surgeon can modify a set of parameters for the placement of the implants 3) A virtual positioning of the implant is proposed to the surgeon who can further modify the planning 4) Once the planning has been validated by the surgeon, the in-house manufacturing process starts.

2.23 Typical low dose CT scan for the MyKnee workflow

2.24 MyKnee® 3D planning user interface

3.1 Schematic representation of the procedure: 1) Creation of a repeatable bone landmarks cloud palpable on CT scan images. 2) Definition of a reference landmarks cloud called Registration Atlas composed by reproducible and repeatable landmarks and the origin and insertion of the knee ligaments. 3) Validation of the RA 4) Calculation of the origin and insertion of the knee ligaments using CT scan and validation using MRI image

3.2 Set of landmarks selected using the "Colour Atlas of Skeletal Landmark Definitions" (Serge Van Sint Jan 2007). FME- Medial Epicondyle, FAM-Tubercle of the Adductor Magnus muscle, FMS-Medial Sulcus**,** FLE-Lateral Epicondyle, centre of tubercle, FUE-Lateral Epicondyle, FBE Lateral Epicondyle**,** FPS-Popliteal Sulcus, FLG-Antero-Lateral ridge of the patellar surface Groove, FMG-Antero-Medial ridge of the patellar surface Groove, FLC-Most distal point of the Lateral Condyle**,** FMC-Most distal point of the Medial Condyle**,** TLR-Lateral Ridge of tibial plateau, TMR-Medial Ridge of tibial plateau**,** TGT -Gerdy Tubercle, TTM-Tibia, Tuberosity medial edge, LCL-Attachment of the collateral Lateral Ligament

4.1 Input and output parameters of the geometrical model

4.2 GMK revision posterior stabilized (PS) model no cruciate retaining (Medacta International SA, Castel San Pietro)

4.3 The image on the left shows an arthritic patient where the MA axes of femur and tibia are not aligned. The image on the right shows the post-operative condition where the angle between the two axes is 180 º

4.4 On the left, femur and tibia components coupling in flexion at 90°. On the right, Extension femur and tibia components coupling (ball and socket) at 90°

4.5 From left to right: varus-valgus femur, varus-valgus tibia, posterior slope tibia, external rotation femur

4.6 The 10% of the preoperative length was considered as the upper limit of elongation for the model output

4.7 ZY-Plane tangent to the bone

4.8 Sensitivity study of the MCL (up) and LCL (down) in the preoperative extension, postoperative extension and postoperative flexion

4.9 Multifiber Model

4.10 Results sensitivity study considering a gap between the femoral and tibial bone cuts of 28mm

4.11 Soft tissue balancing for the TKR preoperative planning surgical procedure

5.1 Input and output parameters of the quasi-static model

5.2 TKR TF model

5.3 Input and output parameters of the quasi static model with patella

5.4 Knee joint modelling

5.5 TKR PF model

6.1 eTibia instrumented implant. The load cells are placed on the tibial tray whilst the antenna is located at the bottom, protected by a plastic tip

6.2 Subject specific musculoskeletal modelling framework to compute the soft tissue balancing

6.3 Geometrical lower limb musculoskeletal model

6.4 The definition of the body joints: ball socket (hip) and hinge (knee and ankle)

6.5 The musculoskeletal model was modified to transmit the forces of the quadriceps through the patella to the tibia

6.6 MRI knee ligaments preoperative position

6.7 Knee maximum moment and knee passive moment developed by the model simulating the Biodex test. The maximum activation of the muscles with positive moment arm (agonist muscles), with respect to the direction of interest (flexion or extension) allowed the calculation of the maximum joint moment.

6.8 Marker set used for static and dynamic trials

6.9 Joint reaction body diagram of the tibia body segment

6.10 Surgical variables (from left): varus-valgus femur, varus-valgus tibia, tibial slope, external rotation femur

6.11 Example of the heat map construction. On the left the curve of the length of the MCL ligaments throughout the gait cycle with a Tibia Varus-Valgus=-2° and gap=26mm. On the right the heat map of the Tibia Varus Valgus parameter. Red color=10% of the initial length, Blue color=-10% of the initial length.

6.12 Knee kinematics compared with healthy subjects (Right), and TKR patient (Left)

6.13 Knee dynamics compared with healthy subjects (Right), and knee kinematics compared with healthy subjects (Left)

6.14 Total knee joint forces predicted (black) during four walking gait trials normalized on the 100% of the gait cycle. The eTibia experimental forces are showed for the same gait trials (red). The vertical blue bar represents the toe-off phase of the gait cycle (toes are leaving the ground)

6.15 Regression line - R^2 Linear = 0.939

6.16 The figure shows the results of the Femur and Tibia varus-valgus parameters. The yellow point represents the postoperative ligament balancing imposed by surgery. The yellow dot represents the real outcome of the surgery

6.17 The figure shows the results of the Femur External Rotation and Tibia Posterior Slope parameters. The yellow point represents the postoperative ligament balancing imposed by surgery. The yellow dot represents the real outcome of the surgery

6.18 Patient with Posterior Stabilized Implant

6.19 Patient with Sphere Implant

6.20 The figure shows the knee joint kinematics of the model compared with the healthy subjects. Our model detects accurately the knee angle in the heel-strike phase, as showed in the picture taken during the trial in the gait laboratory.

7.1 Optimized TKR surgery procedure that shows pre-operatively the elongation of the ligaments after the operation

7.2 Optimized TKR surgery procedure that employs pre-operatively planned, custom-made cutting guides

Chapter 1

Introduction

1.1 Background

Total knee replacement (TKR) is certainly the most effective treatment for knee osteoarthritis (OA), a degenerative disease of the cartilage tissue, which requires 600.000 people each year in United States to have one of their joints replaced with an artificial implant (Bozic et al., 2010). This number is expected to increase significantly due to the aging of the population and the obesity epidemic (Bhandari et al., 2012).

TKR is a surgical procedure that aims to reduce pain and re-establish proper kinematic analysis of the joint by replacing the damaged surfaces of the knee condyles and the tibial plate with metallic alloy components (Liddle et al., 2013). In addition, a plastic insert, placed between the metallic or ceramic components, aims to replace the cartilage function.

Throughout the years, TKR have proven to be very effective after 10 years from the operation by significantly reducing the knee joint pain. Among the knee OA symptoms, acute pain during physical activities is the most critical factor which affects heavily the patients' quality of life (Hochberg et al., 2013). When TKR started to be widespread, elderly patients with a very limited post-surgery lifestyle expectation, were the typical candidates. Thus, the surgical procedure was tuned on this population, favouring low impacts activities over mobility.

Unlike the medical literature, which reported a successful rate of 90 % (Colizza et al., 1995), over 40% of the patients declared a poor quality of their lifestyle after the surgery by reporting a reduced range of motion, joint stiffness and pain (Mannion et al., 2009). In addition, an excessive physical activity represents the second leading factor for the failure of TKR which is defined with a very severe end point: re-operation, also called revision surgery. Not surprisingly half of the patients undergoing to a revision surgery are under 65 (Heck et al., 1998), meaning that the surgical procedure didn't meet the demand of a younger population with higher expectations in terms of lifestyle.

Furthermore, the revision surgery is a very complex procedure, after which patients could expect less improvement and a higher risk of complications than after their primary total knee replacement (Stambough et al., 2014).

In order to achieve stability and mobility, the surgical procedure must assure a correct alignment of the mechanical axis along with a proper balance of the knee soft tissue (Bellemans et al., 2005). Currently, the surgical procedures have considerably improved in placing the artificial components on the patient, by introducing subject-specific cutting guides, which starting from a CT-based pre-operative planning, provide an easy way to produce precise bone cuts, essential to accurately position the implant with respect to the skeleton (Maniar and Singhi, 2014). However, the preoperative planning procedure is still completely based on the surgeon's experience, as the current preplanning software is not able to predict how the knee soft tissue will be affected by the new position of tibia and femur.

The most common causes for TKR failure are: knee instability, patella-femoral complications, misalignment, and component loosening (Narkbunnam and Chareancholvanich, 2012; Parratte and Pagnano, 2008; Seil and Pape, 2011). In general, most of the above factors for failure can be attributed to surgical techniques which inadequately addresses the problem of balancing the knee soft tissues (Bozic et al., 2010; Fehring et al., 2001; Lonner et al., 1999; Sharkey, 2002).

The definition of soft tissue balancing after TKR is not straightforward, however it can be simply said that the stability of the knee must be restored after the surgery. This concept might be used to refer to a prosthetic knee joint where the following characteristics are preserved: a) a full range of movement; b) symmetrical medial-lateral balance at full extension and 90 degrees of flexion; c) correct varus-valgus alignment in both flexion and extension; d) absence of medial-lateral tightness or laxity; e) correct patellar tracking; and f) correct rotational balance between the femoral and the tibial components (Babazadeh et al., 2009).

The surgeons pay great attention to how the prosthetic components are positioned with respect to the bones, so as to ensure the preoperative kinematic analysis is retained, this concept will be extensively defined in the next chapter ; but there is not yet a validated procedure to check in advance how a given position of the implant will affect all the knee soft tissue (e.g. ligaments, tendons, and other connective tissues that wrap the knee joint). Therefore, the balancing of the soft tissue is treated intra-operatively as a consequence of the positioning of the prosthetic component and not as *a priori* requirement. The most

popular surgical techniques to achieve a soft tissue balance are the balanced resection and measured resection (Ranawat et al., 2006; Whiteside et al., 2000). To assess the soft tissue balancing, surgeons manually apply a varus-valgus moment to the joint to evaluate the relative tightness or laxity of the soft tissues and assess the frontal plane balance. Based on this and on a following subjective assessment of the flexion-extension movement, if balance has not been achieved, the tightest among the ligaments of the knee is released. Despite the continual advancements made to the surgical procedures, the intraoperative balancing of the soft tissue is still completely based on the surgeon's experience (Matsuda et al., 2005).

Among the different surgical procedures for TKR surgery, few years ago in the market were introduced a tool that were able to guide the surgeon to perform the cut on the bone, this new technology is based on subject specific cutting blocks that are personalized using the specific anatomy of the patient. The procedure is characterized by a complex three-dimensional preoperative planning based on computed tomography (CT) or magnetic resonance images (MRI). Based on the specific manufacturers' software along with the other inputs from the surgeon, custom disposable patient-specific cutting blocks are manufactured to assure an accurate resection of the bone during the surgery. The surgeon' preferences are called preoperative planning parameters and are correlated with the orientation of the planes cut. The preoperative planning successfully addresses the problem of having aligned the components to the mechanical axes but it doesn't take into account the soft tissue balancing.

A computational model to predict the outcome of the TKR represents a viable solution toward optimal soft tissue balancing. For this reason, the biomechanical research community is strongly engaged in knee modelling and a number of recent papers made available in vivo measurements obtained from instrumented prostheses (Bergmann et al., 2007, 2001; D'Lima et al., 2012; Benjamin J Fregly et al., 2012; Westerhoff et al., 2009), to help the modelling community to improve and validate their findings.

The ultimate goal of this dissertation is to help the surgeon in placing the prosthetic implants on the patient providing robust indications on the knee soft tissue balancing in the preoperative planning.

1.2 Motivation and Rationale

In TKR surgery the soft tissue balancing relies completely on the surgeon's experience, this means that different surgeons with the same clinical data may opt to a different treatment option and then to a different outcome. The introduction of subject-specific musculoskeletal computational models aims to help the clinicians in taking the best treatment option to adopt, providing information that are based on principles of physics and physiology.

When TKR started to be widely adopted, most of the patients were well over 65, and with limited life style expectations. Surgical procedures were tuned on this population, and privileged stability over mobility. Therefore, the design of the implants and the surgical technique were focused on meeting the needs of a non-active population, which are: the reduction of the pain, the preservation of the stability, an acceptable range of motion compatible with low impact day life activities. However, along with the aging of the population, also the people between 45 and 64 now represent a relevant fragment of the TKR market. These younger patients have different needs after a TKR, they have a longer live expectancy and more importantly they require of having a more active lifestyle. For this reason the surgical technique should meet the new demands (Jones and Huo, 2006), providing implant design with a longer lifespan along with a specific design that aim to re-establish a proper range of motion together with a good performance in higher impact lifestyle activities. It has been reported that among the causes that lead to a revision surgery there is an excessive active life style within the first two years after the primary TKR (Heck et al., 1998).

To achieve stability and mobility a TKR procedure requires an accurate planning, in order to ensure an optimal balancing of the soft tissues, and an accurate execution, in order to achieve accurate skeletal positioning.

In this context the Medacta International SA (Castel San Pietro, Switzerland) group, which is an industrial company active in the field of production and sale of medical devices, offer a product for TKR surgery, called *MyKnee*® that allows the personalization of the surgical instrumentation (cutting guides) through a CT-based patient specific pre-operative planning. The process starts with a baseline CT or MRI scan of the knee patient and these data are successively transmitted to the Medacta International database. The imaging is then used to create a 3D bone knee model of the patient allowing the creation of patient specific anatomical cutting blocks that can fit the patient knee morphology

without using any alignment jig to position them during the surgery. The anatomical cutting block is a tool that aims to reduce to a minimum the subjectivity of the surgeon in placing the prosthetic components with respect to the bones during the surgery. The term "subjectivity" in TKR for the surgeon is defined as their ability to cut the bone perpendicularly to the mechanical axes. Without the cutting guides the accuracy relies only on the specific ability of the surgeon. Medacta manufactures this tool, after the surgeon has inspected and confirmed the surgical parameters that define the orientation of the implants. The success of the TKR surgery is strictly correlated with the preplanning phase, through which the surgeon can change the surgical parameters that directly influence the final pose of the implants on the patient. In addition, a 3D model of the femur and the tibia are delivered to the surgeon with the resection line drawn to help the surgeon in resecting the exact amount of bone. The balancing of the knee soft tissue is completed ignored in the *MyKnee*® procedure and left to the surgeon intra-operatively. In many cases he has to re-plan the surgery to address the balancing of the soft tissue and this happens in almost 50% of the surgeries (Barrack et al., 2012).

The main goal of this dissertation was to create a patient specific modelling framework to be added to the *MyKnee*® preoperative planning to take into account the knee soft tissue balancing along with the surgical parameters that define the placement of the prosthetic components to assure mechanical stability (Figure 1.1).

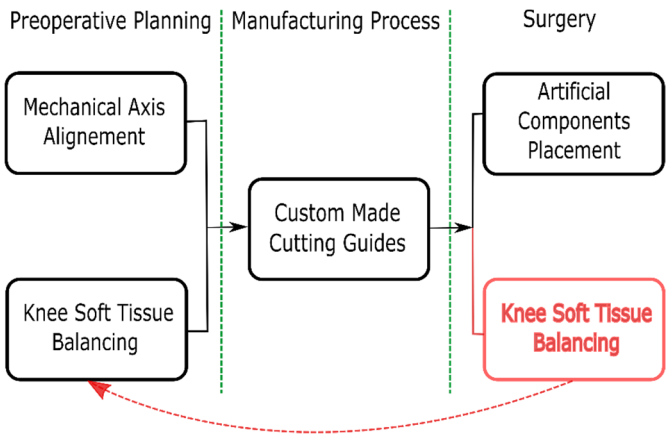

Figure 1.1 – *Current TKR surgery procedure that employs pre-operatively planned, custom-made cutting guides*

The level of subjectivity for TKR is due to the fact that the surgeons, performing a conventional TKR has no tools to understand how a given position of the implants would

affect the soft tissue balance of the knee. Due to the subjective nature of this surgical decisions, two surgeons on the same patient might place the implant differently achieving different elongation of the ligaments (Benjamin J. Fregly et al., 2012). One way to help the surgeons would be to develop objective knee computational models that are able to predict the best positioning of the implants to produce the best outcome for the patients.

1.3 Specific Aims

The specific aims of this dissertation are:

1) To develop a procedure to estimate the origin and insertions of the knee ligaments from computed tomography (CT) images;
2) To develop an optimized subject specific preoperative planning framework based on static and kinetostatic knee models to compute the soft tissue balance for TKR surgery;
3) To develop a dynamic musculoskeletal model, called *life style simulator* for TKR surgery, to compute preoperatively the knee soft tissue balancing in dynamic daily live activities such as walking.

This dissertation describes through the chapters, the use and the development of different approaches for knee modelling to compute the knee soft tissue balancing. In addition to the computational knee modelling, a procedure to calculate the origins and insertions of the knee ligaments has been developed as primary input for the models. This procedure is extensively described in the Chapter 3 and it represents the first step to create subject specific knee models from the CT images. The estimation of these points on the patient's anatomy relies on the construction of a registration atlas created using the "Multibody Models of the Human Knee Project (Bloemker et al., 2012; Guess et al., 2010) where the data is based on three cadaver knees that were physically tested in a dynamic knee simulator. The dataset also includes the ligaments properties, such as the origin and insertion location. The validation of this study was conducted on a dataset where both CT and magnetic resonance images (MRI) were available, meaning that the level of accuracy obtained by such procedure is the same level of accuracy obtained using MRI images where the soft tissue is rather visible. This procedure represents a crucial

step in this study because the preoperative length of each ligament will be used to calculate the maximum acceptable elongation (warning threshold) in the postoperative position when the prosthetic components are implanted.

The study comprises the development of subject specific models of some patients where the output is the percentage of elongation calculated on the preoperative length of the ligaments. During the preoperative planning the surgeon can change a set of parameters that defines the orientation of the cut on the bone and consequently the placement of the prosthesis. The subject specific models will be able to perform a sensitivity analysis of the preoperative parameters to assess the knee soft tissue balancing.

Subject specific geometric models and one quasi-static models were developed to create the preoperative planning framework to be added to the existent in house *MyKnee*® Medacta software. The comparison between the two models has been then performed observing how the output changed considering substantial differences in terms of forces, number of bones and fibers included in the model. Verifying that the static model has no difference in terms of output, the model with a minor computational cost will be implemented in the Medacta framework.

The first study in Chapter 4 is a subject specific geometric model developed on a dataset of seven patients that underwent a TKR surgery using a posterior stabilized prosthetic implant no cruciate retaining. The model predicts the post-operative soft tissue balancing examining the knee at two fixed angles, 0 and 90 degrees of flexion. The postoperative position of the knee was accurately simulated thanks to the particular constraints of the prosthesis. In the static model only the collateral lateral ligament (LCL) and the medial collateral ligament (MCL) have been included to assess the knee soft tissue balancing. By that a multi-fibre model, that includes all the fibres that composes the knee soft tissue, have been developed on one patient of the dataset to assess that the analysis of soft tissue balancing can be limited to the investigation of the ligaments, which ultimately represent the most stressed structures in TKR surgery.

The study in Chapter 5 is a subject specific quasi-static model, developed on the same dataset and it is composed by the femoral component, the tibial insert, and the two collateral ligaments (MCL and LCL). The two rigid bodies are linked by a kinematic joint, which define how the femur component moves respect to the grounded tibial insert. The contact between the femoral component and the tibial insert was modelled using the fundamentals of the Elastic Foundation theory (Johnson, 1985) in which the contacting solids may be considered rigid bodies except for a thin layer of elastic material of

thickness at the surfaces (Blankevoort et al., 1991; D'Lima et al., 2007; Johnson, 1985). The method for defining each ligament used in this study is the force-displacement curve that was first introduced by Blankevoort et al. (1991). The lateral collateral (LCL) and the medial collateral (MCL) ligaments were both modelled as one bundle element, the non-linear behaviour has been represented using one dimensional non-linear springs and non-linear splines which take the toe region into account. The simulation reached the convergence when the translational and angular accelerations of the femoral component were less than a small user-defined tolerance. A second patient-specific model was developed for each patient, adding the patella, the patellar tendon and the rectus femoris muscle, which is one of the major extensors of the knee.

The computational dynamic musculoskeletal subject specific model in Chapter 6 is created using the experimental data of the "Grand Challenge Competition to Predict In Vivo Knee Loads" (Benjamin J Fregly et al., 2012). The experimental data included the tibio-femoral *in vivo* contact forces of a patient that underwent to a TKR surgery obtained from a telemetric force measuring sensor embedded in the knee prosthesis. Thus, the model has been validated comparing the predictions with the experimental data, in terms of knee joint reaction forces during gait level walking trials. In fact the primary aim of the competition was to help the biomechanical community in creating computational models that could accurately predict the kinematic analysis of gait, while reproducing correctly the tibio-femoral forces along with the muscular forces. The model developed includes 4-body segments (pelvis, femur, shank, foot) of the right lower limb and 44 active muscles. The open-source dynamic solver OpenSim software, developed by Stanford University (Delp et al., 2007), was used to construct the musculoskeletal models and to solve the inverse kinematic analysis and dynamics problems together with the static optimization tool. NMS Builder (SCS srl, Italy) software was used to visualize the medical images, the 3D geometry, and to perform the virtual palpation and the registration between the landmark clouds. The collateral lateral ligaments (LCL and sMCL) were included in the model and the sensitivity study has been conducted by varying step-by-step each surgical parameters during the dynamic task simulated.

All of the studies within this dissertation consist of computational methods that estimate the elongation of the ligaments performing a sensitivity analysis of the surgical parameters that the surgeon can change in the preoperative planning. In this series of studies, these models have been tailored to examine specific research questions for Medacta International SA (Castel San Pietro, Switzerland). However, the proposed

methodology in this dissertation can be expanded to address separate research questions and have the potential to be used in a commercial pre-operative setting or within a manufacturer's design cycle.

References

Babazadeh, S., Stoney, J.D., Lim, K., Choong, P.F.M., 2009. The relevance of ligament balancing in total knee arthroplasty: how important is it? A systematic review of the literature. Orthop. Rev. (Pavia). 1, e26. doi:10.4081/or.2009.e26

Barrack, R.L., Ruh, E.L., Williams, B.M., Ford, a. D., Foreman, K., Nunley, R.M., 2012. Patient specific cutting blocks are currently of no proven value. J. Bone Jt. Surg. - Br. Vol. 94–B, 95–99. doi:10.1302/0301-620X.94B11.30834

Bellemans, J., Vandenneucker, H., Vanlauwe, J., 2005. (iv) Total knee replacement, in: Current Orthopaedics. pp. 446–452. doi:10.1016/j.cuor.2005.09.007

Bergmann, G., Deuretzbacher, G., Heller, M., Graichen, F., Rohlmann, A., Strauss, J., Duda, G.N., 2001. Hip contact forces and gait patterns from routine activities, in: Journal of Biomechanics. pp. 859–871. doi:10.1016/S0021-9290(01)00040-9

Bergmann, G., Graichen, F., Bender, A., Kääb, M., Rohlmann, A., Westerhoff, P., 2007. In vivo glenohumeral contact forces-Measurements in the first patient 7 months postoperatively. J. Biomech. 40, 2139–2149. doi:10.1016/j.jbiomech.2006.10.037

Bhandari, M., Smith, J., Miller, L.E., Block, J.E., 2012. Clinical and economic burden of revision knee arthroplasty. Clin. Med. Insights. Arthritis Musculoskelet. Disord. 5, 89–94. doi:10.4137/CMAMD.S10859

Blankevoort, L., Kuiper, J.H., Huiskes, R., Grootenboer, H.J., 1991. Articular contact in a three-dimensional model of the knee. J. Biomech. 24, 1019–1031. doi:10.1016/0021-9290(91)90019-J

Bloemker, K.H., Guess, T.M., Maletsky, L., Dodd, K., 2012. Computational Knee Ligament Determined Zero-Load Lengths Modeling Using Experimentally 33–41.

Bozic, K.J., Kurtz, S.M., Lau, E., Ong, K., Chiu, V., Vail, T.P., Rubash, H.E., Berry, D.J., 2010. The epidemiology of revision total knee arthroplasty in the United States. Clin. Orthop. Relat. Res. 468, 45–51. doi:10.1007/s11999-009-0945-0

Colizza, W.A., Insall, J.N., Scuderi, G.R., 1995. The posterior stabilized total knee prosthesis. Assessment of polyethylene damage and osteolysis after a ten-year-minimum follow-up. J. Bone Joint Surg. Am. 77, 1713–20.

D'Lima, D.D., Fregly, B.J., Patil, S., Steklov, N., Colwell, C.W., 2012. Knee joint forces: prediction, measurement, and significance. Proc. Inst. Mech. Eng. H. 226, 95–102. doi:10.1177/0954411911433372

D'Lima, D.D., Patil, S., Steklov, N., Colwell, C.W., 2007. An ABJS Best Paper: Dynamic intraoperative ligament balancing for total knee arthroplasty. Clin. Orthop. Relat. Res. 463, 208–212. doi:10.1097/BLO.0b013e318150dc2c

Delp, S.L., Anderson, F.C., Arnold, A.S., Loan, P., Habib, A., John, C.T., Guendelman, E., Thelen, D.G., 2007. OpenSim: Open-source software to create and analyze dynamic simulations of movement. IEEE Trans. Biomed. Eng. 54, 1940–1950. doi:10.1109/TBME.2007.901024

Fehring, T.K., Odum, S., Griffin, W.L., Mason, J.B., Nadaud, M., 2001. Early failures in total knee

arthroplasty. Clin. Orthop. Relat. Res. 315–318. doi:10.1097/00003086-200111000-00041

Fregly, B.J., Besier, T.F., Lloyd, D.G., Delp, S.L., Banks, S.A., Pandy, M.G., D'Lima, D.D., 2012. Grand challenge competition to predict in vivo knee loads. J. Orthop. Res. 30, 503–13. doi:10.1002/jor.22023

Fregly, B.J., Besier, T.F., Lloyd, D.G., Delp, S.L., Banks, S. a., Pandy, M.G., D'Lima, D.D., 2012. Grand challenge competition to predict in vivo knee loads. J. Orthop. Res. 30, 503–513. doi:10.1002/jor.22023

Guess, T.M., Thiagarajan, G., Kia, M., Mishra, M., 2010. A subject specific multibody model of the knee with menisci. Med. Eng. Phys. 32, 505–515. doi:10.1016/j.medengphy.2010.02.020

Heck, D. a, Melfi, C. a, Mamlin, L. a, Katz, B.P., Arthur, D.S., Dittus, R.S., Freund, D. a, 1998. Revision rates after knee replacement in the United States. Med. Care 36, 661–669. doi:10.1097/00005650-199805000-00006

Hochberg, M.C., Yerges-Armstrong, L., Yau, M., Mitchell, B.D., 2013. Genetic epidemiology of osteoarthritis: recent developments and future directions. Curr. Opin. Rheumatol. 25, 192–7. doi:10.1097/BOR.0b013e32835cfb8e

Johnson, K.L., 1985. Contact Mechanics, Journal of the American Chemical Society. doi:10.1115/1.3261297

Jones, R.E., Huo, M.H., 2006. Rotating Platform Knees: An Emerging Clinical Standard. In the Affirmative. J. Arthroplasty. doi:10.1016/j.arth.2006.01.021

Liddle, A.D., Pegg, E.C., Pandit, H., 2013. Knee replacement for osteoarthritis. Maturitas 75, 131–136. doi:10.1016/j.maturitas.2013.03.005

Lonner, J.H., Siliski, J.M., Scott, R.D., 1999. Prodromes of failure in total knee arthroplasty. J. Arthroplasty 14, 488–492. doi:10.1016/S0883-5403(99)90106-7

Maniar, R.N., Singhi, T., 2014. Patient specific implants: scope for the future. Curr. Rev. Musculoskelet. Med. 7, 125–30. doi:10.1007/s12178-014-9214-2

Mannion, A.F., Kämpfen, S., Munzinger, U., Kramers-de Quervain, I., 2009. The role of patient expectations in predicting outcome after total knee arthroplasty. Arthritis Res. Ther. 11, R139. doi:10.1186/ar2811

Matsuda, Y., Ishii, Y., Noguchi, H., Ishii, R., 2005. Varus-valgus balance and range of movement after total knee arthroplasty., The Journal of bone and joint surgery. British volume. doi:10.1302/0301-620X.87B6.15256

Narkbunnam, R., Chareancholvanich, K., 2012. Causes of failure in total knee arthroplasty. J. Med. Assoc. Thai. 95, 667–73.

Parratte, S., Pagnano, M.W., 2008. Instability after total knee arthroplasty. Instr. Course Lect. 57, 295–304.

Ranawat, A.S., Gupta, S.K., Ranawat, C.S., 2006. The P.F.C. sigma RP-F total knee arthroplasty: designed for improved performance. Orthopedics 29, S28–S29.

Seil, R., Pape, D., 2011. Causes of failure and etiology of painful primary total knee arthroplasty. Knee Surgery, Sport. Traumatol. Arthrosc. 19, 1418–1432. doi:10.1007/s00167-011-1631-9

Sharkey, P.F., 2002. Why are total knee arthroplasties failing today? Clin. Orthop. Relat. Res. 404, 7–13.

doi:10.1097/01.blo.0000036002.13841.32

Stambough, J.B., Clohisy, J.C., Barrack, R.L., Nunley, R.M., Keeney, J.A., 2014. Increased risk of failure following revision total knee replacement in patients aged 55 years and younger. Bone Jt. J. 96–B, 1657–1662. doi:10.1302/0301-620X.96B12.34486

Westerhoff, P., Graichen, F., Bender, A., Rohlmann, A., Bergmann, G., 2009. An instrumented implant for in vivo measurement of contact forces and contact moments in the shoulder joint. Med. Eng. Phys. 31, 207–213. doi:10.1016/j.medengphy.2008.07.011

Whiteside, L.A., Saeki, K., Mihalko, W.M., 2000. Functional medical ligament balancing in total knee arthroplasty. Clin. Orthop. Relat. Res. 45–57.

Chapter 2

Literature Review

This chapter aims to provide the reader the necessary background information about the total knee replacement surgery technique and the knee joint modelling methods available in the literature. In the first part of the chapter a detailed description of the knee physiology and anatomy is presented, with a particular focus on the properties and the function of the knee ligaments. The total knee replacement, as cure for knee osteoarthritis, is extensively described including the most employed surgical procedures available in the market, principally focusing on the preoperative planning surgery technique. The Medacta *MyKnee*® preoperative planner software is described in detail to show how a predictive model for knee soft tissue balancing might be embedded in such framework. The last part of the chapter is dedicated to the knee joint modelling and the musculoskeletal dynamic models available in literature.

2.1 Anatomic reference terminology

The description of the human body and its movement requires a standardized anatomic reference. Three anatomical planes are defined for the anatomical position and the axes of movement, the planes are sagittal, frontal (coronal), and transverse (Figure 2.1). The relative location is described using spatial and directional indications:

- anterior (close to the front of the body)
- Posterior (close to the back of the body)
- superior (close to the head)
- inferior (close to the feet)
- medial (close to the midline of the body)
- lateral (away from the midline of the body)

The extremities of the body, upper and lower, are described using the terms *proximal* and *distal*. Proximal is referred to a position along a segment which is closer to the main mass of to the body (Zatsiorsky, 2002), while distal refers to a spatially distant part.

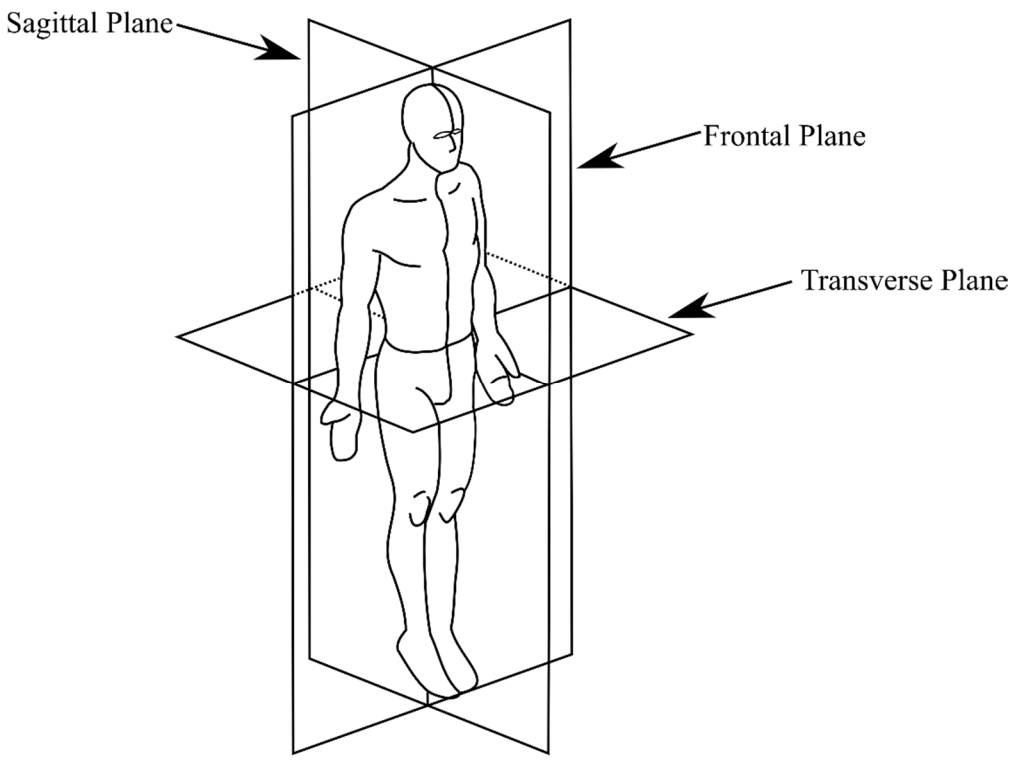

Figure 2.1 – *The Anatomical references planes*

2.2 The knee joint

2.2.1 Anatomy and physiology of the knee joint

The knee is the largest joint in the human body and it is composed by four bones: the femur, the tibia, the fibula and the patella (Figure 2.2). This articulation is substantially constituted by two different joints that work synergistically during the movements.

Figure 2.2 – *The knee joint (http://bit.ly/1ojwwwS)*

The contact between the femur and the tibia composes the tibia-femoral joint which has six degrees of freedom (three rotations and three translations). Despite the number of the degrees of freedom, the tibia-femoral joint is essentially a synovial joint with a single degree of freedom in flexion-extension with a range of motion that goes from 0° up to 135°. More precisely, the relative movement between the femur and tibia is not a pure hinge joint, in fact the shape of the knee condyles along with the tibial plate allow two contemporary movements: sliding and rolling during the flexion-extension movement. Further the tibia-femoral joint allows a slight internal and external rotation whilst the remaining degrees of freedom are locked by the presence of a large variety of structures that, acting as a constraint, limit the movement of the bones conferring stability to the joint. These structures are the knee ligaments, the synovial capsule, the patella, and the tendons of the extensor and flexor muscle group.

The contact between the distal femur and the patella composes the patella-femoral joint. The posterior side of the patella lies congruently on the femoral trochlea, which having a slightly concave shape, allows the sliding of the patella on the femur like a rope in a pulley. This joint mechanism, called trochlea, composes the patella-femoral joint.

There are a large variety of structures that stabilize the patella such as the alar ligaments, the patellar ligament, the articular capsule of the knee joint, and the tendons of the quadriceps muscle group.

The two joints work synergistically: during the flexion-extension movement of the knee joint the patella moves from the frontal part of the femur to the most distal part following the femoral trochlea shape which can be roughly approximated as an arc of circle. The flexion extension movement ranges approximately from 0° up to 135° while the varus-valgus is very limited with a range of motion between 3° and 4°, the medial rotation of the femur is almost limited by the ligaments.

2.2.2 Structure of the knee joint

The knee joint is entirely protected by a variety of structures such as the synovial joint capsule, that along with muscles and ligaments ensure stability and prevent excessive motion. These structures surrounding the joint can be divided in five compartments: anterior, posterior, medial, lateral, and central compartment.

The frontal compartment (Figure 2.3) is composed by the anterior synovial capsule, the patella, and the patellar tendon which represent the distal attachment of the quadriceps femoris muscle group (vastus lateralis, vastus intermedialis, vastus medial, and rectus femoris muscle).

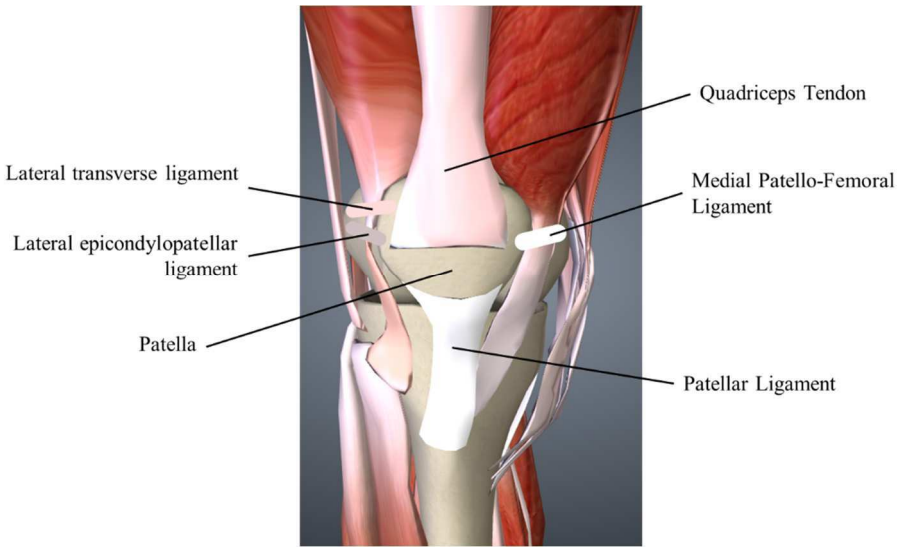

Figure 2.3 – *Frontal view of the knee joint (http://bit.ly/1ojwwwS)*

The four bundles of the quadriceps femoris merge distally to form a solid connection called quadriceps tendon that attaches to the superior and anterior edges of the patella. This tendon attaches to the distal patella while the patellar tendon, which connect the patella with the tibia, originates from the proximal edge. The patellar tendon is a thick bundle (averagely 5 cm) that origin from the base of the patella and insert to the tibial tuberosity of the tibia. This strong structure, composed by the quadriceps tendon, the patella, and the patellar ligament allows the extension movement of the knee joint. The patella is also connected medially and laterally with the femur through the medial patello-femoral ligament, the lateral epicondylopatellar ligament, and the lateral transverse ligament (Figure 2.3). There are superficial bundles on the patella's frontal surface, called medial and lateral retinaculum that connect the quadriceps tendon and the patellar ligament with the anterior synovial joint capsule conferring stability to the whole joint.

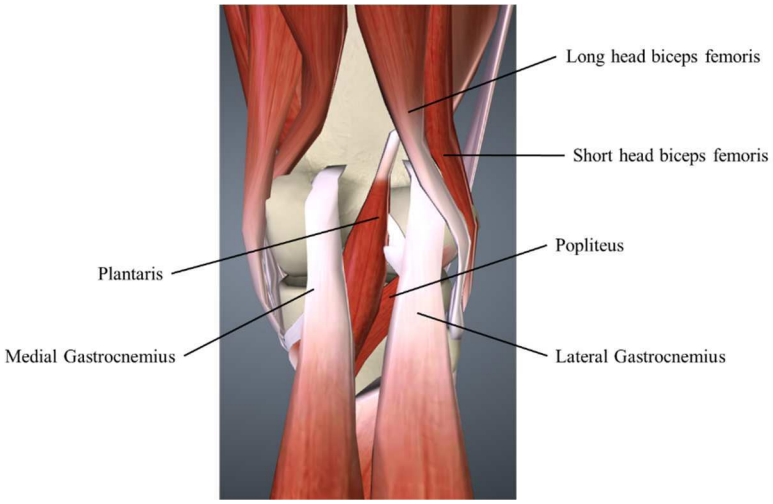

Figure 2.4 – *Posterior view of the knee joint (http://bit.ly/1ojwwwS)*

The posterior compartment (Figure 2.4) is composed by the posterior synovial capsule, which ensures the stability of the knee in extension, and the muscle attachments that insert on the femur and the tibia. The gastrocnemius muscle, which is the major flexor of the knee, is composed by two heads that originate from both the knee condyles, lateral and medial respectively. Other extensors of the knee that are attached to the posterior compartment of the femur are: the plantaris, the popliteus, the semimembranosus, and the short and long head of the biceps femoris muscle.

The medial compartment is composed by the internal synovial capsule, the medial collateral ligament (MCL), and the muscle attachments on the tibia (Figure 2.5). The muscle that insert on the medial compartment are: the semimembranosus, the semitendinosus, the gracilis, and the sartorius muscle (LaPrade et al., 2007).

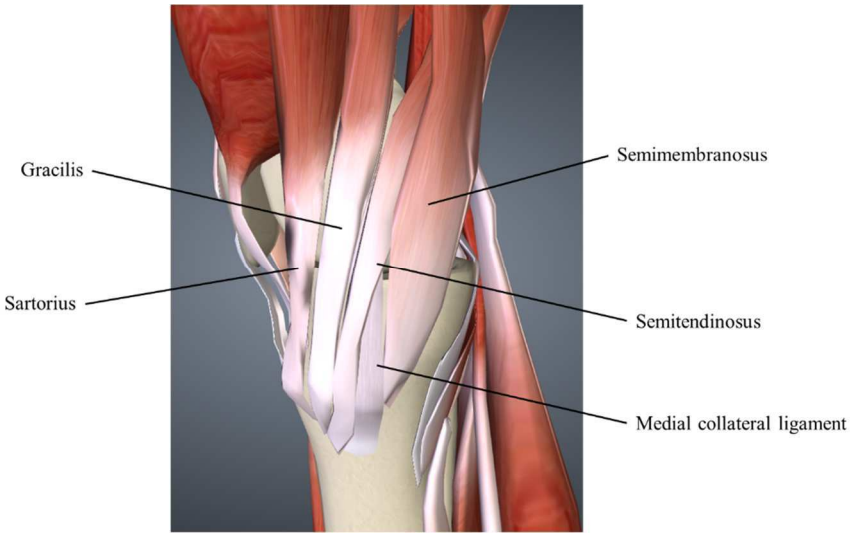

Figure 2.5 – *Medial view of the knee joint (http://bit.ly/1ojwwwS)*

These muscles are classified as extensors of the knee, however given the orientation of the fibres and the attachments points they also control the valgus rotation of the knee.

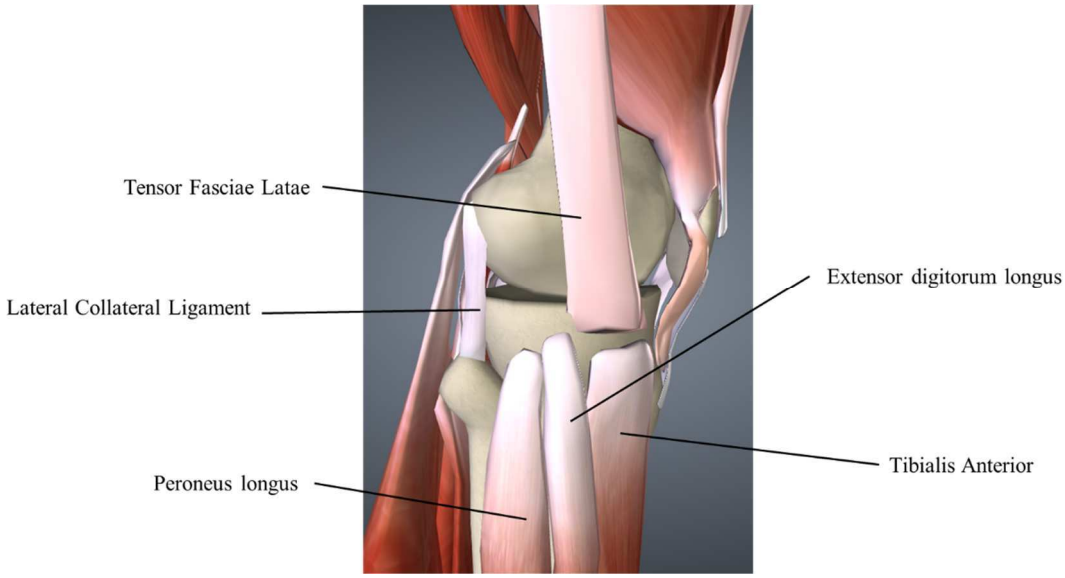

Figure 2.6 – *Lateral view of the knee joint (http://bit.ly/1ojwwwS)*

The lateral compartment (Figure 2.6) is composed by the external synovial capsule, the lateral collateral ligament (LCL), and the attachments of several muscles. The tensor fasciae latae muscle is a continuous of the iliotibial tract which insert to the tibia and its function is to keep the balance of the pelvis during locomotive physical activities. The other muscles are flexors and extensors of the ankle and they are the peroneus longus, the tibial anterior, and the extensor digitorum muscle.

The central compartment (Figure 2.7), also called the central pivot, represents the core of knee movement and it is mostly controlled by anterior and posterior cruciate ligaments (ACL and PCL, respectively). The cruciate ligaments cross each other in the transverse, frontal, and sagittal plane. This compartment is the primary stabilizer and limit the anterior-posterior movement, the internal and external tibial rotation are almost neglected. In particular, the ACL, which originates from the intercondylar eminence of the tibia and insert to the posterior face of the lateral knee condyle, limits the hyperextension of the knee and the anterior sliding of tibial plateau. The PCL, which originates from the intercondylar eminence of the tibia to the lateral aspect of the medial femoral condyle, controls the posterior sliding of the tibial plateau.

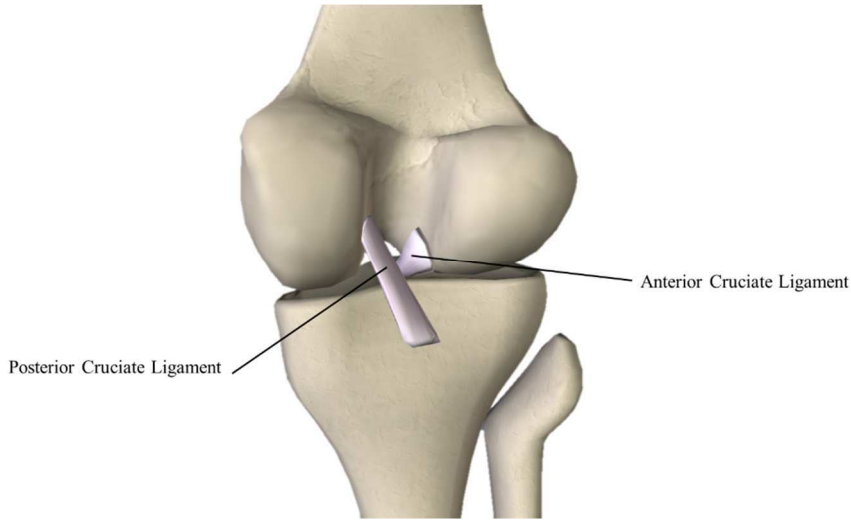

Figure 2.7 – *Central compartment of the knee joint (http://bit.ly/1ojwwwS)*

The distal femur and proximal tibia are separated by a fibrocartilaginous structure called menisci which helps the knee joint in terms of stability, lubrication, and load distribution (Hutton, 1993). There two menisci placed on the tibial plate, the lateral and the medial, both are shaped as semi-lunar cartilages (Figure 2.8). This configuration creates two concavities on the tibial plate to receive the femur condyles ensuring structural integrity to the whole knee during tension and torsion movements. Structurally the menisci are composed by inhomogeneous collagen fibre layers (Hutton, 1993) that are able to transduce applied compression and shear forces into tensile stress. In fact the menisci has a higher water content that allow to endure very high knee joint loads. During the most common life activities such as walking compressive knee forces can be as high as three body weight (Taylor et al., 2004).

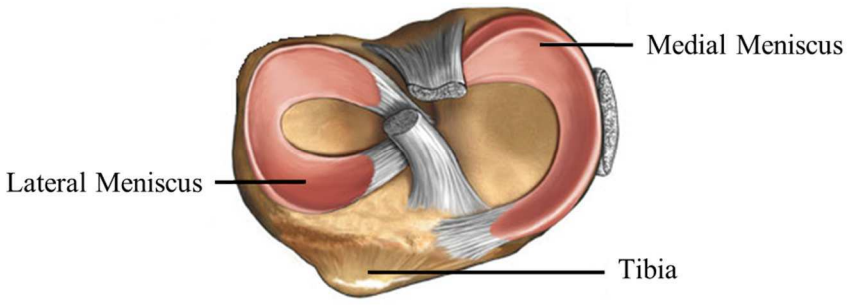

Figure 2.8 – *Axial view of the knee menisci cartilage*

The functional role of the meniscus is crucial in maintaining a good quality of lifestyle given the importance and the centrality of the knee joint in the daily life activities. The tear of the menisci can represent the initial stage of the knee cartilage deterioration (Englund et al., 2009; Michael et al., 2010), better known as knee osteoarthritis.

2.2.3 Knee osteoarthritis

The knee joint is subjected to a wide range of injuries such as the ligaments tear, bones fracture, meniscus injuries, or tendons rupture. However, the most common disease affecting the knee joint function is the osteoarthritis (OA) which is described as a degenerative process of the knee cartilage (Figure 2.9) with no cure (Michael et al., 2010), that require 600.000 people in USA each year to have one of their joints replaced with an artificial components (Bhandari et al., 2012). Although the elderly population is the typical target for this pathology (Neogi and Zhang, 2013), the standard is rapidly shifting to younger patients due to the aging of the population and the obesity epidemic, and these numbers are expected to grow up in the next few decade (Bhandari et al., 2012). The causes of OA are unknown; however evidences have proven that the origin is multifactorial. Many epidemiological studies have attempted to describe the aetiology of OA finding two types of risk factors, endogenous (age, sex, ethnic origin) and exogenous (trauma, overweight, lifestyle) (Hochberg et al., 2013). Although the risk factors might suggest a sort of guidelines to prevent or delay the occurrence of this pathology, the genetic factors indubitably play a key role (Hochberg et al., 2013).

Figure 2.9 – *Degeneration of knee cartilage (osteoarthritis)*

The cartilage loss is caused by a break of the normal degenerative and regenerative/healing processes of the knee cartilage. Micro tears start to appear at cellular level in the most stressed areas of the cartilage leading overtime to overall degeneration (Das and Farooqi, 2008). This degenerative progression results in thinning of the knee cartilage which is usually detected by x-ray, measuring the thickness between the femur and the tibia. At latter stage the articular cartilage results thinned and fragmented, in severe cases it can completely disappear leaving the femoral surface uncovered. The symptoms correlated with OA are joint pain, stiffness, and restriction of the joint function. The pain is mainly associated with physical activity, the knee joint is loaded and the movement creates a friction between the bones that rub against each other given the absence of the cartilage function. For this reason, OA represents a dramatic change in peoples' quality of life especially for younger patients that have high lifestyle expectations.

Many studies on the treatment of OA have proven that a changing in lifestyle such as losing weight or decreasing physical exercise may achieve sufficient results in preventing or delaying the occurrence of this disease (Cooper et al., 2000; Hunter and Eckstein, 2009). However, since the regeneration of the articular cartilage is not possible, unloading the joint or the normal rest does not heal or reverse the OA symptoms (O'Driscoll, 1998). Thus, in patients with symptoms of severe pain and impaired ability to perform daily activities changes in lifestyle are not valid, therefore surgical procedures are commonly considered. Traditionally, the surgical treatment aims to restore the damaged bony surfaces using artificial components, this operation is known as knee joint replacement (Bellemans et al., 2005a; Bhandari et al., 2012; Walker et al., 2010).

2.3 Knee Ligaments

2.3.1 Introduction

The human ligaments connect bone with bone and their primary role is to act as a mechanical stabilizer to the joints guiding the motion and preventing excessive displacement. Generally they are attached to the bone through four progressive zones: ligament, fibrocartilage, mineralized fibrocartilage and bone (Woo et al., 1987). The mechanical behaviour of the ligaments steams from the particular organization of the collagen fibres. In fact these fibres are composed by tropocollagen molecules (Brodsky and Persikov, 2005) which are organized into helical chains of cross-striated fibrils that confers to the ligaments unique mechanical properties under tensile loading (Figure 2.10).

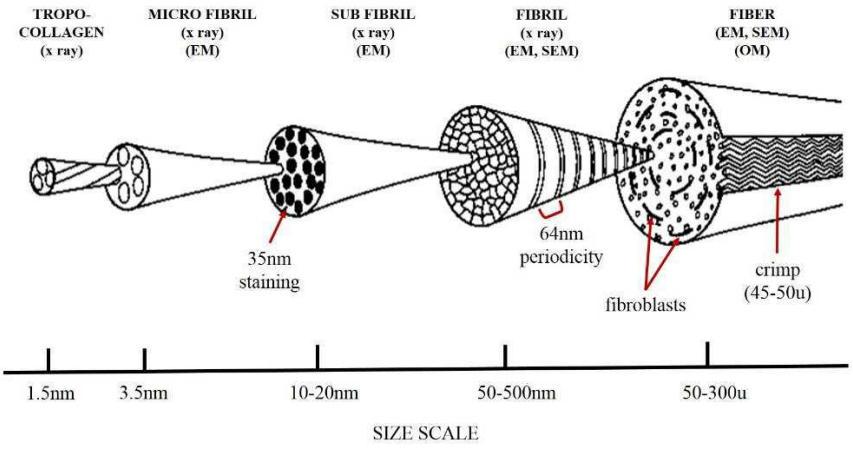

Figure 2.10 – *Human ligament structure. Image modified from* Woo et al., 1999

In fact, the cross-linked chains of the collagen fibres give stiffness to the tissue allowing to work efficiently under mechanical stress. The ligaments have unique properties and it's very difficult to find an artificial material with the same characteristics, for this reason it has been proposed the use of autogenous tissue graft in case of ligaments rupture, however the long-term clinical results appear to be dubious (Arnoczky et al., 1982).

The structure and the biochemical composition of ligaments are identical in humans and in many animal species such as rats, rabbits, dogs and monkeys, so the extrapolation regarding these structures in humans can be made from animal experimental results (Proffen et al., 2012).

Among the number of structures that surround the knee, the four major ligaments are the prime responsible for the stability and the motion of such important joint of the human locomotor system.

The major ligaments of the knee are four:

- The medial collateral (MCL) ligament origins from the medial epicondyle of the femur and inserts on the post-medial edge of the metaphysis of the tibia.
- The lateral collateral (LCL) ligament originates from the lateral epicondyle of the femur and inserts on the head of the fibula.
- The anterior cruciate (ACL) ligament originates from the post-lateral aspect of the intercondylar fossa of the femur and inserts on the anterior part of intercondylar eminentia of the tibia.
- The posterior cruciate (PCL) ligament originates from antero-lateral aspect of the intercondylar fossa of the femur and inserts on the posterior part of intercondylar eminentia of the tibia (S. L.-Y. Woo et al., 2006).

Each knee ligament is divided by different bundles which have different tensioning pattern during flexion and extension. The ACL and PCL are both composed by two bundles: anteromedial (AM) and posteromedial (PM) (Yagi et al., 2002). The MCL and LCL have in addition another bundle called medial bundle (ML) (Park et al., 2006). The contribution of each bundles during flexion-extension movement allow to understand the mechanical properties of the ligaments and more importantly the stability of the joint when a partial rupture of the knee ligaments occurs (Harner et al., 1995).

The knee ligaments assure stability to the joint by preventing an excessive motion, for each plane of knee mobility the ligaments divide in primary and secondary stabilizers. The MCL and ACL are primary and secondary stabilizers respectively for the varus movement, whilst the varus is controlled by the PCL and LCL. Further the LCL and PCL are particularly active in preventing the motion at 45° and 90° of flexion, respectively. The cruciate ligaments play a primary role when anterior/posterior displacement of the

tibia relative to the femur occurs. The external rotation of the knee joint is controlled by the MCL during the flexion with the ACL as a secondary constraint.
In extension the ACL acts as the main stabilizer and the LCL as a second costraint, when the knee is flexed, the cruciate ligaments allow a correct internal rotation movement, while in extension, the ACL is the primary stabilizer and the LCL is secondary stabilizer (Marshall et al., 1977).

2.3.2 Mechanical Properties of Ligaments

Measuring the mechanical behavior of human soft tissue remains challenging. As human soft tissue is anisotropic, non-linear and inhomogeneous in nature, its properties are difficult to characterize.

The human ligaments have a non-linear viscoelastic behavior in response to tensile loading test, which derives directly from the composite and anisotropic structures this tissue is made of. In fact, the ligaments work more efficiently when the load is transferred bone to bone along the axial direction, experimental tests have discovered time-dependent properties such as creep, hysteresis, or tension-relaxation proving the non-linear behavior of the ligament under tensile loading. Designing experiments for material characterization of knee ligaments poses several problems and has therefore been a subject of much debate. Two issues are the measurement of specimen cross sectional area for the computation of stress and the measurement of surface strain. The typical result of a bone-ligament-bone (BLB) specimen of knee ligament loaded with forces applied on the extremities is shown in figure 2.11 (Girgis et al., 1975, Markolf et al., 1990, (Arms et al., 1984; Beynnon et al., 1992, Quapp and Weiss, 1998; Woo et al., 1999). Although the best solution would be to examine the isolated ligaments, however in most cases the specimen is too small and premature failure occurs at the clamp sites (Lyon et al., 1989).

Different methods have been described that are either based on contact or noncontact measurement techniques. Classically, several types of strain gauges have been used. The major downside of these measurement tools is that they are invasive in nature and act as single-point gauges, which can only record strain from one small area. Even several strain gauges cannot show regional strain and strain gradients and thus could miss critical

details. Moreover, many designs only measure strain in one direction (uni-directional strain).

The measure of the ligament surface strain has been tackled using different methods in the past decades, many studies utilized strain gages sutured or adhered to the ligament bundle to measure ligament displacement at various knee position (Berns et al., 1992; Gardiner et al., 2001) and it represented the most used method. The typical setup includes uniaxial strain gauges that are able to measure the strain of the ligament along the direction of the applied force, however, more strain gauges can be combined together to form a rosette (Salo et al., 2015), which is able to detect deformations also in different directions. Other studies (Quapp and Weiss, 1998; Woo et al., 1999) have used extensometer to measure the ligament's strain to understand how the knee position and the muscle contraction affect the ligaments biomechanics. Delport et al. (2012) have sutured two calibrated extensometers (Type 634.12F-24, MTS, Eden Prairie, MN, USA) to the lateral and medial superficial collateral ligaments with the knee unloaded and in full extension. A preliminary test of the fixation of the extensometers showed that strains could be detected with an accuracy of better than 1%.

In the study conducted by Pioletti et al. (1999), BLB specimens were placed in a custom-made device to perform uniaxial dynamical tests on isolated ligaments. The strain was measured with a linear displacement transducer (VIBROMETER, WG 173, Fribourg, Switzerland) placed on the moving end of the ligament. The advantages of using this "contact" technique is represented by the moderate cost of the experimental setup and the accuracy of the results achieved in measuring the ligaments mechanical behavior, however these conventional techniques are very invasive and strain measurement techniques, such as using extensometers, disturb the strain state in the ligament and result in point measurements that do not account for the vastly varying strain distribution resulting from material in-homogeneity. Also, this conventional approach is not capable to measure ligament cross-sectional area and surface strain distribution.

To address this issue, others studies have adopted optical technique for the measurement of strains (Woo et al., 1983) that are capable of measuring ligament cross-sectional area and surface strain distribution which are necessary information to develop a proper constitutive model of the ligaments for biomechanical models of the knee. The

non-contact methods employed tool such as surface digitization system (ATOS^{TM}: Advanced Topometric Sensor), 3D photogrammetric device (Tyson et al., 2002) (ARAMIS^{TM}), and laser micrometers (Lee et al., 1988, Iaconis et al., 1987). Another approach is the image-based strain measurements that are non-invasive. Many of them optically track surface markers on the specimen during deformation to inversely calculate displacements and strain. Their resolution is mainly defined by the distance between the markers on the surface and was low in many setups (Mazzocca Noble). Digital image correlation (DIC) is an optical method for strain measurement that uses image recognition to analyse and compare digital images acquired from the surface of a substrate instead of surface markers (Zhang). By tracing a randomly applied high contrast speckle pattern using white light, displacement and strain within the specimen can be calculated from subsequent images. The initial imaging processing defines unique correlation areas known as macro-image facets, typically 5–20 pixels square, across the entire imaging area. Each facet is a measurement point that can be thought of as an extensometer point and strain rosette.

2.3.3 Tensile properties of ligaments

The structural properties of the bone-ligament-bone complex are normally determined via tensile test, where a tensile load is applied along the axial direction at constant rate the ligament. A typical result of a tensile test is a curve that is nonlinear and concave upward (Figure 2.11).

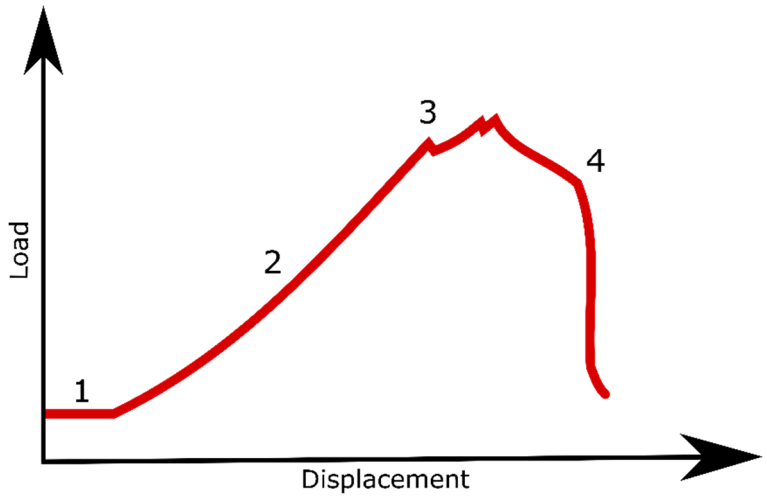

Figure 2.11 – *Ligament force-displacement curve modified from Benjamin & Ralphs, 1997*

This is the typical ligament force-displacement curve obtained from a tensile test, the curve is commonly divided into four regions:

- *Region 1* is the “toe region” (nonlinear behaviour)
- *Region 2* is the linear behaviour
- *Region 3* appears when isolated collagen fibres begin to fail
- *Region 4* is the rupture of ligament

The unique behaviour of this tissue suggests that initial elongation is the result of a change in the helical configuration of the relaxed collagen chains. In this region the tissue can be stretched applying a small load, the collagen fibres lose their wavy pattern and they become more straight (Woo et al., 1991). Applying more load increases rapidly the stiffness of the ligament and at this stage a bigger amount of force is required to produce the same displacement.

The relationship between force and displacement (stress and strain) of the ligaments is quantified by calculating the modulus of elasticity. In fact, this parameter has been calculated for tendons and ligaments in several studies (Benjamin and Ralphs, 1997; Pioletti et al., 1998).The strain (ε) is defined as the deformation per unit of length and it is calculated by placing markers on the ligament in the region of interest. The formula to calculate the strain is (Woo et al., 1999):

$$\varepsilon = \frac{(l - l_0)}{l_0}$$

where

- l_o is the initial length (distance between the markers)
- l is the length after the application of the load.

Experimentally the strain has been obtained using many measuring devices that were sutured directly on the soft tissue measuring the variations along the axial direction. These devices are mercury strain gauges (Aglietti et al., 1993; Berns et al., 1992), Hall-effect strain transducers, or differential-variable-reluctance-transducer (Arms et al., 1983). Other experimental studies have enrolled non-contact method such as the video

dimension analyser system or the motion capture system, both use a video camera and an image processing system (Woo et al., 1986). The determination of a correct value of the initial length is fundamental because an incorrect initial length of ligament would naturally lead to the incorrect calculation of ligament strain; the optical video system seems to reduce errors (Woo et al., 1983).
The stress, defined in newton per square millimetre, is the load per unit cross-sectional area of a ligament. The formula is:

$$\sigma = \frac{F}{A}$$

where

- F is the force applied
- A is the cross-sectional area.

The modulus of elasticity is based on a linear relationship between force and displacement, and this is the formula:

$$E = \frac{\sigma}{\varepsilon}$$

(σ = stress, ε = strain)

2.3.4 Viscoelastic properties of ligaments

Many studies have discovered experimentally time and history dependent viscoelastic properties of these viscoelastic properties of the knee ligaments are:

- creep (progressive increase of the ligament length applying the same force through time)
- tension-relaxation (a decrease of the tension when the ligament is maintained at a fixed length)
- hysteresis (energy dissipation after constant loading and unloading) (Figure 2.12).

In particular, Woo et al. (1989) noticed that during cyclic loading/unloading of the ligament at specific intervals, the force-displacement curve moved along the deformation axes increasing the area of the loading cycle. The progressive deformation is not recoverable and it becomes bigger at every loading cycle. This mechanical response confirmed the presence of non-elastic structures in the ligaments which guide the non-linear behaviour under tensile stress test.

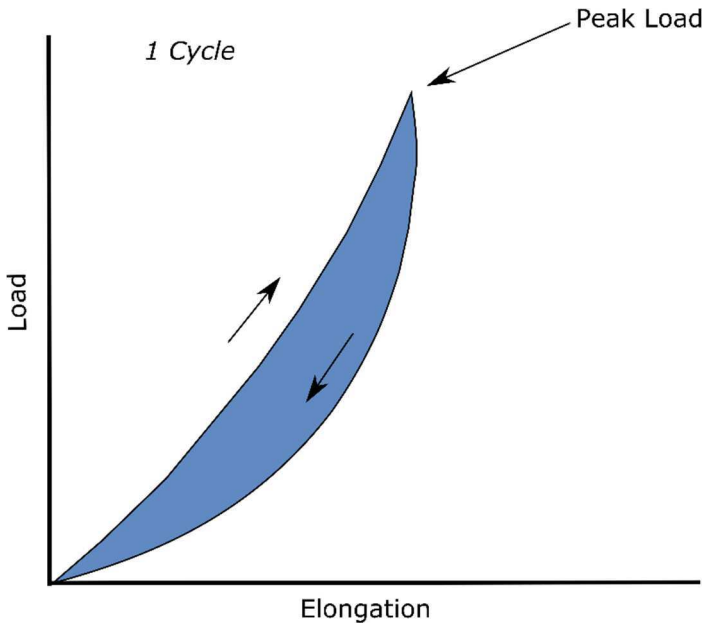

Figure 2.12 – *Typical loading (top) and unloading curves (bottom) from tensile testing of knee ligaments. The two nonlinear curves form a hysteresis loop. The area between the curves, called the area of hysteresis, represents the energy lost within the tissue. Image modified from Benjamin and Ralphs, 1997*

Many authors have investigated the behaviour of the ligaments under repetitive loading/unloading testing: in 1983, Woo et al. reported an experiment in which a bone-ligament-bone complex is subjected to a 10 cycles of preconditioning to a low "overall strain" value of 2%, followed by testing to a failure at a stretch rate of 2 cm/min.

2.3.5 Damage threshold in quasi-static distraction of human knee

The mechanical behaviour of ligament is studied by elongating the structure to the point of rupture while measuring associated increase length and tension. From literature it's possible to find the value of the strain at failure of bone-ligament-bone complex of animals during a tensile loading test. In 1983, Woo et al. tested the MCL of dogs, rabbit and swine for a tensile testing of the bone-ligament structure. The results suggest that the bone-MCL-bone don't show a linear structural behaviour, in particular all the ligaments showed this nonlinear relation. The strain at failure obtained in this study is 14±1% for the dog specimen, 12±1% for the swine and 7±1% for the rabbit. It's very important to point out that during the tensile test some bone complex failed at the mid-ligament substance level whereas others failed with a combination of ligament substance tear together with tibial avulsion. Thus, the averaged "overall strains" at failure for the specimens did not truly represent the ultimate strain of its MCL substance because probably the "overall strain" at failure is probably lower than the actual ultimate strain values, since most of the specimens fail by tibial avulsion. The methodology permitted also the study of the regional strain variation along the ligament substance. The tibial region demonstrated higher strain values than the femoral region for all three animal groups. It's interesting to underline that the deformation near or at the ligament insertion sites to bone are larger than the mid-substance. It is conceivable that larger deformation near insertion may predispose these areas to higher incidence of tensile failure (Arms et al., 1983). According to the experimental tests conducted to calculate the strain to failure (Table 2.1), the ultimate strain ranges between 15% and 20% of the initial length, confirming that the ligaments are the first stabilizers for the mechanical stability of the knee joint. The table below showed the ultimate strain of different human knee ligaments obtained during tensile loading test (Quapp and Weiss, 1998). The results revealed that, although the experimental set up and the specimens were different, there is a 5% of difference between all the studies, confirming that the average ultimate strain for a human knee ligament is around 17% of the initial length. It might be said that despite the differences between the specimens (age, sex, type of ligament), the results are remarkably similar, meaning that the collagen structure of the tissue remained constant over different ligaments and subjects. The experimental set ups used in these studies were non-contact (optical) (S. L. Y. Woo et al., 2006) and clamp to clamp devices (Quapp and Weiss, 1998).

Specimen Type	Tangent Modulus(MPa)	Tensile Stress (MPa)	Ultimate Strain ($\%$)
Human MCL (Quapp et al. 1997)	332.2±58.3	38.6±4.8	**17.1±1.5**
Human PCL, anterolateral bundle (Race et al. 1994)	248±119	35.9±15.2	**18.0±5.3**
Human ACL, LCL, PCL (Butler et al. 1986)	345.0±22.4	36.4±2.5	**15.0±0.8**
Human pPCL (Race and Amis 1994)	N.A.	N.A.	**19.5±5.4**
Human aPCL (Race and Amis 1994)	N.A.	N.A.	**18.0±5.3**

Table 2.1 – *The tests were performed using non-contact strain measurement technique except the Butler et al. study*

2.4 Total Knee Replacement

2.4.1 Introduction

Total Knee Replacement (TKR) is a surgical procedure aimed to replace the damaged surfaces of the knee joint with artificial components. The femoral and tibial surfaces are replaced by a metallic component called femoral component and tibial tray, respectively. A polyethylene tibial insert is placed between the femoral component and the tibial tray, replacing the cartilage function, while a patellar button replaces the patellar surface (Figure 2.13).

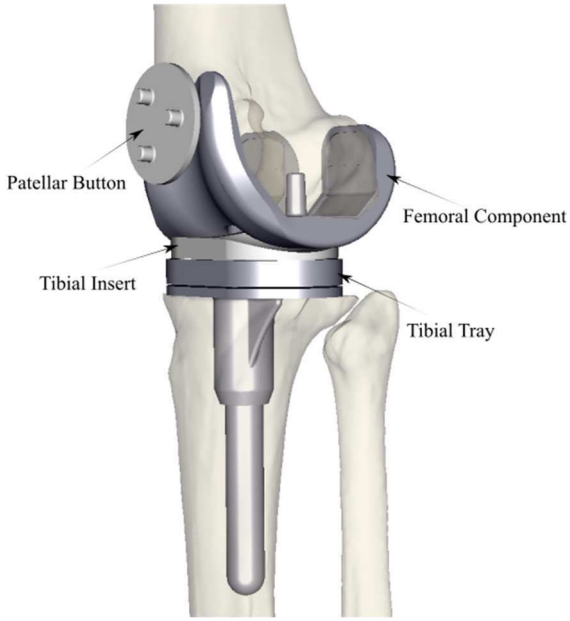

Figure 2.13 - *The procedure consists of replacing the surface of distal femur and the proximal tibia with high resistant metallic components. The femoral surface is replaced by a femoral metallic component while tibia surface by a tibial metallic baseplate. Between the femoral component and the tibial baseplate, a plastic insert is inserted to replace the cartilage function*.

The first design of knee replacement was created by Gluck (Wessinghage, 1991), who in 1890 presented a prototype made of ivory, which was attached to the bone through cement made of colophony, pumice, and plaster of Paris. The proposed model was a hinged design, which attempted to simplify the knee mechanics by limiting the motion to the flexion-extension movement. In the seventies some studies defined a primitive concept for the most recent total knee replacement designs, which eliminated the mechanical connection from the joint, relying upon the soft tissue to provide articular stability. Gunston (1971) created a metallic prosthesis for the femur and a polyethylene

insert for the tibia that were attached to the bones using a cement made of polymethyl-methacrylate (PMMA). The design was thought as a uni-compartimental prosthesis, which could replace the surface of either medial/lateral compartment of the femur or both. The first type of total condylar knee replacement was introduced by Freeman and Swanson (Freeman et al., 1973), which implanted the first model of total condylar prosthesis in 1970. This concept represents the start of the modern era of total knee replacement design; in fact, improved versions of this prosthetic model are still currently used in clinic. Insall et al. (Insall et al., 1976) refined the total condylar knee replacement improving in the frontal plane the congruency between the trochlea of the femoral component and the polyethylene patellar component. The tibial component was designed to enhance the stability, there was an intercondylar spine and the tibial plates were cup shaped to receive the knee condyles. The components were attached to the bone through cement and short-term good results were reported (Insall et al., 1976). This total condylar knee prosthetic implant is still considered the gold standard in total knee replacement surgery and it represents the design concept on which all contemporary TKRs are based (Persona® Knee – *Zimmer, USA*; GMK Sphere® - *Medacta International SA, Switzerland*). Despite the considerable success of this novel design in terms of short-term outcome, the major cause for failure was loosening of the components (Moreland, 1988) and the failure rates were considerably high (Tew and Waugh, 1982). Many studies reported the negative effect of the bone cement such as heat-related failures (Mjoberg et al., 1986) and chemical toxicity (Stürup et al., 1994), resulting in bone resorption and osteolytic activity (Goodman et al., 1991; Schmalzried et al., 1992). This led the research to explore new methods for fixation such as the press-fit implants where a roughened metal surface allows the bony growth in microscopic pores (Hungerford et al., 1989). The Freeman-Swanson model has represented a base to develop more complex prosthetic implants such as the fixed-bearing knees, where the polyethylene tibial insert is locked with the tibial tray. The high congruency of the contact surface provides low contact stress but in the other hand it produces a high torque at the bone-implant surface predisposing to component loosening. Most recent total knee replacement designs present mobile-bearings, which allow movement of the insert relative to the tray. The mobile-bearing design provides in principle both congruity and mobility, allowing low contact stress and low constraint force to improve wear resistance and, theoretically, to minimize loosening. The latest achievements in design and material science have led to incremented life expectancy of TKR implants, where the femoral component and the tibial tray are usually

made of titanium or cobalt-chrome steel (Co-CR-Ba), while tibial insert and patellar button are usually made of ultra-high molecular weight polyethylene (UHMWPE).

Many studies in literature have reported the effectiveness of the TKR in the long-term clinical results (Callaghan, 2001; Colizza et al., 1995) in terms of significant pain reduction over 10-15 years after the surgery; TKR failure is measure as 10 % of implants retrieved within 10 years, as reported in outcome registers (Figure 2.14). The increasing number of osteoarthritis patients due to the progressive aging of the population and the introduction of minimally invasive surgical procedures have boosted the demand of total knee replacement surgeries, which now present in most clinical studies success rate of 90%, when measured in term of revisions (Callaghan, 2001; Colizza et al., 1995; Emmerson et al., 1996; Ranawat et al., 1997).

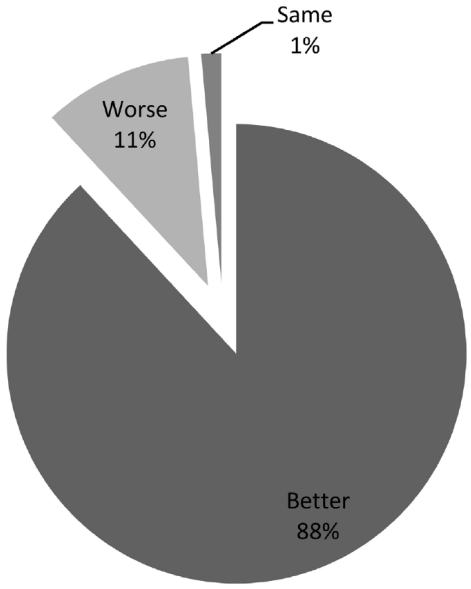

Figure 2.14 - *Proportion of patients achieving optimal and suboptimal outcome (figures from* (Baker et al., 2012)*).*

According to this failure criterion, only 10% of implants fail, most of the time for reasons other than the device design (Baker et al., 2012). Thus, this light TKR appears to be a successful procedure.

However, over 40% of patients are unhappy of the life style their TKR offer (Mannion et al., 2009).

When TKR started to be widely adopted, most of the patients were well over 65, and with limited life style expectations. Surgical procedures were tuned on this population, and privileged stability over mobility. As the indication broadened, younger and younger patients were enrolled; today 45% of the patients are under 65 (Baker et al.,

2012) years old. Also, the expectations in term of active life style in the ageing population changed considerably. Hence, nearly half of patients are not satisfied.

In order to achieve stability and mobility a TKR procedure requires an accurate planning, in order to ensure an optimal balancing of the soft tissues, and an accurate execution, in order to achieve accurate skeletal positioning. The second part has been drastically improved by the introduction of subject-specific cutting guides, which starting from a CT-based pre-operative planning, provide an easy way to produce precise bone cuts, essential to accurately position the implant with respect to the skeleton (Maniar and Singhi, 2014). However, the planning step is still entirely left on the surgeon experience, as the current planning tools are not able to predict which soft tissue balancing a certain planning would produce.

2.4.2 Surgical Principles

The aim of the total knee replacement surgery is to restore the correct mechanical alignment of the lower limb, along with the optimal soft tissue balance (Bellemans et al., 2005b) (Figure 2.15); meaning that, considering the lower limb fully extended, the mechanical axis lies on the connecting line between the center of the femoral head and the center of the ankle passing through the center of the femur condyles and the tibial spine (Luo, 2004).

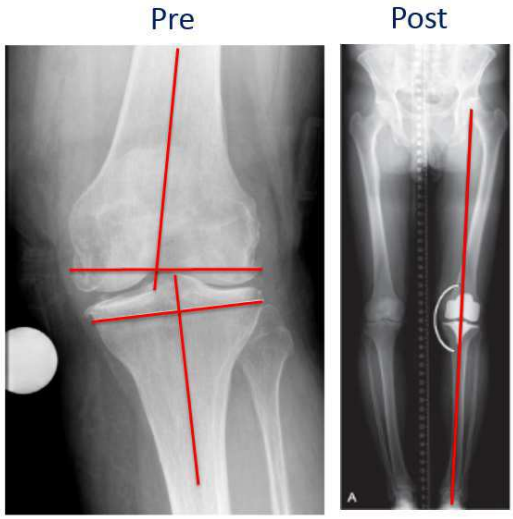

Figure 2.15 - *Restoration of preoperative varus deformity (left) to correct alignment after TKA (right)*

The most common surgical approach used by the surgeons is the vertical midline skin incision and a medial para-patellar approach. The intention is to replace the amount of bone and cartilage that have been lost secondary to the arthritic process and that resected as part of the TKR, with a similar thickness of polyethylene and metal provided by the prosthetic components. After exposing the joint with some elevation of the medial retinaculum, the knee is flexed. Depending on the particular surgical technique the surgeon performs the tibial and femoral cut following certain criteria.

The surgical procedure starts typically exposing the knee through a medial para-patellar incision on the skin, the length ranges from 136 mm up to 151.8 mm (Maniar and Singhi, 2014) depending by the technique utilized. The first step is to detach the patella from the knee opening the synovial capsule and removing the structures such as the epicondylopatellar ligaments to expose the distal femur and the proximal tibia. Once the patella is moved laterally, the surgeon clean out the remained structures in the medial portion between the femur and the tibia included either both the cruciate ligaments, or

just the anterior cruciate ligament (ACL). After there is the most delicate part of the procedure where the surgeon shapes the bones to fit the implants by removing measured fragments of the bones. The surgical procedure comprises five cuts on the femur: 1) distal cut 2) anterior and posterior cuts 3) two chamfer cuts (Brooks, 2009), and one on the proximal tibia (Figure 2.16).

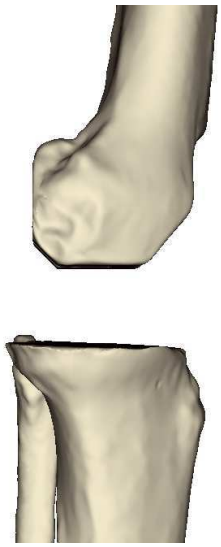

Figure 2.16 – *TKR surgical procedure*

The two parallels cut on the femur and the tibia are the most important since they dictate the position of the final implant and the orientation of the remaining cuts. Among the surgical techniques that allow to achieve an optimal orientation of the cut, the most common are: conventional TKR (cTKR), computer assisted surgery (CAS-TKR), and patient specific instrumentation (PSI-TKR). The cTKR and the PSI allow the surgeons to perform the cut using a mask, called cutting block, attached to the bone during the surgery which guides the jig to remove the bone. The position of the cutting block on the bone is crucial and it relies on specific bony landmarks such as the knee condyles. The PSI surgical technique relies upon a complex patient specific preoperative planning (Hafez et al., 2006) based on CT or MRI images, that allow the manufacturing of patient specific instrumentation that fit accurately the patient's anatomy. The cTKR instead employs generic cutting blocks of different size to try to fit different bony anatomies with the same aim of PSI (Bäthis et al., 2004). The CAS uses a motion capture system which through rigid body markers attached on the patient's bone, tracks their motion helping to define the orientation of the cuts in the three dimensional space (Bae and Song, 2011). These techniques take into account the alignment of the femoral and tibial components with respect to the mechanical axis of the lower limb, the balancing of the soft tissue is not

included. Therefore, to address the balancing problem the surgical procedure includes some methods to check and eventually adjust the tension of the soft tissue.

The most popular techniques are: the balanced resection and the measured resection. Balanced resection is performed by first cutting the tibial bone and then applying a symmetrical tension to both ligaments, with the extended knee, using tensors, knee balancer or laminar spreaders (Ranawat et al., 2006; Whiteside et al., 2000). The same procedure is then applied with the flexed knee and setting the femoral component rotation so to maintain the established tension on the balanced ligaments, which is not easy to achieve since heavily influenced by the size of the femoral component (Heesterbeek et al., 2009; Lee et al., 2011). Measured resection entails the cuts of both the femur and tibia bones before the ligaments balancing. After the cuts, a trial prosthesis implant is placed between the bones and the knee is tested in extension and in flexion. The total amount of bone that is cut should correspond to the thickness of the prosthesis but femoral and tibial preparations are performed independently (Winemaker, 2002). The artificial components are then placed on the bones and afterwards the surgeon will perform some manual testing to check the range of motion and the stability of the joint. To conclude the procedure, the wound is closed using stiches or staples and a bandage will then be applied for the recovery process.

2.4.3 TKR failure

Clinical failure of TKR is defined with a very severe end point: re-operation, also called revision surgery. The occurrence of these revisions represents a dramatic change in the patients' quality of life and also denotes an underestimated problem in terms of economic burden. In fact, the total costs associated with each total knee replacement surgery have been estimated to exceed US$49,000, and this number is expected to continue to increase, in concert with the rapidly increasing number of total knee replacement performed every year (Bhandari et al., 2012). Furthermore, the revision surgery is a very complex procedure, after which patients could expect less improvement and a higher risk of complications than after their primary total knee replacement (Stambough et al., 2014). Thus, the definition of new methods that aim to limit the number and risk of revision surgeries is compelling to reduce the economic burden of TKR.

The most common causes for TKR failure are: knee instability, patella-femoral complications, misalignment, and component loosening (Narkbunnam and Chareancholvanich, 2012; Parratte and Pagnano, 2008; Seil and Pape, 2011). Instability, resulting from excessive laxity of the soft tissue, represents the 22% of the TKR revision causes (Sharkey, 2002). Patients that present instability suffer pain, effusions, and inability to navigate curbs and inclined planes (Fehring et al., 2001). Patella-femoral complications can be associated to an incongruent tibio-femoral rotation, commonly caused by internal rotation of the tibial plate or the femoral component (Barrack et al., 2001; Berger et al., 1998). The wrong patellar tracking can lead to anterior pain, patellar fracture, and patellar instability, and limitations in the ROM. Component loosing is considered as a consequence of polyethylene wear (Sharkey, 2002), it results up to 34% of late stage surgeries revision. Accelerated wear has been observed in patient with excessive soft tissue tension, both medially and laterally (Gallo et al., 2013; Kuster and Stachowiak, 2002), that leads to a greater mechanical stress between the femoral and tibial component. In general, most of the above factors for failure can be attributed to surgical techniques which inadequately addresses the problem of balancing the knee soft tissues (Bozic et al., 2010; Fehring et al., 2001; Lonner et al., 1999; Sharkey, 2002).

2.4.4 The relevance of the Soft Tissue Balancing in TKR

The definition of soft tissue balancing for TKR is not straightforward. This concept might be used to refer to a prosthetic knee joint where the following characteristics are preserved:

a) a full range of movement;
b) symmetrical medial-lateral balance at full extension and 90 degrees of flexion;
c) correct varus valgus alignment in both flexion and extension;
d) absence of medial-lateral tightness or laxity;
e) correct patellar tracking; and
f) correct rotational balance between the femoral and the tibial components (Babazadeh et al., 2009).

In terms of surgical procedure, the above factors should be ensured by the creation of a balanced flexion-extension gap between the femoral and tibial cut, which dictates the thickness of the final implant (Dennis et al., 2010; Heesterbeek et al., 2010). This is usually pursued during the surgery by subsequent adjustment of the flexion extension gap (Figure 2.17) in attempt to obtain equal sized rectangular gaps in both extension and flexion positions (Griffin et al., 2000) to avoid soft tissue laxity where the gap is bigger and overstuffing of the joint where the gap is smaller (Bellemans et al., 2005b).

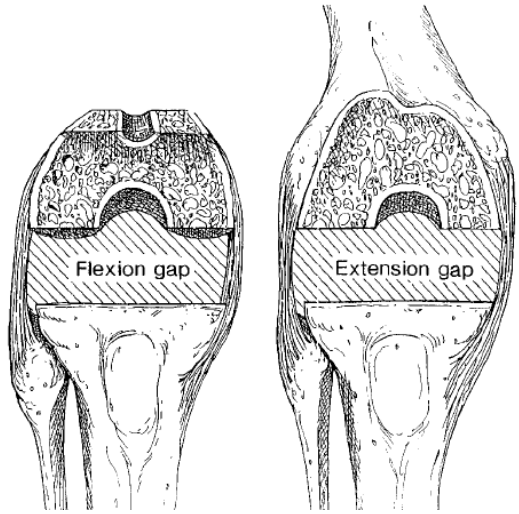

Figure 2.17 – *Flexion – Extension gap during Total Knee Replacement Surgery* (Griffin et al., 2000)

The most popular surgical techniques to achieve gap balance are balanced resection and measured resection and they have been already described in the previous

paragraph. However, after the gap balancing procedure, surgeons manually apply a varus-valgus moment to the joint to evaluate the relative tightness or laxity of the soft tissues and assess coronal plane balance. Based on this and on a following subjective assessment of the flexion-extension movement, if balance has not been achieved, the tightest among the ligaments of the knee is released (Unitt et al., 2008). Increasing the size of the flexion and extension gap after extensive releasing procedure may alter the alignment (Yoshii et al., 1991) and adversely affects the clinical outcome (Martin and Whiteside, 1990). Many surgical devices have been developed to assist the balancing in TKR, including spacers (D'Lima et al., 2007), tensors (Insall et al., 1985), electronic instrument (Miller et al., 2001). Tensors and spacers, are used to replace trial prosthesis implant during TKR (Freeman et al., 1978; Insall et al., 1985), whereas electronic devices are sensors that measure the pressure in the medial and lateral compartments (Fetto et al., 2011). All the above methods focus on the frontal plane with the aim of creating the desired varus-valgus stability and produce an even distribution of the forces on the medial and lateral compartments. Despite all the improvements allowed by these techniques, intraoperative tension is still usually judged subjectively (Matsuda et al., 2005) and soft tissue balancing is still completely based on the surgeon's subjective criteria. The creation of new tools able to help the surgeon is crucial for the reduction of these soft tissue related complications and for the minimization of the number of revision procedures after TKR.

2.4.5 Preoperative Planning for TKR

Since the first conventional TKR (cTKR) surgeries in the seventies, the primary objective was to increase the accuracy of the placement of the artificial components on the patient. One of the crucial aims in TKR is to place the femoral component perpendicular to the mechanical axis of the leg in the frontal plane. Failure to do so may adversely affect the long term outcome of TKR (Bäthis et al., 2004; Blakeney et al., 2011; Narkbunnam and Chareancholvanich, 2012). Many studies have demonstrated that the effect of misalignment in the frontal plane, exceeding the 3 degrees, may lead to a premature failure of the implant caused by component loosing due to an inaccurate kinematics (Jeffery et al., 1991; Moreland, 1988; Rand and Coventry, 1988).

To overcome these complications, computer assisted navigation (CAS) in TKR was introduced to minimize the number of these outliers in misalignment and component loosing (Figure 2.18). Navigation consists of three elements: computer, motion capture system, and rigid body marker (Bae and Song, 2011). The tracking system visualizes the rigid body markers attached on the patient's bone, and tracks their motion with the help of computer processing within the three dimensional space.

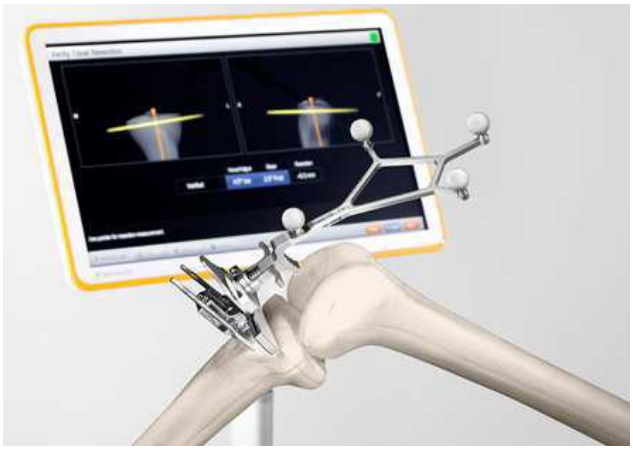

Figure 2.18 - *CAS system*

This technique successfully improved the accuracy (Delp et al., 1998; Dutton et al., 2008; Dutton and Yeo, 2009; Mason et al., 2007; Victor and Hoste, 2004) achieving a more accurate postoperative alignment through more precise and reproducible bony resection and ligament balancing. However, the CAS has some important limitations, such as an increased risk of complications due to the pin attached to the bone (Bonutti et

al., 2008; Novicoff et al., 2010), that slowed the wide application in the clinical routine. Furthermore, the procedure is longer than the cTKR with higher cost, for all these reasons many surgeons didn't adopt the CAS, at the price of having a less accurate postoperative alignment. More importantly many published studies have not found statistically significant differences between CAS and cTKR based on the Knee Society score (KSS), Western Ontario and McMaster Universities Osteoarthritis Index (WOMAC) or University of California Los Angeles activity score (UCLA). Only one prospective study (Chin et al., 2005) reported better five-year KSS results in the CAS TKA group.

Patient-specific instrumentation (PSI) for total knee replacement was introduced in the market few years ago as a sub category of CAS. PSI is characterized by a complex three-dimensional preoperative planning based on computed tomography (CT) or magnetic resonance images (MRI). Based on the specific manufacturers' software along with the other inputs from the surgeon, custom disposable patient-specific cutting blocks are manufactured to assure an accurate resection of the bone (Figure 2.19).

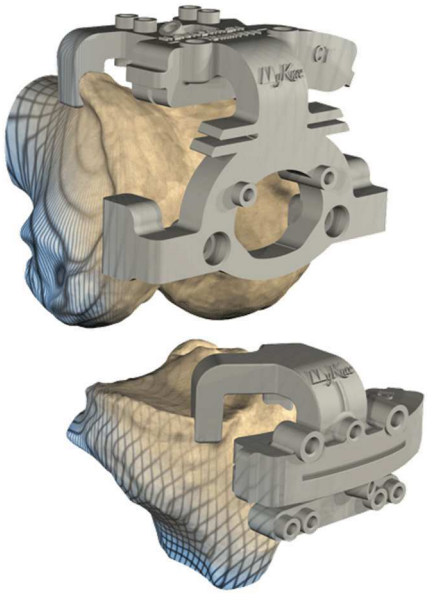

Figure 2.19 – *Preoperatively planned cutting blocks*

In the preplanning protocol the surgeon can change a set of parameters about the orientation of the cutting planes and the depth of cuts on femoral and tibial sides, respectively. The pre-operative parameters that can be adjusted by the surgeon are:

- Femur Varus/Valgus
- Tibia Varus/Valgus

- Tibial slope
- External rotation

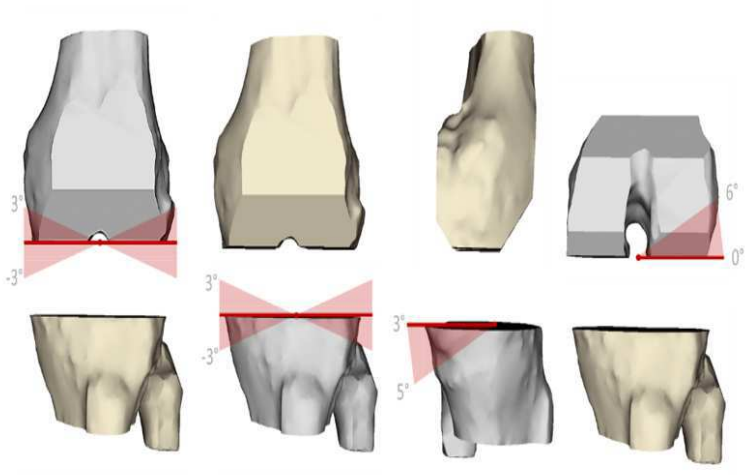

Figure 2.20 – *Surgical variables (from left): varus-valgus femur, varus-valgus tibia, tibial slope, external rotation femur*

The cutting blocks are meant to fit accurately the bone surface, assuring a better alignment of the cuts to the mechanical axes compared to the generic jigs used in the cTKR. The advantages of using the PSI TKR is meant to be a faster, more accurate, and cost effective surgery due to the reduction of numbers of trays used during the surgery. In fact, pre-operative planning with three-dimensional models obtained from medical images, aims to assess the size and orientation of the implants to be used, thereby ensuring that components of the correct size are available during the surgery. It's important to notice that the medical images needed to perform a TKR preoperative planning is a low dose CT scan (Henckel et al., 2006), which limits the minimum the radiations on the patient and the cost of the exam. Also, this exam is routinely prescribed by the clinicians to assess the pathologic condition of the patient before the surgery (Mohanlal and Jain, 2009). Although many studies reported that the PSI TKR improved the accuracy of implant positioning compared with the cTKR, there are some issues that are matter for a debate. The limitations are mostly given by the fact that there are often some changes that deviate from the steps of the original preoperative planning. The causes that provoke the failure of the preoperative planning are many and it is likely that an experienced PSI surgeon can make fewer changes during the surgery, but this factor can never be eliminated completely. However, many studies have reported that the surgery time is effectively shorter only without considering the time for the pre-operative planning, which is usually considered as the central part of the procedure.

In the literature there are many studies that compared the three techniques and the results are very controversial (Chin et al., 2005; Hoffart et al., 2012; Manzotti and Confalonieri, 2013). Therefore, to understand the performance of the preoperative planning for PSI the outcomes of patients divided by three groups were compared: cTKR, CAS TKR, and PSI TKR. The three groups have been compared respect to:

a) Postoperative alignment
b) Intraoperative advantages
c) Surgical time
d) Cost savings

a) The postoperative alignment has been evaluated in a retrospective randomized study of Noble et al. (2012) of 15 PSI and 14 cTKR, reporting a significantly better mechanical axes alignment with PSI with respect to cTKR (1,7 deg versus 2,8 deg, respectively). On the other hand, Barret et al. found no difference in component alignment and mechanical axes restoration between the three groups, Nunley et al. (Nunley et al., 2012), Victor et al. (Victor and Hoste, 2004), arrived at same conclusion. However, it must be said that cTKR and CSA TKR align the component respect to the mechanical axis, which is the line that connects the centre of hip, knee, and ankle, respectively. The PSI TKR instead, has the unique ability to align the prosthesis with respect to the kinematic axis, achieving better results in terms of malposition of the components (Dossett et al., 2012; Nogler et al., 2012) and ligament balancing (Walker et al., 2014). The benefits of having the components aligned to the mechanical axes are better range of motion, less instability, less stiffness, and less pain in the postoperative rehabilitation (Howell et al., 2013). Howell et al. in a prospective study of 198 patients that underwent to a PSI TKE, reported no failure and high functional recovering after 28 months in 75% of the cohort. However, the assessment of restoration of the mechanical/kinematic axes needs to be further evaluated in order to understand the real validity of the PSI TKR.

b) There are different factors to be considered in the intraoperative advantages. The length of incision is definitely smaller in the PSI TKR because the jigs used to cut the bones are less invasive, Nobles et al. (Noble et al., 2012) reported a decrease in skin incision compared to the cTKR (136 mm PSI TKR, 151.8 mm cTKR, p=0.014). Although the size of the tibial and femoral component is based on CT

images or MRI, many studies reported a mismatch during the surgery. Vunderlinckx et al. (Vundelinckx et al., 2013) reported a change in the femoral size in 19.4% of the 31 PSI TKR patients operated, Spencer et al. (Spencer et al., 2009) found no change required in the size of the femoral and tibial component. Conversely, Lusting et al. (Lustig et al., 2013) observed a change in the femoral size of 48% of the 45 PSI TKR patients and 50% in tibial size (to be rewritten). This discrepancy is mainly due to the fact that the surgeon adjusts the soft tissue balancing also changing the size of the components, obtaining e.g. a bigger gap between the femoral and tibial plane to balance the ligaments. Therefore, during the surgery one size below and one above the preplanned size, should be available in the trays. To balance the soft tissue or to adapt the changing in size of the implants, re-cuts of the bone maybe required. The PSI TKR procedure has a higher number of intraoperative re-cuts than the cTKR (Hamilton et al., 2013), mainly on the femur which is the most important cut. This may be due to the fact that to avoid an irreversible over resection of the bone, the preoperative planning tends to minimize the thickness obtained by the femoral cut, demanding a recut.

c) The aim of PSI TKR was to decrease the number of surgical steps eliminating the uncertainty of fitting the jigs (cTKR) or refereeing the cuts to external landmarks (CSA TKR). Nobles et al. reported a significantly reduction of the surgical time of PSI TKR respect to cTKR (121.4 versus 128.1 minutes), the CAS TKR is the longest procedure because of the placement of the markers on the patient's bone (Barrett et al., 2014). On the contrary, there are studies in literature (Hamilton et al., 2013; Roh et al., 2013) which report a comparable time between the two procedures, the loss of time was attributed to the change in plan needed for ligament balancing. The current literature review suggests that a deep knowledge and experience in using PSI TKR may ultimately improve the procedure in terms of surgical time.

d) The decrease of the overall costs of the procedure is the most effective benefits of the PSI TKR (Barrack et al., 2001; Watters et al., 2011). The use of patient-specific instrumentation reduces the number of trays used during the surgery, the turnover time is smaller, the number of personnel employed is decreased, and the cost of maintaining the inventory of both instruments and implants is minor. The shorter operation time allows the surgeon to have more surgeries per session with

less personnel employed, Watters et al. (Watters et al., 2011) reported in their study savings of 391$ per PSI TKR surgery with respect to the cTKR. The reduction is due to the operation time shorter of 13 minutes (101 $) and the employing of fewer trays (290 $). However, these studies don't include the cost of the imaging (CT or MRI) and the fabrication of the custom cutting blocks (Barrack et al., 2001). The PSI TKR is certainly a cost-saving procedure, however the savings don't justify the cost of the preoperative planning whenever there are some complications during the surgery or the patient undergo to a revision surgery. Only a significant reduction of the revisions surgery can ultimately admit the wide application of subject specific preoperative planning (Slover et al., 2012).

Conclusively, the advantages of using preoperative planning for TKR have attracted a lot interest, considering the results and the possibility to expand and improve further this surgical technique. However, currently available techniques that employs patient-specific instrumentation don't take into account the soft tissue balance, in fact the femoral component rotation is place using the measured resection method. This might represent a limitation because this approach might have less accuracy in placing the femoral component when compared to the gap-balancing results. (Dennis et al., 2010; Fehring et al., 2001).

2.4.6 Myknee® Medacta – Preoperative Planning for TKR

Medacta International SA is world-leading manufacturer of orthopaedic implants, neurological system, and instrumentation. The company has been founded in 1999 and the fast growth in the past years is due to the revolutionary approach in standard of care breakthroughs in hip replacement with the AMIS system and total knee replacement with MyKnee preoperative planning system technology. In 2013 Medacta documented 110.000 AMIS technique surgical procedure for hip arthroplasty and 15.000 procedures performed via the MyKnee patient-specific technology. Nowadays the Medacta group, based in Switzerland, operates in 30 countries worldwide.

MyKnee® – Patient Matched Technology

MyKnee® is the preoperative planning system which allows the manufacturing of subject-specific cutting blocks (Figure 2.20) to be used in the surgery. The surgeon can visualize and assess the 3D planning based on CT or MRI through the Medacta website. All the MyKnee® workflow is managed in house by Medacta, which provides constant assistance to the surgeon thanks to a dedicated personal technician.

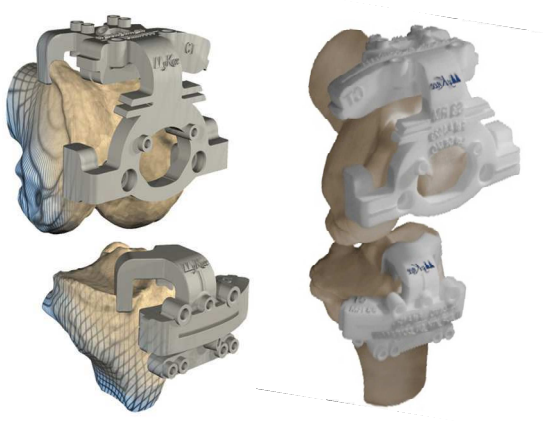

Figure 2.21 - *Medacta® cutting blocks*

This system is a versatile tool available for total knee replacement and uni-compartimental knee replacement, it permits to have a preoperative planning based on different surgical techniques such as bone referencing (MyKnee®), ligament balance based (MyKnee® LBS).

The MyKnee® workflow comprehends (Figure 2.21):

1) The MRI or low dose CT scan images of the patient's leg is uploaded on the Medacta portal
2) Starting from the 3D reconstruction of the bone morphology the surgeon can modify a set of orientation parameters for the placement of the implant
3) A virtual positioning of the implant is proposed to the surgeon who can further modify the planning
4) Once the planning has been validated by the surgeon, the in-house manufacturing process starts

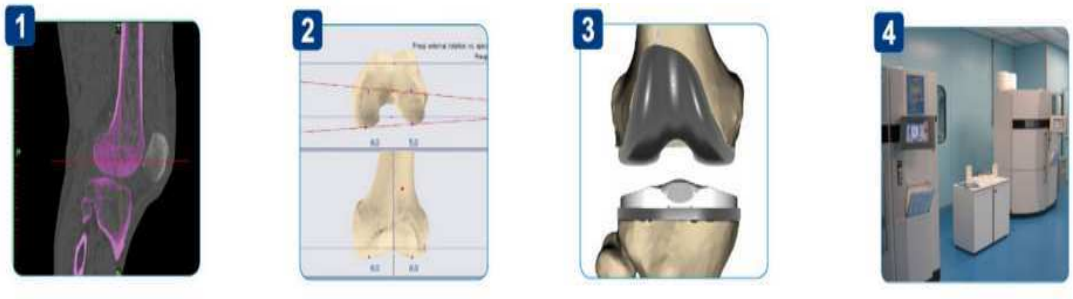

Figure 2.22- *MyKnee® workflow - 1) The MRI or CT images upload on the Medacta portal 2) Starting from the 3D reconstruction of the bone morphology, the surgeon can modify a set of parameters for the placement of the implants 3) A virtual positioning of the implant is proposed to the surgeon who can further modify the planning 4) Once the planning has been validated by the surgeon, the in-house manufacturing process starts.*

The Medacta's protocol requires a low dose CT scan (Figure 2.22) of hip, knee, and ankle separately, this minimizes the exposition of the patient to the x-rays.

Figure 2.23 – *Typical low dose CT scan for the MyKnee® workflow*

The recommended settings for the CT scan images are (Table):

	Ankle and Hip	Knee
Rows x Columns	512 x 512 pixels	512 x 512 pixels
Slice thickness	2 - 4mm	0.5 - 1mm
Spacing between slices	2 - 4mm	0.5 - 1mm
FOV	Max 200mm	Max 200mm

Table 2.2 – *CT scan image settings for MyKnee® workflow*

This procedure accesses the base to create the custom cutting blocks that can fit the subject-specific knee morphology without using any alignment jig to position them during the surgery. The cutting blocks guide the femoral and tibial cut planned by the surgeon during the pre-operative planning phase in order to re-establish a proper kinematic of the knee after the surgery. The crucial part of the preoperative planning is the adjustment of the orientation parameters in the MyKnee® user interface (Figure 2.22). The interactive 3D web planning is based on the surgeon's specific preferences and allows the changing the position of the implants. The surgeon can change the orientation parameters during the preoperative planning, before the creation of the anatomical cutting blocks. The surgeon can change the orientation parameters during the preoperative planning, before the creation of the anatomical cutting blocks. The surgeon can change the orientation parameters during the preoperative planning, before the creation of the anatomical cutting blocks.

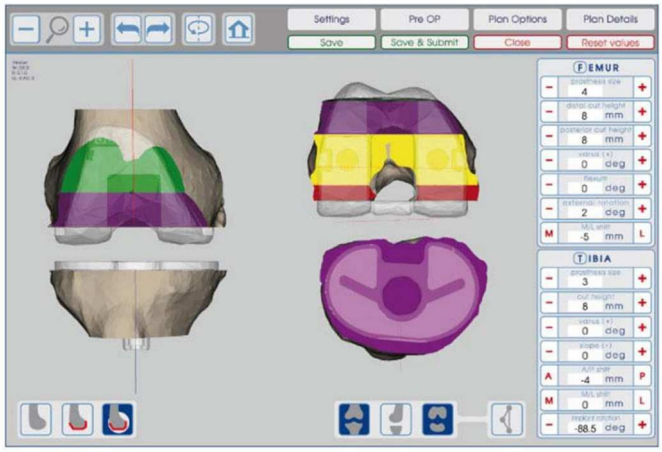

Figure 2.24 - *MyKnee® 3D planning user interface*

The orientation parameters, called surgical variables in this dissertation, are:

1) the varus-valgus femur cutting plane orientation on the frontal plane (from -3º to 3º degrees, with a step of 1º)
2) the varus-valgus tibia cutting plane orientation on the frontal plane (from -3º to 3º degrees, with a step of 1º)
3) the external rotation femur condyle cutting plane orientation on the frontal plane (from 0º to 6º, with a step of 1º)
4) the posterior slope tibial cutting plane orientation on the sagittal plane (from 3º to 5º, with a step of 1º)

The surgeon can change the orientation parameters during the preoperative planning, before the creation of the anatomical cutting blocks. Once these parameters are inspected and eventually corrected, the surgeon sends online the confirmation for manufacturing and delivering of the surgical instrumentation and also the plastic models of femur and tibia bones. The surgeon uses this personalized instrumentation before the bones cut trying the anatomical cutting blocks on the plastic model for examination. Afterward, the cutting guides can be placed to the patient in the same manner until a good fit is obtained. In addition, after the cut, the surgeon can compare the amount of bone removed using the resection line on the plastic model.

The MyKnee® pre-operative procedure assists the surgeon to re-establish the preoperative kinematic of the knee after the surgery. The achievement of mechanical stability, and the alignment of the joint, realizes performing the correct alignment of the mechanical axes between femur and tibia.

2.5 Computational Knee Models

2.5.1 Overview knee joint models

The number of studies that have investigated the computational modelling of the human knee is massive. The knee is one of the largest and more complex joint forming the musculoskeletal system, and given its central role in locomotive activities, is also subject to a large variety of injuries and degenerative pathologies. Understanding the mechanics and the forces placed on the knee structures might lead to understand the causes and improve surgical techniques such as the TKR. The study of the biomechanics of the knee has started in the first decade of the 19th century; however, the first models available in the literature (Goodfellow and O'Connor, 1978) that attempted to describe the function of the knee, were published only in the seventies. In the recent years a lot of studies have been conducted to understand the knee biomechanics and in literature there are different approaches: kinematic, static-kinetostatic, and dynamic models. In literature dynamic models of the knee are often embedded in a total body or lower limb dynamic musculoskeletal models, for this reason this matter will be discussed in a separated section in this chapter.

The kinematic models were entirely based on the physical description of the knee anatomy considering passive conditions and unloaded state (Goodfellow et al., 1978). The hypothesis behind this theory lies on the fact that when the external forces applied to the knee are negligible, the passive motion is balanced by the major passive structures and the particular shape of the contact surfaces within the range of motion. This theory is better known as the four-bar linkage mechanism (Levitskii et al., 1972; Sancisi et al., 2009), and it is composed by two crossed bar which are fixed at one end, and connected by a coupler in the other. The length of these bars is equal to the length of the anterior and posterior cruciate ligaments. Since this model is in 2D, more complex models have been developed to analyses forces and movement out of the sagittal plane. In particular, these models didn't take into account all the movements coupled with the flexion extension of the knee such as the tibial rotation. Parenti Castelli (2004) developed several models based on the theory of spatial equivalent mechanism. The rigid bodies are connected through different constraints that represent the passive structures of the knee. For example, describing the passive motion of the human ankle joint (Di Gregorio et al., 2007) the ligaments were considered as two bars given the isometric behaviour of the fibres throughout the entire range of motion. Sancisi et al. (2011) developed a new

mechanism including the patella that simulates the passive knee motion and it is simpler from a mechanical point of view. This knee 3D model of the patella-femur relative motion is combined with a previous simplified model of the femur-tibia relative motion, providing a new methodology to improve the design of the prosthetic implants (Sancisi and Parenti-Castelli, 2011a).

A second approach has been developed in the literature, describing the knee motion as a set of equations including the equilibrium equations of the system along with the mathematical representation of the passive structure and contact surfaces (Blankevoort et al., 1991). The description of the motion of the tibia with respect to the femur has been conducted in many models considering rigid or deformable bodies. The mathematical description of the articular surfaces is realized approximating the anatomical curvature of the bones with simple geometries such as sphere, planes, or cylinders. Advanced technique such as the B-spline least square fitting surface allows the approximation of more complex contacting surfaces (Ma and Kruth, 1995; Parenti-Castelli et al., 2004; Sancisi and Parenti-Castelli, 2011b). In many studies the patella was not included in the knee model, analyzing only the movement of the femur with respect to the tibia. However, Sancisi and Parenti-Castelli (2011) developed a one degree of freedom knee model, that took into account the relative motion of the patella and the femur, where the ligaments were modeled as isometric rigid links. The accuracy results of this study was validated performing experimental tests.

The second static approach is largely used in the literature and when the forces are not taken into account and the model is defined as static (Blankevoort et al., 1991). In the static configuration the positions of the rigid bodies are determined through the definition of a three dimensional reference system and the transformations are represented by 4x4 matrices. In homogeneous coordinates:

$$\left[\begin{array}{ccc|c} r_{11} & r_{12} & r_{13} & t_x \\ r_{21} & r_{22} & r_{23} & t_y \\ r_{31} & r_{32} & r_{33} & t_z \\ 0 & 0 & 0 & 1 \end{array}\right]$$

The 3x3 submatrix represented by the *r*-scalar coefficients represents the rotation matrix while the 3x1 *t*-vector describes the translation vector in the specified 3D reference system. The rotation matrix is descripted as a composition of 3 elementary rotations

around the Cartesian axis called Euler angles. Sometime these angles are also referred as *yaw/pitch/roll*. The three Euler angles are:

$$\theta_x = atan2(r_{32}, r_{33})$$

$$\theta_y = atan2(-r_{31}, \sqrt{r_{32}^2 - r_{33}^2}$$

$$\theta_z = atan2(-r_{21}, -r_{11})$$

Given the three angles θ_x, θ_y, θ_z the rotation matrix R is calculated as follows:

$$X = \begin{bmatrix} 1 & 0 & 0 \\ 0 & \cos\theta_x & -\sin\theta_x \\ 0 & \sin\theta_x & \cos\theta_x \end{bmatrix}$$

$$Y = \begin{bmatrix} \cos\theta_y & 0 & \sin\theta_y \\ 0 & 1 & 0 \\ -\sin\theta_y & 0 & \cos\theta_y \end{bmatrix}$$

$$Z = \begin{bmatrix} \cos\theta_z & -\sin\theta_z & 0 \\ \sin\theta_z & \cos\theta_z & 0 \\ 0 & 0 & 1 \end{bmatrix}$$

$$R = ZXY$$

The position of the rigid bodies in the static model can be predicted considering the geometry and the forces that are considered constant throughout the simulation. Thus, this approach might result particularly relevant for TKR knee models where the geometry of the sliding surfaces that guides the motion are well defined. The development of these models allows the calculation of the length of structures such as the ligaments in particular positions within the range of motion. One of the main advantages of using a static approach is the modest computational cost given the known mathematical description of the knee model.

When the model follows a series of equilibrium states to reach the convergence and the inertial and viscous properties are neglected, it is defined as kinetostatic or quasi-static (Wismans et al., 1980). The forces and moments are equilibrated considering specific constraints at fixed flexion-extension angles, and this allow to understand some

complex function of the knee that comes from the contribution of passive structures such as the ligaments. The literature has emphasized the importance to investigate the behaviour of the passive structures in terms of force and deformation as a function of the knee angle (Blankevoort and Huiskes, 1996) and the contact forces between the femur and the tibia. The majority of the studies calculated the elongation of the ligaments given the experimental measurements of knee kinematics, measuring the distance between the femoral and tibial insertion point.

Other methods employed computational algorithms such as the finite element methods and elastic springs (Weiss and Gardiner, 2001) to obtain the deformation of ligaments applying different loading conditions at various flexion angles. The elastic springs approach has been adopted widely by the researcher given the high computational cost of the finite element method. The non-linear behaviour of the ligaments is characterized through non-linear springs that aim to represent the toe region of the force displacement curve (H. Bloemker, 2012; Weiss and Gardiner, 2001). The toe region occurs in the initial stretching of the fibre and it ends when the ligament becomes taut (Weiss et al., 2005) assuming a linear behaviour. In the linear region the ligament is represented as a linear spring with a stiffness parameters *k*. Many studies in literature have used non-linear one-dimensional spring expressed by the force-displacement curve (Baldwin et al., 2009; Franci et al., 2008; Ottoboni et al., 2010; Sancisi and Parenti-Castelli, 2011a, 2011c, 2010; Yang et al., 2010) to define the mechanical properties of the knee ligaments. Blankevoort et al. (Blankevoort et al., 1991) defined the zero-load length (l_0) as the length of the fibre when it first becomes taut, the reference length (l_r) as the length of the fibre at the reference position (knee is extended), and the reference strain (ε_r) as the strain at the reference position.

The force displacement curve is described by the following equations:

$$1) \qquad f = \begin{cases} \frac{1}{4} k \varepsilon^2 / \varepsilon_l & 0 \le \varepsilon \le 2\varepsilon_l \\ k(\varepsilon - \varepsilon_l) & \varepsilon > 2\varepsilon_l \\ 0 & \varepsilon > 0 \end{cases}$$

$$2) \qquad \varepsilon = \left(\frac{l - l_0}{l_0}\right)$$

where:

f = the tensile force of the ligament

k = the ligament stiffness

$2\varepsilon_l$ = the level at which the ligament moves from the non-linear region (toe region) to the linear region of the force-displacement curve

ε = the strain of the ligament

l = length of the ligament

This approach is relatively easy to implement in a knee model, however it employs generalized values of the reference strain, obtained from the literature, with the reference length to calculate the zero-load length. This method does not take into account the subject specific properties of the ligament, due to this the force and displacement values might be unlikely given the significant differences between different subjects. Some studies have represented the ligament structure as a single bundle fibre (Wismans et al., 1980), whereas others used more than one line to take into account the anatomical structures (Andriacchi et al., 1983; Bertozzi et al., 2007; Bloemker et al., 2012; Franci et al., 2008; Sancisi and Parenti-Castelli, 2011c, 2010). The use of a high number of bundles to describe the ligaments is widely adopted in literature and strictly correlated with the objective of the study, however in this approach the mechanics of the ligaments is rather complex and a higher number of parameters need to be defined. Since the definition of these soft tissue related parameters is very complex even when cadaveric data are available, the estimation of the same parameters for a living subject has an even greater source of error that effect the calculation of the ligament's force and displacement.

The quasi-static models developed in literature included also the contact forces between the femoral and tibial surface when the kinematics was not measured experimentally. In this case the ligaments forces are considered in concert with the contact forces to define the relative position of the bones that composes the knee. The contact between articular surfaces has been solved using methodologies of different complexity. The most used contact modelling is based on the assumption that the bodies are rigid and the contact surfaces can be approximated with 2D polynomials, 3D polynomials, or spheres and planes. However, this analytical approach neglects the possibility to evaluate the pressure distribution on the contact area, which is rather important in total knee replacement models. Also, the idealization of the contact doesn't take into account the real contact forces produced by the deformation of the compliant materials. Therefore,

one theory based on the Hertz contact theory has been developed to calculate forces and deformations of known geometries using the linear elasticity theory. On the other hand, the elastic foundation theory has been developed to compute the contact between more complex objects using triangular meshes that can represent the contact surfaces. This methodology implies that the bodies may be considered rigid but for a thin layer of elastic material of thickness *h*. As a result, a "bed of springs" on the surface (Johnson, 1985) of each body is obtained to produce the push-back forces generated during the contact. The springs represent an elastic layer of known thickness covering a rigid substrate on both bodies, where each spring is independent from its neighbours. The springs are defined by a stiffness *k*,

$$k = \frac{(1-p)\cdot E}{(1+p)\cdot(1-2p)\cdot h}$$

where:

E = Young's modulus

p = Poisson's ratio

h = thickness

The stiffness takes into account the material properties of the body to calculate the deformation caused by the contact and the magnitude of the force generated. This methodology allows to estimate the distribution of the pressure on the contact area, many studies have used this approach to understand the pressure on the prosthetic implants in order to reduce the wear of the plastic components (Jayabalan et al., 2007).

2.2.15 Computational Dynamic Musculoskeletal Models

The human movement is the direct result of the coordinated passive and active action of several anatomic structures that work together to ensure freedom of movement. The anatomic structures are the skeletal system and the muscles that represent the passive and active part, and they form the musculoskeletal system. The skeletal system provides the framework that allows the moment while the muscles provide the energy to move the joints. The ligaments create the joints that are links between bones, the tendons represent the attachment sites for the muscles. The muscles span across the skeletal system pulling our bones and joints into the exact position to perform different physical activities. For a selected movement of the joint the muscles are divided in agonists and antagonists, the first group produces force shortening the length while the antagonist provide stability to the movement lengthening the fibres (co-contraction mechanism). Many studies in literature have modelled the human musculoskeletal system through a number of rigid bodies interconnected by joints and spanned by musculotendon actuators that simulates the actions of the muscles.

Since the forces and moments that govern a musculoskeletal model cannot be measured directly *in vivo*, the biomechanical research community is strongly engaged in knee modelling and a number of recent papers made available in vivo measurements obtained from instrumented prostheses (Bergmann, 2008; D'Lima et al., 2012; Fregly et al., 2012; Westerhoff et al., 2009). Among them there is the free access database "orthoload" (www.orthoload.com) (Julius Wolff Institute- Charity Berlin, 2001) which made available the contact forces of hip, shoulder, knee, and vertebral body, obtained by patients instrumented with telemetric prosthesis. A more complete dataset has been released by the "Grand Challenge Competition to Predict In Vivo Loads" which provides the knee contact forces, motion capture data, ground reaction forces, EMG, fluoroscopy, and pre and post-operative computed tomography (CT) images. The availability of these *in vivo* measurements, in concert with the availability of software such NMS Builder (SCS srl, Italy) and OpenSim, allowed the research community to create and validate musculoskeletal models able to predict *in vivo* muscles and contact forces.

The availability of this *in vivo* measurement in mainly due to the development of an innovative implantable device that is able to detect accurately the forces produced by the contact of the knee and the tibia during dynamic activities (D'Lima et al., 2005; Kirking et al., 2006). D'Lima et al. (2005) instrumented a tibial prosthesis four force

transducers located at the four corners of the tibial tray, powered by external coil induction. These transducers were able to detect the total compressive forces on the tibial tray and the location of the centre of pressure. A microprocessor performed the processing of the signal that was transmitted through an antenna to an external receiver. The external receiver was connected to a computer for data acquisition and processing. The accuracy of the telemetry device was validated performing *ex vivo* and successively *in vivo* tests. The use of an instrumented prosthesis is extremely invasive, considering the number of components that composes the telemetric devices, for this reason the cohort of patients is very limited and this represents the main limitation.

The prediction of muscle forces represents a challenging task because the number of muscle is generally bigger than the joints' degrees of freedom. Many studies have proposed optimization theories to solve the distribution problem and simulate the loading conditions. Static optimization is usually employed to solve the indeterminate problem of equilibrating the inter-segmental joint loads using a number of actuators that exceeds the joint's degrees of freedom (Modenese et al., 2013). Martelli et al. (Martelli et al., 2015) have proposed an alternative stochastic modelling that produce a space of solutions in which the best force muscles recruitment strategy can be found to produce muscle and joint forces. The predicted muscle forces are usually evaluated using the surface electromyography (EMG), however this approach is debatable because of the complex relationship between the muscle forces and their EMG signals during dynamic activities (Erdemir et al., 2007). Thelen et al. (Thelen et al., 2014) developed a musculoskeletal model for the co-simulation of neuromuscular dynamics a knee joint mechanics during human walking. The contact between the femoral and the tibial surface has been modelled using the elastic foundation theory and the model was based on forward dynamic analysis. A computed muscle control algorithm (CMC) was used to modulate the muscle activations to track measured joint angle trajectories during level walking. Marra et al. (Marra et al., 2014) proposed a musculoskeletal modelling framework which comprehended two separate knee models, one employing the traditional hinge joint solved using an inverse dynamic, and another using an 11 degrees of freedom which was solved using a force dependent kinematics (FDK). The authors pointed out the importance to have a robust workflow to build a reliable subject-specific musculoskeletal architecture using advanced morphed techniques to scale the cadaver anatomy to a patient implanted with a telemetric prosthesis. Hast and Piazza (Piazza and Delp, 2001) represented the knee as a "dual-joint", the first joint was a typical idealized joint solved using an inverse

dynamic for the estimation of the muscle forces, the second joint was 12 degrees of freedom knee model based on forward dynamics with elastic foundation contact at the tibiofemoral and patella-femoral articulations. The paper of Manal et al. (Manal and Buchanan, 2013) employed an electromyogram-driven modelling approach to predict knee joint reaction forces for two different gait patterns (normal walking and medial thrust gait). The model evaluated the accuracy of the prediction of joint reaction forces with respect to the experimental data, not only for normal walking but also for novel gait patterns. The predictive capabilities of validated musculoskeletal models gained gradually clinical relevance because the possibility to validate the muscle forces and the ligament forces as indirect measurements of the joint reaction forces (Erdemir et al., 2007).

References

Aglietti, P., Buzzi, R., D'Andria, S., Zaccherotti, G., 1993. Patellofemoral problems after intraarticular anterior cruciate ligament reconstruction. Clin. Orthop. Relat. Res. 195–204. doi:10.1097/00003086-199303000-00025

Andriacchi, T.P., Mikosz, R.P., Hampton, S.J., Galante, J.O., 1983. Model studies of the stiffness characteristics of the human knee joint. J. Biomech. 16, 23–29. doi:10.1016/0021-9290(83)90043-X

Arms, S., Boyle, J., Johnson, R., Pope, M., 1983. Strain measurement in the medial collateral ligament of the human knee: an autopsy study. J Biomech 16, 491–496.

Arnoczky, S.P., Tarvin, G.B., Marshall, J.L., 1982. Anterior cruciate ligament replacement using patellar tendon. An evaluation of graft revascularization in the dog. J. Bone Joint Surg. Am. 64, 217–224.

Babazadeh, S., Stoney, J.D., Lim, K., Choong, P.F.M., 2009. The relevance of ligament balancing in total knee arthroplasty: how important is it? A systematic review of the literature. Orthop. Rev. (Pavia). 1, e26. doi:10.4081/or.2009.e26

Bae, D.K., Song, S.J., 2011. Computer assisted navigation in knee arthroplasty. Clin. Orthop. Surg. 3, 259–267. doi:10.4055/cios.2011.3.4.259

Baker, P.N., Deehan, D.J., Lees, D., Jameson, S., Avery, P.J., Gregg, P.J., Reed, M.R., 2012. The effect of surgical factors on early patient-reported outcome measures (PROMS) following total knee replacement. Bone Joint J. 94–B, 1058–1066.

Baldwin, M. a, Laz, P.J., Stowe, J.Q., Rullkoetter, P.J., 2009. Efficient probabilistic representation of tibiofemoral soft tissue constraint. Comput. Methods Biomech. Biomed. Engin. 12, 651–659. doi:10.1080/10255840902822550

Barrack, R.L., Schrader, T., Bertot, A.J., Wolfe, M.W., Myers, L., 2001. Component rotation and anterior knee pain after total knee arthroplasty. Clin. Orthop. Relat. Res. 46–55.

Barrett, W., Hoeffel, D., Dalury, D., Mason, J.B.B., Murphy, J., Himden, S., 2014. In-vivo alignment comparing patient specific instrumentation with both conventional and computer assisted surgery (CAS) instrumentation in total knee arthroplasty. J. Arthroplasty 29, 343–7. doi:10.1016/j.arth.2013.06.029

Bäthis, H., Perlick, L., Tingart, M., Lüring, C., Zurakowski, D., Grifka, J., 2004. Alignment in total knee arthroplasty. A comparison of computer-assisted surgery with the conventional technique. J. Bone Joint Surg. Br. 86, 682–687. doi:10.1302/0301-620X.86B5.14927

Bellemans, J., Vandenneucker, H., Vanlauwe, J., 2005a. (iv) Total knee replacement. Curr. Orthop. 19, 446–452. doi:10.1016/j.cuor.2005.09.007

Bellemans, J., Vandenneucker, H., Vanlauwe, J., 2005b. (iv) Total knee replacement, in: Current Orthopaedics. pp. 446–452. doi:10.1016/j.cuor.2005.09.007

Benjamin, M., Ralphs, J.R., 1997. Tendons and ligaments - An overview. Histol. Histopathol. doi:10.1016/B978-0-323-09138-1.00007-3

Berger, R.A., Crossett, L.S., Jacobs, J.J., Rubash, H.E., 1998. Malrotation causing patellofemoral complications after total knee arthroplasty., Clinical orthopaedics and related research.

Bergmann, G., 2008. Orthoload.com [WWW Document]. Charité Univ. Berlin. URL http://www.orthoload.com/?page_id=7

Berns, G.S., Hull, M.L., Patterson, H.A., 1992. Strain in the Anteromedial Bundle of the Anterior Cruciate Ligament Under Combination Loading. J. Orthop. Researrh 10167–176. doi:10.1002/jor.1100100203

Bertozzi, L., Stagni, R., Fantozzi, S., Cappello, A., 2007. Knee model sensitivity to cruciate ligaments parameters: A stability simulation study for a living subject. J. Biomech. 40. doi:10.1016/j.jbiomech.2007.02.018

Bhandari, M., Smith, J., Miller, L.E., Block, J.E., 2012. Clinical and economic burden of revision knee arthroplasty. Clin. Med. Insights. Arthritis Musculoskelet. Disord. 5, 89–94. doi:10.4137/CMAMD.S10859

Blakeney, W.G., Khan, R.J.K., Wall, S.J., 2011. Computer-assisted techniques versus conventional guides for component alignment in total knee arthroplasty: a randomized controlled trial. J. Bone Joint Surg. Am. 93, 1377–1384. doi:10.2106/JBJS.I.01321

Blankevoort, L., Huiskes, R., 1996. Validation of a three-dimensional model of the knee. J. Biomech. 29, 955–961. doi:10.1016/0021-9290(95)00149-2

Blankevoort, L., Kuiper, J.H., Huiskes, R., Grootenboer, H.J., 1991. Articular contact in a three-dimensional model of the knee. J. Biomech. 24, 1019–1031. doi:10.1016/0021-9290(91)90019-J

Bloemker, K.H., Guess, T.M., Maletsky, L., Dodd, K., 2012. Computational Knee Ligament Determined Zero-Load Lengths Modeling Using Experimentally 33–41.

Bonutti, P., Dethmers, D., Stiehl, J.B., 2008. Case report : femoral shaft fracture resulting from femoral tracker placement in navigated TKA. Clin. Orthop. Relat. Res. 466, 1499–502. doi:10.1007/s11999-008-0150-6

Bozic, K.J., Kurtz, S.M., Lau, E., Ong, K., Chiu, V., Vail, T.P., Rubash, H.E., Berry, D.J., 2010. The epidemiology of revision total knee arthroplasty in the United States. Clin. Orthop. Relat. Res. 468, 45–51. doi:10.1007/s11999-009-0945-0

Brodsky, B., Persikov, A. V., 2005. Molecular structure of the collagen triple helix. Adv. Protein Chem. doi:10.1016/S0065-3233(05)70009-7

Brooks, P., 2009. Seven cuts to the perfect total knee. Orthopedics 32. doi:10.3928/01477447-20090728-27

Callaghan, J.J., 2001. Mobile-bearing knee replacement: clinical results: a review of the literature. Clin. Orthop. Relat. Res. 221–225.

Chin, P.L., Yang, K.Y., Yeo, S.J., Lo, N.N., 2005. Randomized control trial comparing radiographic total knee arthroplasty implant placement using computer navigation versus conventional technique. J. Arthroplasty 20, 618–26. doi:10.1016/j.arth.2005.04.004

Colizza, W.A., Insall, J.N., Scuderi, G.R., 1995. The posterior stabilized total knee prosthesis. Assessment of polyethylene damage and osteolysis after a ten-year-minimum follow-up. J. Bone Joint Surg. Am. 77, 1713–20.

Cooper, C., Snow, S., McAlindon, T.E., Kellingray, S., Stuart, B., Coggon, D., Dieppe, P. a, 2000. Risk factors for the incidence and progression of radiographic knee osteoarthritis. Arthritis Rheum. 43, 995–1000. doi:10.1002/1529-0131(200005)43:5<995::AID-ANR6>3.0.CO;2-1

D'Lima, D.D., Fregly, B.J., Patil, S., Steklov, N., Colwell, C.W., 2012. Knee joint forces: prediction, measurement, and significance. Proc. Inst. Mech. Eng. H. 226, 95–102. doi:10.1177/0954411911433372

D'Lima, D.D., Patil, S., Steklov, N., Colwell, C.W., 2007. An ABJS Best Paper: Dynamic intraoperative ligament balancing for total knee arthroplasty. Clin. Orthop. Relat. Res.

463, 208–212. doi:10.1097/BLO.0b013e318150dc2c

D'Lima, D.D., Townsend, C.P., Arms, S.W., Morris, B. a., Colwell, C.W., 2005. An implantable telemetry device to measure intra-articular tibial forces. J. Biomech. 38, 299–304. doi:10.1016/j.jbiomech.2004.02.011

Das, S.K., Farooqi, A., 2008. Osteoarthritis. Best Pract. Res. Clin. Rheumatol. 22, 657–675. doi:10.1016/j.berh.2008.07.002

Delp, S.L., Stulberg, S.D., Davies, B., Picard, F., Leitner, F., 1998. Computer assisted knee replacement. Clin. Orthop. Relat. Res. 49–56.

Dennis, D.A., Komistek, R.D., Kim, R.H., Sharma, A., 2010. Gap balancing versus measured resection technique for total knee arthroplasty, in: Clinical Orthopaedics and Related Research. pp. 102–107. doi:10.1007/s11999-009-1112-3

Di Gregorio, R., Parenti-Castelli, V., O'Connor, J.J., Leardini, A., 2007. Mathematical models of passive motion at the human ankle joint by equivalent spatial parallel mechanisms. Med. Biol. Eng. Comput. 45, 305–313.

Dossett, H.G., Swartz, G.J., Estrada, N. a., LeFevre, G.W., Kwasman, B.G., 2012. Kinematically Versus Mechanically Aligned Total Knee Arthroplasty. Orthopedics 160–170. doi:10.3928/01477447-20120123-04

Dutton, A.Q., Yeo, S.-J., 2009. Computer-assisted minimally invasive total knee arthroplasty compared with standard total knee arthroplasty. Surgical technique. J. Bone Joint Surg. Am. 91 Suppl 2, 116–130. doi:10.2106/JBJS.H.01549

Dutton, A.Q., Yeo, S.-J., Yang, K.-Y., Lo, N.-N., Chia, K.-U., Chong, H.-C., 2008. Computer-assisted minimally invasive total knee arthroplasty compared with standard total knee arthroplasty. A prospective, randomized study. J. Bone Joint Surg. Am. 90, 2–9. doi:10.2106/JBJS.F.01148

Emmerson, K.P., Moran, C.G., Pinder, I.M., 1996. Survivorship analysis of the Kinematic Stabilizer total knee replacement: a 10- to 14-year follow-up. J. Bone Joint Surg. Br. 78, 441–5.

Englund, M., Guermazi, A., Lohmander, S.L., 2009. The Role of the Meniscus in Knee Osteoarthritis: a Cause or Consequence? Radiol. Clin. North Am. doi:10.1016/j.rcl.2009.03.003

Erdemir, A., McLean, S., Herzog, W., van den Bogert, A.J., 2007. Model-based estimation of muscle forces exerted during movements. Clin. Biomech. (Bristol, Avon) 22, 131–54. doi:10.1016/j.clinbiomech.2006.09.005

Fehring, T.K., Odum, S., Griffin, W.L., Mason, J.B., Nadaud, M., 2001. Early failures in total knee arthroplasty. Clin. Orthop. Relat. Res. 315–318. doi:10.1097/00003086-200111000-00041

Fetto, J.F., Hadley, S., Leffers, K.J., Leslie, C.J.D.O., Schwarzkopf, R., 2011. Electronic measurement of soft-tissue balancing. Bull. NYU Hosp. Jt. Dis. 69, 285–288.

Franci, R., Sancisi, N., Parenti-Castelli, V., 2008. A three-step procedure for the modelling of human diarthrodial joints, in: Proceedings of the RAAD 2008, 17th International Workshop on Robotics in Alpe-Adria-Danube Region. pp. 1–10.

Freeman, M.A., Todd, R.C., Bamert, P., Day, W.H., 1978. ICLH arthroplasty of the knee: 1968--1977. J. Bone Joint Surg. Br. 60–B, 339–344.

Freeman, M.A.R., Swanson, S.A. V, Todd, R.C., 1973. Total replacement of the knee using the Freeman-Swanson knee prosthesis. Clin. Orthop. Relat. Res. 94, 153–170.

Fregly, B.J., Besier, T.F., Lloyd, D.G., Delp, S.L., Banks, S. a., Pandy, M.G., D'Lima, D.D., 2012. Grand challenge competition to predict in vivo knee loads. J. Orthop. Res. 30, 503–513. doi:10.1002/jor.22023

Gallo, J., Goodman, S.B., Konttinen, Y.T., Wimmer, M.A., Holinka, M., 2013. Osteolysis around total knee arthroplasty: A review of pathogenetic mechanisms. Acta Biomater. doi:10.1016/j.actbio.2013.05.005

Gardiner, J.C., Weiss, J. a, Rosenberg, T.D., 2001. Strain in the human medial collateral ligament during valgus loading of the knee. Clin. Orthop. Relat. Res. 266–274. doi:10.1097/00003086-200110000-00031

Goodfellow, J., O'Connor, J., 1978. The mechanics of the knee and prosthesis design. J. Bone Jt. Surgery, Br. Vol. 60, 358–369.

Goodfellow, J.W., O'connor, J.J., Shrive, N.G., 1978. Prosthetic joint device.

Goodman, S.B., Lee, J., Smith, R.L., Csongradi, J.C., Fornasier, V.L., 1991. Mechanical overload of a single compartment induces early degenerative changes in the rabbit knee: a preliminary study. J. Investig. Surg. 4, 161–170.

Griffin, F.M., Insall, J.N., Scuderi, G.R., 2000. Accuracy of soft tissue balancing in total knee arthroplasty. J. Arthroplasty 15, 970–973. doi:10.1054/arth.2000.6503

Gunston, F.H., 1971. Polycentric knee arthroplasty. Prosthetic simulation of normal knee movement. J. Bone Joint Surg. Br. 53, 272–277. doi:10.1097/01.blo.0000214423.59829.04

H. Bloemker, K., 2012. Computational Knee Ligament Modeling Using Experimentally Determined Zero-Load Lengths. Open Biomed. Eng. J. doi:10.2174/1874230001206010033

Hafez, M. a, Chelule, K.L., Seedhom, B.B., Sherman, K.P., 2006. Computer-assisted total knee arthroplasty using patient-specific templating. Clin. Orthop. Relat. Res. 444, 184–192. doi:10.1097/01.blo.0000201148.06454.ef

Hamilton, W.G., Parks, N.L., Saxena, A., 2013. Patient-specific instrumentation does not shorten surgical time: A prospective, randomized trial. J. Arthroplasty 28, 96–100. doi:10.1016/j.arth.2013.04.049

Harner, C.D., Xerogeanes, J.W., Livesay, G. a, Carlin, G.J., Smith, B. a, Kusayama, T., Kashiwaguchi, S., Woo, S.L., 1995. The human posterior cruciate ligament complex: an interdisciplinary study. Ligament morphology and biomechanical evaluation. Am. J. Sports Med. 23, 736–745. doi:10.1177/036354659502300617

Heesterbeek, P., Keijsers, N., Jacobs, W., Verdonschot, N., Wymenga, A., 2010. Posterior cruciate ligament recruitment affects antero-posterior translation during flexion gap distraction in total knee replacement. An intraoperative study involving 50 patients. Acta Orthop. 81, 471–477. doi:10.3109/17453674.2010.501743

Heesterbeek, P.J.C., Jacobs, W.C.H., Wymenga, A.B., 2009. Effects of the balanced gap technique on femoral component rotation in TKA. Clin. Orthop. Relat. Res. 467, 1015–1022. doi:10.1007/s11999-008-0539-2

Henckel, J., Richards, R., Lozhkin, K., Harris, S., Rodriguez Baena, F.M., W Barrett, A.R., Cobb, J.P., Manager R W Barrett, P.A., 2006. Very low-dose computed tomography for planning and outcome measurement in knee replacement THE IMPERIAL KNEE PROTOCOL. J Bone Jt. Surg [Br] 8888, 1513–18. doi:10.1302/0301-620X.88B11

Hochberg, M.C., Yerges-Armstrong, L., Yau, M., Mitchell, B.D., 2013. Genetic epidemiology of osteoarthritis: recent developments and future directions. Curr. Opin. Rheumatol. 25, 192–7. doi:10.1097/BOR.0b013e32835cfb8e

Hoffart, H.-E., Langenstein, E., Vasak, N., 2012. A prospective study comparing the functional outcome of computer-assisted and conventional total knee replacement. J. Bone Joint Surg. Br. 94, 194–9. doi:10.1302/0301-620X.94B2.27454

Howell, S.M., Howell, S.J., Kuznik, K.T., Cohen, J., Hull, M.L., 2013. Does a kinematically aligned total knee arthroplasty restore function without failure regardless of alignment category? Knee. Clin. Orthop. Relat. Res. 471, 1000–1007. doi:10.1007/s11999-012-2613-z

Hungerford, D.S., Krackow, K.A., Kenna, R. V, 1989. Cementless total knee replacement in patients 50 years old and under. Orthop. Clin. North Am. 20, 131–145.

Hunter, D.J., Eckstein, F., 2009. Exercise and osteoarthritis. J. Anat. doi:10.1111/j.1469-7580.2008.01013.x

Hutton, C.W., 1993. Knee Meniscus: Basic and Clinical Foundations. Ann. Rheum. Dis. 52, 556.

Insall, J.N., Binazzi, R., Soudry, M., Mestriner, L.A., 1985. Total Knee Arthroplasty. Clin. Orthop. Relat. Res. 192.

Insall, J.N., Ranawat, C.S., Aglietti, P., Shine, J., 1976. A comparison of four models of total knee-replacement prostheses. J Bone Jt. Surg Am 58, 754–765.

Jayabalan, P., Furman, B.D., Cottrell, J.M., Wright, T.M., 2007. Backside wear in modern total knee designs. HSS J. 3, 30–34. doi:10.1007/s11420-006-9033-0

Jeffery, R.S., Morris, R.W., Denham, R. a, 1991. Coronal alignment after total knee replacement. J. Bone Joint Surg. Br. 73, 709–14.

Johnson, K.L., 1985. Contact Mechanics, Journal of the American Chemical Society. doi:10.1115/1.3261297

Julius Wolff Institute- Charity Berlin, 2001. Orthoload.com. http://www.orthoload.com/.

Kirking, B., Krevolin, J., Townsend, C., Colwell, C.W., D'Lima, D.D., 2006. A multiaxial force-sensing implantable tibial prosthesis. J. Biomech. 39, 1744–51. doi:10.1016/j.jbiomech.2005.05.023

Kuster, M.S., Stachowiak, G.W., 2002. Factors affecting polyethylene wear in total knee arthroplasty. Orthopedics 25, s235–s242.

LaPrade, R.F., Engebretsen, A.H., Ly, T. V, Johansen, S., Wentorf, F.A., Engebretsen, L., 2007. The anatomy of the medial part of the knee. J. Bone Jt. Surg. (American Vol. 89, 2000–2010. doi:10.2106/JBJS.F.01176

Lee, D.S., Song, E.K., Seon, J.K., Park, S.J., 2011. Effect of Balanced Gap Total Knee Arthroplasty on Intraoperative Laxities and Femoral Component Rotation. J. Arthroplasty 26, 699–704. doi:10.1016/j.arth.2010.06.005

Levitskii, N.I., Sarkissyan, Y.L., Gekchian, G.S., 1972. Optimum synthesis of four-bar function generating mechanism. Mech. Mach. Theory 7, 387–398. doi:10.1016/0094-114X(72)90048-1

Lonner, J.H., Siliski, J.M., Scott, R.D., 1999. Prodromes of failure in total knee arthroplasty. J. Arthroplasty 14, 488–492. doi:10.1016/S0883-5403(99)90106-7

Luo, C.F., 2004. Reference axes for reconstruction of the knee. Knee. doi:10.1016/j.knee.2004.03.003

Lustig, S., Scholes, C.J., Oussedik, S.I., Kinzel, V., Coolican, M.R.J., Parker, D. a., 2013. Unsatisfactory Accuracy as Determined by Computer Navigation of VISIONAIRE Patient-Specific Instrumentation for Total Knee Arthroplasty. J. Arthroplasty 28, 469–473.

doi:10.1016/j.arth.2012.07.012

Lyon, R.M., Woo, S.L., Hollis, J.M., Marcin, J.P., Lee, E.B., 1989. A new device to measure the structural properties of the femur-anterior cruciate ligament-tibia complex. J. Biomech. Eng. 111, 350–354. doi:10.1115/1.3168390

Ma, W., Kruth, J.P., 1995. Parameterization of randomly measured points for least squares fitting of B-spline curves and surfaces. Comput. Des. 27, 663–675. doi:10.1016/0010-4485(94)00018-9

Manal, K., Buchanan, T.S., 2013. An electromyogram-driven musculoskeletal model of the knee to predict in vivo joint contact forces during normal and novel gait patterns. J. Biomech. Eng. 135, 21014. doi:10.1115/1.4023457

Maniar, R.N., Singhi, T., 2014. Patient specific implants: scope for the future. Curr. Rev. Musculoskelet. Med. 7, 125–30. doi:10.1007/s12178-014-9214-2

Mannion, A.F., Kämpfen, S., Munzinger, U., Kramers-de Quervain, I., 2009. The role of patient expectations in predicting outcome after total knee arthroplasty. Arthritis Res. Ther. 11, R139. doi:10.1186/ar2811

Manzotti, A., Confalonieri, N., 2013. A Prospective Comparison of Patient Specific Instrumentation and Navigation in Unicompartimental Knee Replacement. Orthop. Proc. 95–B, 271.

Marra, M. a, Vanheule, V., Fluit, R., Koopman, B.H.F.J.M., Rasmussen, J., Verdonschot, N.J.J., Andersen, M.S., 2014. A Subject-Specific Musculoskeletal Modeling Framework to Predict in Vivo Mechanics of Total Knee Arthroplasty. J. Biomech. Eng. 137, 1–12. doi:10.1115/1.4029258

Marshall, J.L., Fetto, J.F., BOTERO, P.M., 1977. Knee ligament injuries: a standardized evaluation method. Clin. Orthop. Relat. Res. 123, 115–129.

Martelli, S., Calvetti, D., Somersalo, E., Viceconti, M., 2015. Stochastic modelling of muscle recruitment during activity. Interface Focus 5, 20140094–20140094. doi:10.1098/rsfs.2014.0094

Martin, J.W., Whiteside, L.A., 1990. The influence of joint line position on knee stability after condylar knee arthroplasty. Clin. Orthop. Relat. Res. 146–156. doi:10.1097/00003086-199010000-00021

Mason, J.B., Fehring, T.K., Estok, R., Banel, D., Fahrbach, K., 2007. Meta-Analysis of Alignment Outcomes in Computer-Assisted Total Knee Arthroplasty Surgery. J. Arthroplasty 22, 1097–1106. doi:10.1016/j.arth.2007.08.001

Matsuda, Y., Ishii, Y., Noguchi, H., Ishii, R., 2005. Varus-valgus balance and range of movement after total knee arthroplasty., The Journal of bone and joint surgery. British volume. doi:10.1302/0301-620X.87B6.15256

Michael, J.W.-P., Schlüter-Brust, K.U., Eysel, P., 2010. The epidemiology, etiology, diagnosis, and treatment of osteoarthritis of the knee. Dtsch. Arztebl. Int. 107, 152–62. doi:10.3238/arztebl.2010.0152

Miller, M.C., Berger, R.A., Petrella, A.J., Karmas, A., Rubash, H.E., 2001. Optimizing femoral component rotation in total knee arthroplasty. Clin. Orthop. Relat. Res. 38–45.

Mjoberg, B., Selvik, G., Hansson, L.I., Rosenqvist, R., Onnerfalt, R., 1986. Mechanical loosening of total hip prostheses. A radiographic and roentgen stereophotogrammetric study. J. Bone Jt. Surgery, Br. Vol. 68, 770–774.

Modenese, L., Gopalakrishnan, A., Phillips, A.T.M., 2013. Application of a falsification strategy to a musculoskeletal model of the lower limb and accuracy of the predicted hip

contact force vector. J. Biomech. 46, 1193–1200. doi:10.1016/j.jbiomech.2012.11.045

Mohanlal, P., Jain, S., 2009. Assessment and validation of CT scanogram to compare per-operative and post-operative mechanical axis after navigated total knee replacement. Int. Orthop. 33, 437–439. doi:10.1007/s00264-008-0639-3

Moreland, J.R., 1988. Mechanisms of failure in total knee arthroplasty. Clin. Orthop. Relat. Res. 49–64. doi:10.1097/00003086-198801000-00010

Narkbunnam, R., Chareancholvanich, K., 2012. Causes of failure in total knee arthroplasty. J. Med. Assoc. Thai. 95, 667–73.

Neogi, T., Zhang, Y., 2013. Epidemiology of Osteoarthritis. Rheum. Dis. Clin. North Am. doi:10.1016/j.rdc.2012.10.004

Noble, J.W., Moore, C. a., Liu, N., 2012. The Value of Patient-Matched Instrumentation in Total Knee Arthroplasty. J. Arthroplasty 27, 153–155. doi:10.1016/j.arth.2011.07.006

Nogler, M., Hozack, W., Collopy, D., Mayr, E., Deirmengian, G., Sekyra, K., 2012. Alignment for total knee replacement: A comparison of kinematic axis versus mechanical axis techniques. A cadaver study. Int. Orthop. 36, 2249–2253. doi:10.1007/s00264-012-1642-2

Novicoff, W.M., Saleh, K.J., Mihalko, W.M., Wang, X.-Q.Q., Knaebel, H.-P.P., 2010. Primary total knee arthroplasty: a comparison of computer-assisted and manual techniques. Instr. Course Lect. 59, 109–17.

Nunley, R.M., Ellison, B.S., Ruh, E.L., Williams, B.M., Foreman, K., Ford, A.D., Barrack, R.L., 2012. Are patient-specific cutting blocks cost-effective for total knee arthroplasty? Clin. Orthop. Relat. Res. 470, 889–894. doi:10.1007/s11999-011-2221-3

O'DRISCOLL, S.W., 1998. Current Concepts Review - The Healing and Regeneration of Articular Cartilage*. J. Bone Jt. Surg. 80, 1795–1812.

Ottoboni, a, Parenti-Castelli, V., Sancisi, N., Belvedere, C., Leardini, a, 2010. Articular surface approximation in equivalent spatial parallel mechanism models of the human knee joint: an experiment-based assessment. Proc. Inst. Mech. Eng. H. 224, 1121–1132. doi:10.1243/09544119JEIM684

Parenti-Castelli, V., Leardini, A., Di Gregorio, R., O'Connor, J.J., 2004. On the Modeling of Passive Motion of the Human Knee Joint by Means of Equivalent Planar and Spatial Parallel Mechanisms. Auton. Robots 16, 219–232. doi:10.1023/B:AURO.0000016867.17664.b1

Park, S.E., DeFrate, L.E., Suggs, J.F., Gill, T.J., Rubash, H.E., Li, G., 2006. Erratum to "The change in length of the medial and lateral collateral ligaments during in vivo knee flexion". Knee 13, 77–82. doi:10.1016/j.knee.2004.12.012

Parratte, S., Pagnano, M.W., 2008. Instability after total knee arthroplasty. Instr. Course Lect. 57, 295–304.

Piazza, S.J., Delp, S.L., 2001. Three-dimensional dynamic simulation of total knee replacement motion during a step-up task. J. Biomech. Eng. 123, 599–606. doi:10.1115/1.1406950

Pioletti, D., Rakotomanana, L., Leyvraz, P., 1999. Strain rate effect on the mechanical behavior of the anterior cruciate ligament-bone complex. Med. Eng. Phys. 21, 95–100. doi:S1350453399000284 [pii]

Pioletti, D.P., Rakotomanana, L.R., Benvenuti, J.F., Leyvraz, P.F., 1998. Viscoelastic constitutive law in large deformations: Application to human knee ligaments and tendons. J. Biomech. 31, 753–757. doi:10.1016/S0021-9290(98)00077-3

Proffen, B.L., McElfresh, M., Fleming, B.C., Murray, M.M., 2012. A COMPARATIVE

ANATOMICAL STUDY OF THE HUMAN KNEE AND SIX ANIMAL SPECIES. Knee. doi:10.1016/j.knee.2011.07.005

Quapp, K.M., Weiss, J. a, 1998. Material characterization of human medial collateral ligament. J. Biomech. Eng. 120, 757–763. doi:10.1115/1.2834890

Ranawat, A.S., Gupta, S.K., Ranawat, C.S., 2006. The P.F.C. sigma RP-F total knee arthroplasty: designed for improved performance. Orthopedics 29, S28–S29.

Ranawat, C.S., Luessenhop, C.P., Rodriguez, J.A., 1997. The Press-Fit Condylar Modular Total Knee System. Four-to-Six-Year Results with a Posterior-Cruciate-Substituting Design*. J Bone Jt. Surg Am 79, 342–348.

Rand, J. a, Coventry, M.B., 1988. Ten-year evaluation of geometric total knee arthroplasty. Clin. Orthop. Relat. Res. 168–73. doi:10.1097/00003086-198807000-00022

Roh, Y.W., Kim, T.W., Lee, S., Seong, S.C., Lee, M.C., 2013. Is TKA using patient-specific instruments comparable to conventional TKA? A randomized controlled study of one system knee. Clin. Orthop. Relat. Res. 471, 3988–3995. doi:10.1007/s11999-013-3206-1

Sancisi, N., Caminati, R., Parenti-Castelli, V., 2009. Optimal four-bar linkage for the stability and the motion of the human knee prostheses, in: Atti Del XIX CONGRESSO dell'Associazione Italiana Di Meccanica Teorica E Applicata. pp. 1–10.

Sancisi, N., Parenti-Castelli, V., 2011a. A New Kinematic Model of the Passive Motion of the Knee Inclusive of the Patella. J. Mech. Robot. 3, 41003. doi:10.1115/1.4004890

Sancisi, N., Parenti-Castelli, V., 2011b. A novel 3D parallel mechanism for the passive motion simulation of the patella-femur-tibia complex. Meccanica 46, 207–220. doi:10.1007/s11012-010-9405-x

Sancisi, N., Parenti-Castelli, V., 2011c. A sequentially-defined stiffness model of the knee. Mech. Mach. Theory 46, 1920–1928. doi:10.1016/j.mechmachtheory.2011.07.006

Sancisi, N., Parenti-Castelli, V., 2010. A 1-Dof parallel spherical wrist for the modelling of the knee passive motion. Mech. Mach. Theory 45, 658–665. doi:10.1016/j.mechmachtheory.2009.11.009

Schmalzried, T.P., Kwong, L.M., Jasty, M., Sedlacek, R.C., Haire, T.C., O'Connor, D.O., Bragdon, C.R., Kabo, J.M., Malcolm, A.J., Harris, W.H., 1992. The mechanism of loosening of cemented acetabular components in total hip arthroplasty. Analysis of specimens retrieved at autopsy. Clin. Orthop. Relat. Res. 60–78.

Seil, R., Pape, D., 2011. Causes of failure and etiology of painful primary total knee arthroplasty. Knee Surgery, Sport. Traumatol. Arthrosc. 19, 1418–1432. doi:10.1007/s00167-011-1631-9

Sharkey, P.F., 2002. Why are total knee arthroplasties failing today? Clin. Orthop. Relat. Res. 404, 7–13. doi:10.1097/01.blo.0000036002.13841.32

Slover, J.D., Rubash, H.E., Malchau, H., Bosco, J. a, 2012. Cost-effectiveness analysis of custom total knee cutting blocks. J. Arthroplasty 27, 180–5. doi:10.1016/j.arth.2011.04.023

Spencer, B. a., Mont, M. a., McGrath, M.S., Boyd, B., Mitrick, M.F., 2009. Initial experience with custom-fit total knee replacement: Intra-operative events and long-leg coronal alignment. Int. Orthop. 33, 1571–1575. doi:10.1007/s00264-008-0693-x

Stambough, J.B., Clohisy, J.C., Barrack, R.L., Nunley, R.M., Keeney, J.A., 2014. Increased risk of failure following revision total knee replacement in patients aged 55 years and younger. Bone Jt. J. 96–B, 1657–1662. doi:10.1302/0301-620X.96B12.34486

Stürup, J., Nimb, L., Kramhøft, M., Jensen, J.S., 1994. Effects of polymerization heat and monomers from acrylic cement on canine bone. Acta Orthop. Scand. 65, 20–23.

Taylor, W.R., Heller, M.O., Bergmann, G., Duda, G.N., 2004. Tibio-femoral loading during human gait and stair climbing. J. Orthop. Res. 22, 625–632. doi:10.1016/j.orthres.2003.09.003

Tew, M., Waugh, W., 1982. Estimating the survival time of knee replacements. J Bone Jt. Surg [Br] 64, 579–582.

Thelen, D.G., Won Choi, K., Schmitz, A.M., 2014. Co-simulation of neuromuscular dynamics and knee mechanics during human walking. J. Biomech. Eng. 136, 21033. doi:10.1115/1.4026358

Unitt, L., Sambatakakis, A., Johnstone, D., Briggs, T.W., 2008. Short-term outcome in total knee replacement after soft-tissue release and balancing. J Bone Jt. Surg Br 90, 159–165. doi:90-B/2/159 [pii]\n10.1302/0301-620X.90B2.19327

Victor, J., Hoste, D., 2004. Image-based computer-assisted total knee arthroplasty leads to lower variability in coronal alignment. Clin. Orthop. Relat. Res. 131–9. doi:10.1097/01.blo.0000147710.69612.76

Vundelinckx, B.J., Bruckers, L., De Mulder, K., De Schepper, J., Van Esbroeck, G., 2013. Functional and radiographic short-term outcome evaluation of the Visionaire system, a patient-matched instrumentation system for total knee arthroplasty. J. Arthroplasty 28, 964–70. doi:10.1016/j.arth.2012.09.010

Walker, P.S., Meere, P. a, Bell, C.P., 2014. Effects of surgical variables in balancing of total knee replacements using an instrumented tibial trial. Knee 21, 156–61. doi:10.1016/j.knee.2013.09.002

Walker, P.S., Yildirim, G., Arno, S., Heller, Y., 2010. Future directions in knee replacement. Proc. Inst. Mech. Eng. H. 224, 393–414. doi:10.1243/09544119JEIM655

Watters, T.S., Mather, R.C., Browne, J. a, Berend, K.R., Lombardi, A. V, Bolognesi, M.P., 2011. Analysis of procedure-related costs and proposed benefits of using patient-specific approach in total knee arthroplasty. J. Surg. Orthop. Adv. 20, 112–6.

Weiss, J.A., Gardiner, J.C., 2001. Computational modeling of ligament mechanics. Crit. Rev. Biomed. Eng. 29, 303–371.

Weiss, J.A., Gardiner, J.C., Ellis, B.J., Lujan, T.J., Phatak, N.S., 2005. Three-dimensional finite element modeling of ligaments: Technical aspects. Med. Eng. Phys. 27, 845–861. doi:10.1016/j.medengphy.2005.05.006

Wessinghage, D., 1991. Themistocles Gluck. 100 years artificial joint replacement. Z. Orthop. Ihre Grenzgeb. 129, 383–8. doi:10.1055/s-2008-1040261

Westerhoff, P., Graichen, F., Bender, A., Rohlmann, A., Bergmann, G., 2009. An instrumented implant for in vivo measurement of contact forces and contact moments in the shoulder joint. Med. Eng. Phys. 31, 207–213. doi:10.1016/j.medengphy.2008.07.011

Whiteside, L.A., Saeki, K., Mihalko, W.M., 2000. Functional medical ligament balancing in total knee arthroplasty. Clin. Orthop. Relat. Res. 45–57.

Winemaker, M.J., 2002. Perfect balance in total knee arthroplasty: the elusive compromise. J. Arthroplasty 17, 2–10. doi:http://dx.doi.org/10.1054/arth.2002.29321

Wismans, J., Veldpaus, F., Janssen, J., Huson, a, Struben, P., 1980. A Three-Dimensional Mathematical of the Knee-Joint. J. Biomech. 13, 677–685. doi:10.1016/0021-9290(80)90354-1

Woo, S.L.-Y., Gomez, M.A., Akeson, W.H., 1983. Mechanical properties along the medial collateral ligament. Trans Orthop. Res Soc 8, 7.

Woo, S.L.-Y., Hollis, J.M., Adams, D.J., Lyon, R.M., Takai, S., 1991. Tensile properties of the human femur-anterior cruciate ligament-tibia complex The effects of specimen age and orientation. Am. J. Sports Med. 19, 217–225.

Woo, S.L.-Y., Wu, C., Dede, O., Vercillo, F., Noorani, S., 2006. Biomechanics and anterior cruciate ligament reconstruction. J. Orthop. Surg. Res. 1, 2. doi:10.1186/1749-799X-1-2

Woo, S.L., Debski, R.E., Withrow, J.D., Janaushek, M. a, 1999. Biomechanics of knee ligaments. Am. J. Sports Med. 27, 533–543.

Woo, S.L., Gomez, M.A., Sites, T.J., Newton, P.O., Orlando, C.A., Akeson, W.H., 1987. The biomechanical and morphological changes in the medial collateral ligament of the rabbit after immobilization and remobilization. J Bone Jt. Surg Am 69, 1200–1211.

Woo, S.L., Orlando, C.A., Gomez, M.A., Frank, C.B., Akeson, W.H., 1986. Tensile properties of the medial collateral ligament as a function of age. J Orthop Res 4, 133–141.

Woo, S.L.Y., Abramowitch, S.D., Kilger, R., Liang, R., 2006. Biomechanics of knee ligaments: Injury, healing, and repair. J. Biomech. doi:10.1016/j.jbiomech.2004.10.025

Yagi, M., Wong, E.K., Kanamori, A., Debski, R.E., Fu, F.H., Woo, S.L.-Y., 2002. Biomechanical analysis of an anatomic anterior cruciate ligament reconstruction. Am. J. Sports Med. 30, 660–666.

Yang, N.H., Canavan, P.K., Nayeb-Hashemi, H., Najafi, B., Vaziri, a, 2010. Protocol for constructing subject-specific biomechanical models of knee joint. Comput. Methods Biomech. Biomed. Engin. 13, 589–603. doi:10.1080/10255840903389989

Yoshii, I., Whiteside, L.A., White, S.E., Milliano, M.T., 1991. Influence of prosthetic joint line position on knee kinematics and patellar position. J. Arthroplasty 6, 169–177. doi:10.1016/S0883-5403(11)80013-6

Zatsiorsky, V.M., 2002. Kinetics of human motion, Spine.

Chapter 3

A procedure to estimate the origins and the insertions of the knee ligaments from computed tomography images

The chapter is based on the article:

Ascani, D., Mazzà, C., De Lollis, A., Bernardoni, M., Viceconti, M., 2015. A procedure to estimate the origins and the insertions of the knee ligaments from computed tomography images. J. Biomech. 48, 233–7.

This chapter aims to describe a repeatable and reproducible procedure to estimate the knee ligaments origin and insertion from computed tomography images. Although the knee ligaments are not visible on the CT images, they represent typically the only subject specific data available for a TKR preoperative planning. The estimation of these points on the patient's anatomy rely on the construction of a statistical registration atlas built on data that are based on cadaver specimens. Through an affine transformation between bony landmark clouds the knee ligament origin and insertion are calculated on the patient, the validation of this procedure was conducted on a dataset where both CT and magnetic resonance images (MRI) were available. This accuracy of this methodology is crucial because it will be representing one of the inputs of the knee models developed in the next chapters.

3.1 Introduction

The main role of the ligaments, which connect bone with bone, is to provide mechanical stability to the joints, guiding their movements and preventing excessive motion. The knee is the largest and complex joint of the human body and has four major ligaments: Medial Collateral (MCL), Lateral Collateral (LCL), Anterior Cruciate (ACL) and Posterior Cruciate (PCL). In clinical applications and biomedical research individualized musculoskeletal models are currently used for many purposes such as customized prosthetic implants (Bert, 1996; Reggiani et al., 2007), computer-aided surgery (Zanetti et al., 2005), gait analysis (Kepple et al., 1997) or automated image

segmentation (Ellingsen et al., 2010). In orthopaedic surgery a geometric model of the patient's bone can reproduce the basics morphometry in order to perform a correct computer based surgery (Radermacher et al., 1998). In gait analysis an accurate geometrical model is fundamental to create a realistic musculoskeletal model (Kepple et al., 1997).

Many computational dynamic models of the knee have been developed (Arnold et al., 2010; Blankevoort and Huiskes, 1996; Guess et al., 2013; Kia et al., 2014; Shelburne and Pandy, 2002) to understand the forces and the strains on the knee structures, such as the ligaments, during static and locomotion activities. Improving the accuracy of these models could help to discover the causes of ligaments' injury and guide the surgical treatment in order to improve the functional outcome (Woo et al., 2006). A subject specific model of the knee is also essential for total knee arthroplasty in the preoperative phase in order to assure the durability and the reliability of the joint implant especially for younger patient with a greater physical activity (Zanetti et al., 2005). The accurate estimation of the origin and insertion of these ligaments is a crucial step in all the above applications.

Subject specific models of the knee can be generated using information obtained either *ex vivo,* probing fresh cadavers, or from high resolution Magnetic Resonance Imaging (MRI). Brand et al. (1982) used measurement on three cadavers to obtain a set of lower extremity origin and insertion coordinates. These procedures are complex and cumbersome, therefore many studies utilized a few number of specimens, limiting the impact of the findings. In addition, the data obtained from cadavers have proven to be valid for modelling the knees they have been acquired for, but may likely not translate to other subjects (H. Bloemker, 2012). Many studies proposed methods to create subject specific model by scaling a generic template in order to measure inaccessible point such as the origin and insertions of the knee ligaments (Brand et al., 1982; Lewis et al., 1980). This procedure that involves the scaling of a generic template provides to build one cloud of palpable points on a cadaver specimen and corresponding points on the in vivo subject. Calculating the transformation between these two landmark clouds allows measuring inaccessible points.

The parameters needed to determine an affine transformation are a rotation matrix, a translation vector and a scaling factor. Lew and Lewis (1977) demonstrated that the application of data obtained from cadavers directly to *in vivo* subject is not suitable, some kind of scaling is proper because of the dimension differences between the in vivo

subject and the cadaveric specimens. Morrison (Morrison, 1970), in order to study the mechanics of knee joint in relation to normal walking, developed a technique to scale uniformly along the axes bony landmarks from dry bone data and an experimental subject. Lew and Lewis (1977) formulated a scaling technique that includes the Morrison method to scale inaccessible points from a dried bone specimen to an in vivo subject. This technique provides anisotropic scaling along three mutually orthogonal axes defined in both rigid bodies and is based on the use of four landmarks palpable on the subject and four on the corresponding specimen. The landmarks used to determine the rigid body transformation will contain some errors that come from the palpation of those points on the reference specimen and the experimental subject. Challis (Challis, 1995) suggested a procedure using a linear least-square method which attempted to take into account those errors. Unfortunately this method allows the calculation of the rigid body transformation parameters assuming that the scaling is uniform along the three axes. Anisotropic scaling technique has been presented by Lewis et al. (1980), using eight landmarks on both the specimen and the experimental subject, the results revealed that the anisotropic scaling was more accurate than the isotropic scaling.

In view of all that has been mentioned so far, it can be said that previous studies validated procedures that allow calculating inaccessible points on *in vivo* subjects using different osteometric scaling techniques. In these studies the analysis of human subject *in vivo* has been performed without using CT or MRI scan images. Since only a minimal set of skeletal landmarks can be palpated through external palpation, the number of the landmarks used in the previous methods was very low. Lewis et al. (1980) demonstrated that anisotropic scaling improves the identification of anatomical landmarks locations, particularly when a large number of points were used in the scaling. Also, a detailed description of the landmarks selected were not present in the previous studies, the lack of standard and well defined guidelines for the palpation of the these landmarks affects the accuracy of the rigid body registration (Van Sint Jan and Della Croce, 2005).

The purpose of this study was to create a procedure to estimate the origins and the insertions of the knee ligaments by: providing a reproducible and repeatable anatomical landmark cloud for virtual palpation, creating a registration atlas and using an affine transformation (rotation, translation, anisotropic scaling). The accuracy of this procedure will be assessed through comparison with results obtained from MRI.

3.2 Materials and Methods

The dataset used in this study (D1) has been provided by Medacta International SA (Castel S. Pietro, Switzerland). It consists of seven set of images obtained from seven different patients (64 ± 5 years) who have undergone a Total Knee Replacement. Each patient's dataset includes Computed Tomography (CT) and Magnetic Resonance Imaging (MRI) of pathological knee that underwent surgery and the bone geometries obtained by segmenting the CT data. In addition to D1, a second dataset (D2) has been obtained from the multibody models of the human knee project (Guess et al., 2013, 2010; H. Bloemker, 2012). These models are based on three cadaver knees (Table 3.1) that have been mechanically tested in a dynamic knee simulator. Knee geometries (bone, cartilage, and menisci) were derived from MRI and ligament insertions were obtained from both MRI and probing the cadaver knees. D2 also contains information on ligament modelling, including the origin and insertion locations.

	Age at death	*Gender*	*Right or Left*	*Height(in)*	*Weight(lbs)*
Knee #1	*77*	*Male*	*Right*	*70*	*220*
Knee #2	*55*	*Female*	*Left*	*67*	*160*
Knee #3	*78*	*Female*	*Right*	*65*	*130*

Table 3.1 – *Information regarding each cadaver knee used in this study to create the Registration Atlas*

The first part of this study aims at creating a reproducible and repeatable bone landmarks cloud to be palpated on CT scan images. A detailed standard description of body landmarks through manual or virtual palpation is available in literature (Van Sint Jan, 2007). Among these, a subset of landmarks (Figure 3.2) belonging to the knee, tibia and fibula has been chosen. This landmark cloud has then been identified on each subject dataset through virtual palpation. NMSBuilder (SCS srl, Italy) has been used to visualize the 3D geometry and to perform the virtual palpation (location of anatomical points over a 3D visualization) and the registration between the landmark clouds. The virtual palpation has been performed by four expert operators on both D1 and D2. Each operator performed the virtual palpation on ten knees (cases), repeating the operation three times for each knee (trials). Three operators performed the procedure using NMSBuilder, whereas the fourth one used an in-house tool developed by Medacta International SA. Reproducibility and repeatability were assessed using repeated measures analysis of variance (ANOVA). In particular, a repeated measure ANOVA was performed for each operator considering the "case" as between group factor and the "trial" (3 levels) as within

factor. Three separate ANOVA, one for each test, were then performed considering the operator as between group factor and the cases as within group factor (10 levels).

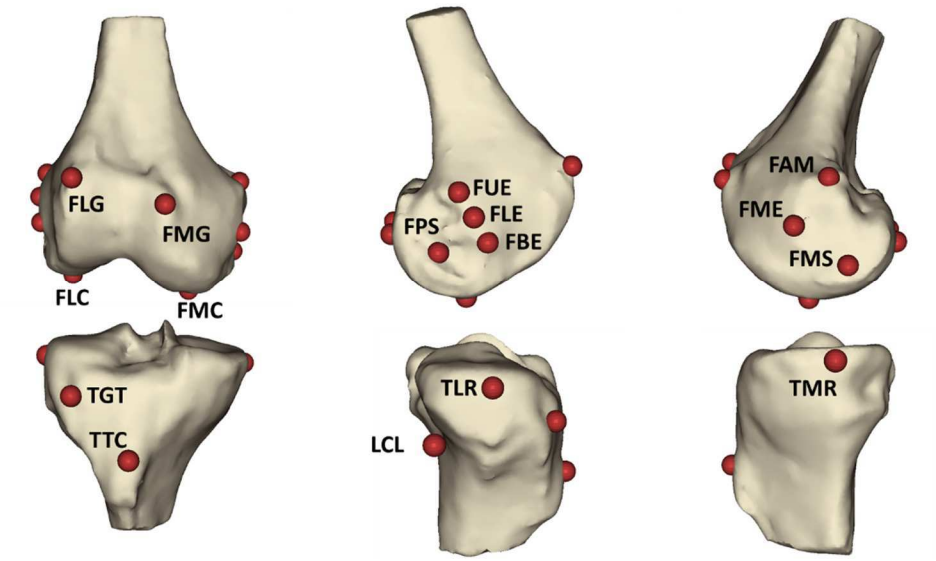

Figure 3.2 – *Set of landmarks selected using the "Color Atlas of Skeletal Landmark Definitions" (Serge Van Sint Jan 2007). FME- Medial Epicondyle, FAM-Tubercle of the Adductor Magnus muscle, FMS-Medial Sulcus, FLE- Lateral Epicondyle, center of tubercle, FUE-Lateral Epicondyle, FBE Lateral Epicondyle, FPS-Popliteal Sulcus, FLG-Antero-Lateral ridge of the patellar surface Groove, FMG-Antero-Medial ridge of the patellar surface Groove, FLC-Most distal point of the Lateral Condyle, FMC-Most distal point of the Medial Condyle, TLR-Lateral Ridge of tibial plateau, TMR-Medial Ridge of tibial plateau, TGT -Gerdy Tubercle, TTM-Tibia, Tuberosity medial edge, LCL-Attachment of the collateral Lateral Ligament*

Once reproducibility and repeatability of the bone landmarks had been assessed, they were palpated on D2 in order to create a reference landmark cloud (C_R), and on D1 in order to create a subject-specific landmark cloud (C_S). Once palpated, the two clouds had to be registered. An affine transformation was used to this purpose to take into account the differences between the landmarks cloud palpated on different subjects. The method that allows the calculation of the parameters that describe an affine transformation between two paired landmark clouds is called, in statistical shape analysis, *Procrustes Analysis* (Grimpampi et al., 2014). In particular, the affine transformation that maps C_R to C_S is composed by a 3x3 transformation matrix, which includes Translation ($T=\langle T_x, T_y, T_z\rangle$), Rotation ($R=\langle R_x, R_y, R_z\rangle$), and scaling ($S=\langle S_x, S_y, S_z\rangle$) parameters. This operation is implemented in Lhp Builder following the method proposed by Berthold and Horn (Horn, 1987). Once T, R and S are calculated, it is possible to register on C_S also those landmarks belonging only to C_R, which, in our case, are the origins and insertions of the four knee ligaments. The ensemble of C_R and of the eight origins and insertions of the knee ligaments composes the so-called Registration Atlas (*RA*). The error associated to the registration procedure is called Procrustes Distances (*PD*) and represents

the geometric distance between C_S and C_R. These values estimate the accuracy of the procedure.

The scaling operation, necessary to take into account anthropometric differences due to age or gender (Fehring et al., 2009), might have as a consequence the fact that landmarks in C_R are not always located on the bone surface. For this reason, a visual inspection needs to be performed after the registration and adjustments need to be taken. These adjustments were performed using an ad-hoc NMS Builder function, names "snap to surface", which allows to move the landmark along the axes characterized by the minimal distance from the closest surface. The repeatability of this operation has been assessed by having one operator repeating it for three times on each case in D1 (after having performed the calculation of the origins and insertions of the knee ligaments using the RA, as described in the following paragraph).

Using the three models from the D2 dataset, four atlases were created: one for each model and one as the average of the previous three (Atlas 1, Atlas 2, Atlas 3, and Atlas M). Not having a proper gold standard available, the four atlases have been compared in terms of Procrustes Distance between the landmarks of C_R registered on the subjects and the landmarks of C_S palpated on the seven subjects.

Once the best RA had been selected, it was used to estimate the origin and the insertions of the knee ligaments of all the cases in D1. Initially, the origin and insertions were calculated through the affine transformation using the CT scan, successively the verification of the positions of those landmarks has been performed using MRI scan where it was possible to estimate the ligaments attachments. In NMSBuilder, the landmarks that represented the origins and insertions of the ligaments were moved whenever the position was considered wrong in according with those images. Then, we compared the distances between the data obtained from the CT scan with those corrected with MRI. To compare the two measurements, the STLs segmented from CT and MRI were registered using a NMS Builder feature called "registration surface" that employs an algorithm based on the iterative closest point (ICP) technique (Besl and McKay, 1992). The ICP technique minimizes the differences between two rigid clouds of points and it results very accurate when the two points cloud have the same shape (Du et al., 2010). The registration errors of the seven patients of the dataset was lower than 1 mm, therefore it did not influence the comparison between the data obtained from the CT scan with those corrected with MRI

The PD distances between the origin and insertions of ligaments calculated with the Registration Atlas and those ones estimated from the MRI were used to run a sensitivity analysis for the estimation of the ligaments length. The estimate of the positions of ligament origins and insertions affect the estimate of the length of a ligament. For each subject, we have a measure of the error in the estimate of these points by comparing CT and MRI based predictions. We considered the standard deviation (SD) of the error found for each origin and insertion point as the expected possible variation of the position of a ligament's attachment. The value of this SD for a given subject is inserted in a sensitivity analysis as a reasonable error in the estimate of the LCL and MCL attachment points to have an indicator of how this would reflect on the ligament length estimate. We run this analysis for one subject (Subject 2), for whom we calculated the length of the ligament as the shortest geometrical distance between the relevant origins and insertions.

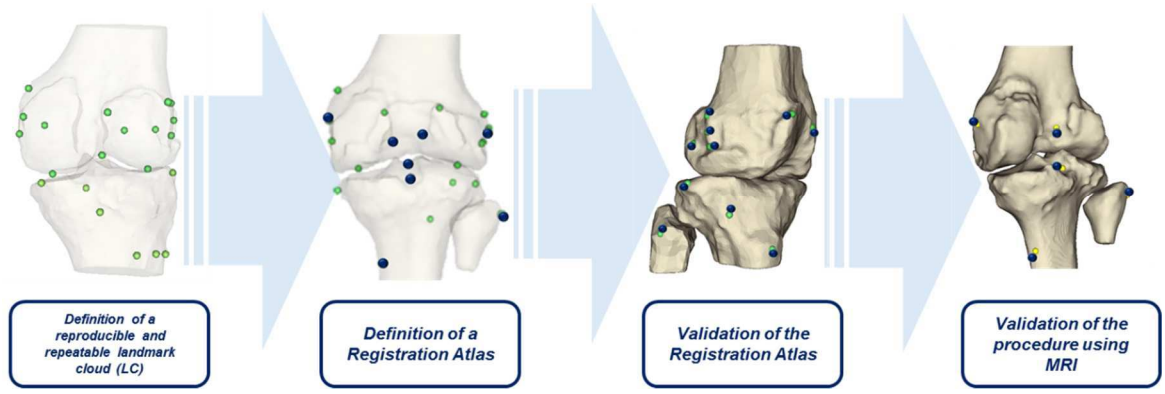

Figure 3.1 - *Schematic representation of the procedure: 1) Creation of a repeatable bone landmarks cloud palpable on CT scan images. 2) Definition of a reference landmarks cloud called Registration Atlas composed by reproducible and repeatable landmarks and the origin and insertion of the knee ligaments. 3) Validation of the RA 4) Calculation of the origin and insertion of the knee ligaments using CT scan and validation using MRI image*

3.3 Results

The results of the ANOVA performed on the data obtained from the various operators showed that the procedure is highly repeatable, with no significant differences observed within (*p=0.748* for trial 1, *p=0.966* for trail 2, and *p=0.992*, for trial 3, respectively) or between operators (*p=0.430* for operator 1, *p=0.572* for operator 2, *p=0.187* for operator 3, and *p=0.685* for operator 4, respectively). These findings suggest that changing the operator does not affect the repeatability and the reproducibility of the virtual palpation of the selected anatomical landmarks cloud. In contrast, the ANOVA revealed that the case factor influences the repeatability of the virtual palpation ($p<0.001$): the specific morphology of a knee or the low resolution of the CT images can be a cause for lower precision in the identification of the landmarks.

Since there was no between-operators effect, the precision of the virtual palpation was evaluated in terms of standard deviation of the landmarks positions, palpated by the four operators over the three trials. The standard deviation ranged from 0.02 mm to 7.71 mm (Table 3.2).

The registration of the four Atlases (Atlas 1, Atlas 2, Atlas 3, and Atlas M) on D2 revealed that the Atlas M gives the best result in terms of PD. The mean PD between the landmarks of C_R registered on the seven subjects, and the landmarks of C_S palpated on the seven subjects (Tables 3.3 and 3.4) was 2.34 ± 0.59 mm for the femur and 1.53 ± 0.50 mm for the tibia, respectively (averaged on the seven subjects).

Landmark	SD Min (mm)	SD Max(mm)
FLE	0.02	5.97
FBE	0.56	2.37
FUE	0.06	2.31
FME	0.38	5.30
FAM	0.16	3.02
FMC	0.08	3.04
FLC	0.04	1.74
FLG	0.16	2.67
FMG	0.06	3.18
FPS	0.23	7.71
FMS	0.31	6.46
TTC	0.1	7.67
TLR	0.03	4.72

TMR	0.11	3.99
TGT	0.22	3.91
LCL	0.03	1.38

Table 3.2 – *The table shows the precision of the landmark positions in terms of Standard Deviation.*

The mean Procrustes distances between the origin and insertions of ligaments calculated with the Registration Atlas M and those estimated from the MRI were 2,1 ± 1,2 mm (0,4 mm < *PD* < 3,9 mm) on the femur and 2,7 ± 1,0 mm (1,4 mm< *PD*< 4,4 mm) on the tibia (averaged over the seven subjects) (Tables 3.5 and 3.6). These results suggest that this procedure is able to calculate the position of the origin and the insertions of the knee ligaments that are rather close to the ones obtainable on the MRI. However, in this chapter the influence of this parameter on the knee motion has not been included, this matter will be extensively tackled in the next chapters.

The "snap to surface" operation was highly repeatable, with the standard deviation of the position of the ligament attachments after the "snap to surface" ranging from 0 to 0.3 mm.

	Mean Distance (mm)	Min (mm)	Max (mm)
SUBJECT 1	2,6 ± 0,8	1,8	4,2
SUBJECT 2	2,2 ± 0,9	1,1	4,5
SUBJECT 3	2,5 ± 1,8	0,3	5,8
SUBJECT 4	2,5 ± 1,6	0,2	5,1
SUBJECT 5	2,6 ± 2,3	0,7	7,3
SUBJECT 6	2,1 ± 0,8	0,7	3,3
SUBJECT 7	1,9 ± 1,1	0,6	4,2

Table 3.3 – *Registration Atlas registered on the seven subjects (femur)*

	Mean Distance (mm)	Min (mm)	Max (mm)
SUBJECT 1	2,1 ± 1,1	0,6	2,9
SUBJECT 2	1,9 ± 1,9	0	3,7
SUBJECT 3	1,1 ± 0,4	0,7	1,6
SUBJECT 4	2,1 ± 1,2	0,5	3,1
SUBJECT 5	1,0 ± 0,6	0,3	1,7
SUBJECT 6	1,3 ± 0,8	0,4	2,2
SUBJECT 7	1,2 ± 0,7	0,4	2,2

Table 3.4 – *Registration Atlas registered on the seven subjects (tibia)*

	Mean Distance (mm)	Min (mm)	Max (mm)
SUBJECT 1	2,5 ± 2,9	0,0	5,5
SUBJECT 2	1,3 ± 2,3	0,1	4,7
SUBJECT 3	3,9 ± 2,8	0,0	6,3
SUBJECT 4	3,1 ± 3,9	0,0	8,0
SUBJECT 5	2,1 ± 1,9	0,0	4,7
SUBJECT 6	0,4 ± 0,7	0,0	1,4
SUBJECT 7	1,3 ± 2,6	0,0	5,3

Table 3.5 – *Mean Distance between the insertion and the origin of the ligaments predicted and the ones estimated on the MRI images (femur)*

	Mean Distance (mm)	Min (mm)	Max (mm)
SUBJECT 1	4,4 ± 4,2	0,0	10,2
SUBJECT 2	2,6 ± 1,8	0,0	4,1
SUBJECT 3	2,5 ± 5,1	0,0	10,2
SUBJECT 4	/	/	/
SUBJECT 5	1,4 ± 1,7	0,0	3,2
SUBJECT 6	2,8 ± 5,6	0,0	11,3
SUBJECT 7	2,7 ± 3,1	0,0	6,1

Table 3.6 – *Mean Distance between the insertion and the origin of the ligaments predicted and the ones estimated on the MRI images (tibia). The subject 4 in not included in this comparison because the MRI data was incomplete*

The sensitivity analysis (Table 3.7) was performed on the Subject 2, having SD of 2.3 mm for the femur and 1.8 for the tibia. It led to an average variation in the estimate of 1.8 mm and 1.7 mm, which represented a variation of 3% and 2% of the ligament length, respectively.

	S1	S2	S3	S4	S5	S6	S7	S8	S9	S10	S11	S12	S13	S14	S15	S16	S17	S18	S19	S20	S21	S22	S23	S24	S25
LCL	52.6	53.3	51.9	50.9	54.2	51.8	52.4	51.3	50.2	53.5	53.4	54.2	52.7	51.8	55.0	54.6	55.2	54.0	52.9	56.2	50.6	51.3	49.9	49.0	52.2
MCL	79.6	79.4	79.9	78.0	81.3	80.0	79.7	80.3	78.3	81.6	79.3	79.1	79.6	77.7	81.0	81.6	81.4	81.9	80.0	83.3	77.6	77.4	77.9	76.0	79.3

Table 3.7 – *Sensitivity study performed on subject 2, all values are expressed in mm. Each of the 25 simulations corresponds to a combination of the possible different errors on origins and insertions.*

Since in the analysed dataset there are larger SD for the patients that may lead to higher length variations, this analysis will be repeated in the next chapter (Chapter 4), where these results are more relevant, including all the patients of the dataset.

3.4 Discussion

This study presented a procedure to estimate, with high accuracy, origins and insertions of the knee ligaments starting from a reproducible and repeatable landmark cloud virtually palpated on a CT scan. The proposed procedure has been evaluated through a comparison with the same estimations as obtained from MRI, which, as shown by Taylor et al. (2013) can be considered as a reliable reference.

Despite many studies have noted the importance of scaling anatomical landmarks from cadaveric specimen to calculate inaccessible points (Brand et al., 1982; Lew and Lewis, 1977; Lewis et al., 1980), we are not aware of other studies providing a methodology to estimate the knee ligaments attachments from a CT scan. Other methods proposed to create subject-specific musculoskeletal models, focused on the mathematical development of the scaling technique needed to estimate the coordinates of bone points not accessible through manual palpation. The results reported show that our methodology allows calculating the knee ligaments attachments with an average RMS error of 2.4 mm on the femur and 2.9 mm on the tibia. The relevance of these errors certainly depends on the practical use of the estimated quantities. A sensitivity analysis of their effects on the estimation of additional parameters, such as ligaments strain during dynamic tasks, could be the objective of further studies. Although our method doesn't have a match with other studies in literature, it is actually quite likely to hypothesize that 2.1 mm and 2.7 mm might be relevant errors when this information is used to estimate the ligaments strain and deformation during dynamic tasks. However, the sensitivity analysis revealed that our method leads to a variation of 2% of the ligament length considering the SD as input. Despite these values are very encouraging, a thorough analysis of this kind would require the development of a more realistic biomechanical model, this matter will be explained in the next chapter.

True accuracy of our estimates should be assessed with *ex vivo* studies. The only study that we are aware of proposing a methodology to estimate inaccessible points that have been validated in-vitro is the one by Kepple et al. (1998), who reported RMS errors of 6.6 mm on the femur and 5.8 mm on the tibia. In a very recent study Pellikaan et al. (2014) reported a mesh morphing based method which allows to estimate the muscle attachment sites of the lower extremity with a mean error smaller than 15 mm, as assessed through ex-vivo testing. This method is based on the assumptions that the bone geometry is strongly correlated with the muscle attachment sites. This assumption, as highlighted

by the authors, was based on clinical experience and it may be not applied to pathological patients (D1) with bone deformities. It has to be pointed out, in addition, that these authors only analysed muscle insertions and data concerning the origins and insertions of the ligaments have not been reported.

The reproducibility analysis showed an absence of significant interactions both between and within factors, confirming that the virtual palpation procedure that provides the input of the method is not operator-dependent. In addition, one of the operators performed the virtual palpation within a different software environment and obtained results that were overlapping to those form the other operators in terms of repeatability. This suggests that the changeover of the virtual palpation software can occur without losing precision.

Repeatability findings suggest that an inevitable source of error for our method lies in the morphological differences between different subjects: some landmarks can be determined more precisely than others (see Table 3.2) since some anatomical regions of knee change substantially from subject to subject (Fehring et al., 2009). The variability we found, in addition, was likely also due to the fact that pathological knees, presenting irregular or deformed surfaces, were part of our dataset. The results showed in Table 3.2 revealed that some landmarks, such as FPS, FMS, and TTC, have a higher SD. The FPS and FMS landmark are located in the medial and lateral sulcus (Figure 3.2), as reported in the "Colours Atlas of Skeletal Landmark Definitions" guideline (Serge Van Sint Jan 2007), and this anatomical area of the femur resulted damaged in most of the patients included in the study. In particular, the presence of osteophytes and deformities due to the sever OA may have misled the operators that have executed the virtual palpation. The TTC bony landmark, which represents the tuberosity of the tibia, is rather easy to identify given the prominent curvature in the anterior part of the tibia. However, one operator completely missed the accurate position of the TTC landmark during the virtual palpation task, negatively affecting the precision of the landmark position in terms of standard deviation. This represents the main limitation of this methodology where the estimation of the origin and insertion of the knee ligaments is strictly correlated with precision of the virtual palpation procedure. Hence, it is conceivably to hypothesize that the expertise of the operators and the use of standard and well-defined guidelines for the definition of the anatomical landmarks for the virtual palpation can both contribute to improve the accuracy of the proposed procedure.

The RA created for the purpose of this study is calculated from three knee specimens obtained from donors of 70 years of age, and has been used to predict the ligament attachments for a population that was only slightly different in terms of age (65 years on average). Future research should be conducted to verify whether the accuracy of the method could be compromised when used in subjects of a different age range.

In conclusion, keeping in mind the generalizability limitations imposed by the number of investigated knees, the proposed procedure can be deemed adequately robust. It allows estimating the origins and the insertions of the knee ligaments from a CT scan with an accuracy level that is equivalent to that reachable using MRI images. As such, this procedure can be used to improve the accuracy of dynamic patient specific knee models in order to have a better understanding of the forces and the strains on the knee structures, such as the ligaments, during static and locomotion activities.

References

Arnold, E.M., Ward, S.R., Lieber, R.L., Delp, S.L., 2010. A model of the lower limb for analysis of human movement. Ann. Biomed. Eng. 38, 269–279.

Bert, J.M., 1996. Custom total hip arthroplasty. J. Arthroplasty 11, 905–915.

Blankevoort, L., Huiskes, R., 1996. Validation of a three-dimensional model of the knee. J. Biomech. 29, 955–961.

Brand, R.A., Crowninshield, R.D., Wittstock, C.E., Pedersen, D.R., Clark, C.R., van Krieken, F.M., 1982. A model of lower extremity muscular anatomy. J. Biomech. Eng. 104, 304–310.

Challis, J.H., 1995. A procedure for determining rigid body transformation parameters. J. Biomech. 28, 733–737.

Ellingsen, L.M., Chintalapani, G., Taylor, R.H., Prince, J.L., 2010. Robust deformable image registration using prior shape information for atlas to patient registration. Comput. Med. Imaging Graph. 34, 79–90.

Fehring, T.K., Odum, S.M., Hughes, J., Springer, B.D., Beaver, W.B., 2009. Differences between the sexes in the anatomy of the anterior condyle of the knee. J. Bone Joint Surg. Am. 91, 2335–2341.

Grimpampi, E., Camomilla, V., Cereatti, A., De Leva, P., Cappozzo, A., 2014. Metrics for describing soft-tissue artefact and its effect on pose, size, and shape of marker clusters. IEEE Trans. Biomed. Eng. 61, 362–367.

Guess, T.M., Liu, H., Bhashyam, S., Thiagarajan, G., 2013. A multibody knee model with discrete cartilage prediction of tibio-femoral contact mechanics. Comput. Methods Biomech. Biomed. Engin. 16, 256–70.

Guess, T.M., Thiagarajan, G., Kia, M., Mishra, M., 2010. A subject specific multibody model of the knee with menisci. Med. Eng. Phys. 32, 505–515.

H. Bloemker, K., 2012. Computational Knee Ligament Modeling Using Experimentally Determined Zero-Load Lengths. Open Biomed. Eng. J.

Horn, B.K.P., 1987. Closed-form solution of absolute orientation using unit quaternions. J. Opt. Soc. Am. A.

Kepple, T.M., Sommer, H.J., Siegel, K.L., Stanhope, S.J., 1997. A three-dimensional musculoskeletal database for the lower extremities. J. Biomech. 31, 77–80.

Kia, M., Stylianou, A.P., Guess, T.M., 2014. Evaluation of a musculoskeletal model with prosthetic knee through six experimental gait trials. Med. Eng. Phys. 36, 335–44.

Lew, W.D., Lewis, J.L., 1977. An anthropometric scaling method with application to the knee joint. J. Biomech. 10, 171–181.

Lewis, J.L., Lew, W.D., Zimmerman, J.R., 1980. A nonhomogeneous anthropometric scaling method based on finite element principles. J. Biomech. 13, 815–824.

Morrison, J.B., 1970. The mechanics of the knee joint in relation to normal walking. J. Biomech. 3, 51–61.

Pellikaan, P., van der Krogt, M.M., Carbone, V., Fluit, R., Vigneron, L.M., Van Deun, J., Verdonschot, N., Koopman, H.F.J.M., 2014. Evaluation of a morphing based method to estimate muscle attachment sites of the lower extremity. J. Biomech. 47, 1144–1150.

Radermacher, K., Portheine, F., Anton, M., Zimolong, A., Kaspers, G., Rau, G., Staudte, H.W., 1998. Computer assisted orthopaedic surgery with image based individual templates. Clin. Orthop. Relat. Res. 354, 28–38.

Reggiani, B., Cristofolini, L., Varini, E., Viceconti, M., 2007. Predicting the subject-specific primary

stability of cementless implants during pre-operative planning: Preliminary validation of subject-specific finite-element models. J. Biomech. 40, 2552–2558.

Shelburne, K.B., Pandy, M.G., 2002. A dynamic model of the knee and lower limb for simulating rising movements. Comput. Methods Biomech. Biomed. Engin. 5, 149–159.

Van Sint Jan, S., 2007. Color atlas of skeletal landmark definitions: guidelines for reproducible manual and virtual palpations. CHURCILL LIVINGSTONE Elsevier, Philiadelphia (PA), USA.

Van Sint Jan, S., Della Croce, U., 2005. Identifying the location of human skeletal landmarks: why standardized definitions are necessary--a proposal. Clin. Biomech. (Bristol, Avon) 20, 659–60.

Woo, S.L.Y., Abramowitch, S.D., Kilger, R., Liang, R., 2006. Biomechanics of knee ligaments: Injury, healing, and repair. J. Biomech.

Zanetti, E.M., Crupi, V., Bignardi, C., Calderale, P.M., 2005. Radiograph-based femur morphing method. Med. Biol. Eng. Comput. 43, 181–188.

Chapter 4

A Subject-Specific Geometric Knee Model to compute the soft tissue balance in TKR Surgery

The model in this chapter is a geometric model developed on a dataset of seven patients that underwent a TKR surgery using a posterior stabilized prosthetic no cruciate retaining implant. The model predicts the post-operative elongation of the knee collateral lateral ligaments examining the knee at two fixed angles, 0º and 90º of flexion. The choice was limited only to two fixed position because the prosthetic implant was designed to have a geometrical congruence between the femoral and tibial components in full extension and at 90 º of flexion. Intermediate positions of the range of motion cannot be calculated geometrically, therefore a more complex model that includes the forces and more structures that surrounds the knee will be developed in the next chapter (Chapter 5). In the geometric model only the collateral lateral ligament (LCL) and the medial collateral ligament (MCL) have been included to assess the knee soft tissue balancing. By that a multi-fibre model, that includes all the fibres that composes the knee soft tissue, have been developed on one patient of the dataset to assess that the analysis of soft tissue balancing can be limited to the investigation of the ligaments, which ultimately represent the most stressed structures in TKR surgery.

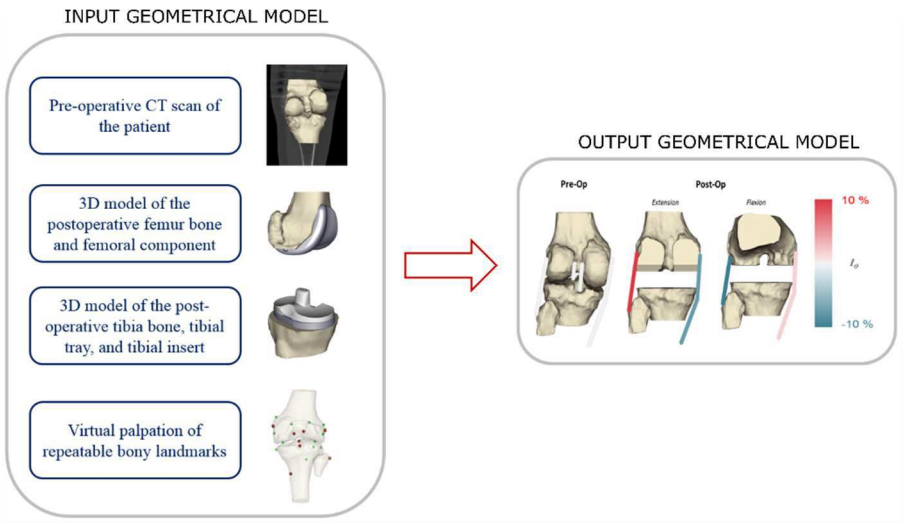

Figure 4.1 – *Input and output parameters of the geometrical model*

4.1 Introduction

One of the primary reasons for TKR failure is the possible damaging of the knee ligaments during the surgical procedure and their possible excessive loosening or stretching caused by the presence of the artificial implant, also referred to as non-optimal ligaments balancing. Problems related with overly tight and overly loose soft-tissue constraint that account for up to 54% of revision surgeries in the early stage (Mulhall et al., 2006), might lead to pain (Babazadeh et al., 2009), stiffness in the joint, and loss of functionality (Heesterbeek et al., 2008). It is important to achieve optimal tension in the knee ligaments to avoid complications after TKR, such as pain and a reduced range of motion (Stambough et al., 2014). The optimal tensions that should be achieved in the knee ligaments after TKR are unknown, therefore the gap-balancing surgical technique aims to create equal rectangular gaps and equal laxities at 0° of flexion, and 90° of flexion during the surgery. However, very few studies have demonstrated the success rate of this methodology (Sikorski, 2008), confirming that the best outcome for TKR surgery is the restoration of the preoperative kinematics. In fact, a non-optimal length of the ligaments leads inevitably to an abnormal kinematics (Ghosh et al., 2012), therefore the preoperative length should be used as a reference to determine whether the balancing after TKR is overly tight or overly loose.

In the market there is a large variety of TKR implants that differs in degrees of constraint, bone and ligaments resection; the most common implants design is the cruciate-retaining (CR) and the posterior-stabilized (PS) models. The CR design requires to cut the anterior cruciate ligament (ACL), the stability is maintained by having a congruent coupling of the contact surfaces, where the axial compression force takes the implant in place and assures stability. The balancing of the soft tissue for the CR implants is very complex because an unbalanced posterior cruciate ligament (PCL) causes tibial anterior subluxation (Heesterbeek et al., 2010). The posterior-stabilized implant requires the resection of both cruciate ligaments (ACL and PCL), the tibial insert provides a pivot that prevents the anterior-posterior movement of the femoral component onto the tibial insert (Walker et al., 2009). Additional categories of TKR implants comprises also the mobile-bearing designs that aim to mimic the natural roll-back movement of the knee joint during the flexion movement: the polyethylene insert can freely rotate and slide on the tibial tray (Most et al., 2003). Most recent models provide asymmetric femoral

condyles implants where the stability is maintained by having a congruent coupling in the medial comportment while the lateral condyle has freedom to move anteriorly and posteriorly (*GMK Sphere*® - *Medacta International SA, Switzerland*). This approach seems to be very promising and recent studies have demonstrated that this implant might reproduce anatomically the kinematics of a healthy knee (Amin et al., 2008; Walker et al., 2010).

Previous studies have investigated the postoperative length of the superficial MCL (MCL) and LCL throughout the knee flexion movement (Ghosh et al., 2012; Jeffcote et al., 2007; König et al., 2011; Thompson et al., 2011), even though the literature about healthy knee is certainly more comprehensive (Bergamini et al., 2011; Harfe et al., 1998; Liu et al., 2011; Park et al., 2006; Sugita and Amis, 2001; Victor et al., 2009; Wang et al., 1973). The studies conducted on the prosthetic knees showed an alteration of the collateral lateral ligament lengths compared with the preoperative data. Findings of the studies for both native and operated knees revealed a near-isometric behavior of the MCL whilst the slackening was significant for the LCL as the knee flexed.

The surgical procedures available in the market do not provide yet any tool to understand in advance how the knee ligaments are affected by the presence of the prosthetic implant. Since a preferred outcome in TKR is the restoration of the native length of the knee ligaments, the purpose of this study is to present a procedure to estimate the postoperative length of the superficial MCL (MCL) and LCL of TKR patients in two static positions: extension (0º) and flexion (90 º). Subject specific models of the knee have been then developed on a TKR patient's dataset to simulate the outcome of the surgery. A biomechanical assessment of this aspect, through a simulation approach, might help the improvement of the surgical procedure that aim to preserve an optimal balancing of the soft tissue.

The specific aims of this chapter are:

a) to create a subject specific geometric model of a TKR patient based on CT scan to estimate the postoperative length of the knee collateral ligaments at 0° and 90° of flexion;
b) to compare the CT- and MRI-based postoperative ligament lengths;
c) to define a criterion, based on the preoperative length (l_0), to judge the acceptability of a postoperative length;
d) to perform a study of the sensitivity of the length estimates to the l_0 of the LCL and MCL;

e) to verify, using an ad hoc multifiber model which, among all the structures that surround the knee, are the most stressed after the TKR surgery.

4.2 Materials and Methods

The dataset used in this study is the same described in Chapter 3, where each patient's dataset includes Computed Tomography (CT) and Magnetic Resonance Imaging (MRI) of pathological knee that underwent surgery. The prosthetic model, used for the surgery, is a GMK posterior stabilized (PS) model no cruciate retaining (Medacta International SA, Castel San Pietro): the tibial tray provides a peg between the medial and the lateral compartment which limits the femoral component slope and constraint the motion of the femoral component (Figure 4.2).

Figure 4.2 - *GMK revision posterior stabilized (PS) model no cruciate retaining (Medacta International SA, Castel San Pietro)*

The stereolithography (STL) files describing the 3D geometries of the lower limb bones (femur, tibia, and fibula) were obtained from the segmentation of both CT and MRI while the STL of the artificial components were provided by the company.

The patella was not included in the dataset. The model was developed entirely using NMSBuilder (SCS srl, Italy), a freely available software that allowed the visualization of STL and DICOM files, the creation of landmark clouds, and the possibility to apply geometrical transformations in the space to 3D geometries.

The femur and tibia STL files have been cut following the surgical procedure extensively described in Chapter 2 (paragraph 2.4.2) and positioned in the extended and flexed post-surgery positions (Figure 4.3).

The surgical principle of the TKR surgery aims to re-align the MA of the lower limb, the angle between the mechanical axes of the femur and tibia must be 180º (Figure 4.3).

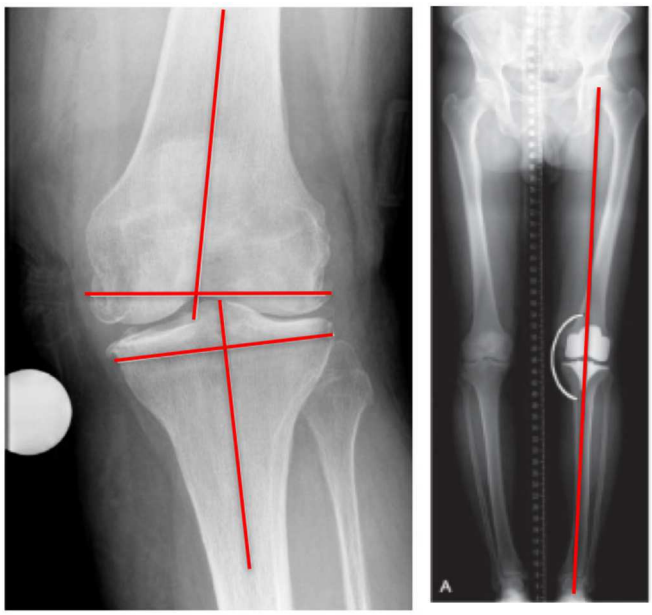

Figure 4.3 – *The image on the left shows an arthritic patient where the MA axes of femur and tibia are not aligned. The image on the right shows the post-operative condition where the angle between the two axes is 180 º*

As showed in Figure 4.2, the alignment of the MA of the lower limb is obtained placing the prosthetic implants perpendicularly to the red line which represents the MA of the patient, and this is currently considered the standard of care (Parratte et al., 2010). The mechanical axis, considering the lower limb fully extended, is the connecting line between the centre of the femoral head and the centre of the ankle passing through the centre of the femur and the tibial spine (Luo, 2004). The definition of the lower limb mechanical axis has been evaluated in NMS Builder allowing the calculation of the position of the femur and tibia after the surgery and the relative roto-translation matrices.

The lower limb planes (sagittal, frontal, transversal) were defined using the mechanical axis and an arbitrary medial lateral direction such as the knee trans-epicondylar axis or alternatively the posterior condyles axis (Luo, 2004). The surgical procedure comprised five cuts on the femur: 1) distal cut 2) anterior and posterior cuts 3) chamfer cuts (Brooks, 2009). The femoral distal cut is then executed on the transversal plane and the height of the cut, along the mechanical axis, is calculated starting from the detection of the distal condyles. Once those points are acquired, the height is calculated moving from the most distal condyle, that conceivably is the less worn, along the

mechanical axis of a quantity related to the surgeon's preference. The femoral distal cut is the most important part of the surgery since it dictates the position of the final implant and the orientation of the remaining cuts. After the distal femoral resection has been made, using antero-posterior femoral sizers, the size of the femur is determined (Ng et al., 2013). Once the femoral size is obtained a customized mask guides the anterior and posterior cuts, this operation is strictly correlated with the specific model of implant, and usually the manufacturer provides specific instructions for the surgical procedure. Afterwards, the chamfer cuts are performed with an inclination of 45º, bridging the distance between the three previous resections (Brooks, 2009). A similar procedure is applied to the tibia, once the mechanical axis has been calculated the tibial cut is performed using the transversal plane orientation previously defined. The height of the cut is then measured starting from the detection of the tibial plate glenoid. The height of the cut, along the mechanical axis, depends on the surgical technique and the cut plane is not perpendicular to the mechanical axis but it is inclined posteriorly by 3º, taking into account the natural slope of the tibia.

Once the bones were cut following the surgical procedure, the prosthetic implant was attached to the bones. The size and the positioning of the implant to the femur and the tibia were performed by the Medacta preplanning software which through an algorithm allows to obtain the best fit to cover the bone cut. The coupling of the femoral component to the tibial insert were calculated considering the geometrical propertied of the implant. In the extended position the curvature of the contacting surfaces can be approximated by a ball and socket coupling (Figure 4.4), allowing to determine accurately the relative position of the femoral component over the tibial insert. In the flexed position at 90º the position is obtained using a specific constraint of the prosthetic implant (Figure 4.4) In fact, the prosthetic implant is designed to posteriorly stabilized, the contact between the peg of the tibial insert and the connection between the lateral and medial compartment of the femoral component limits the movement when the knee is flexed at 90º.

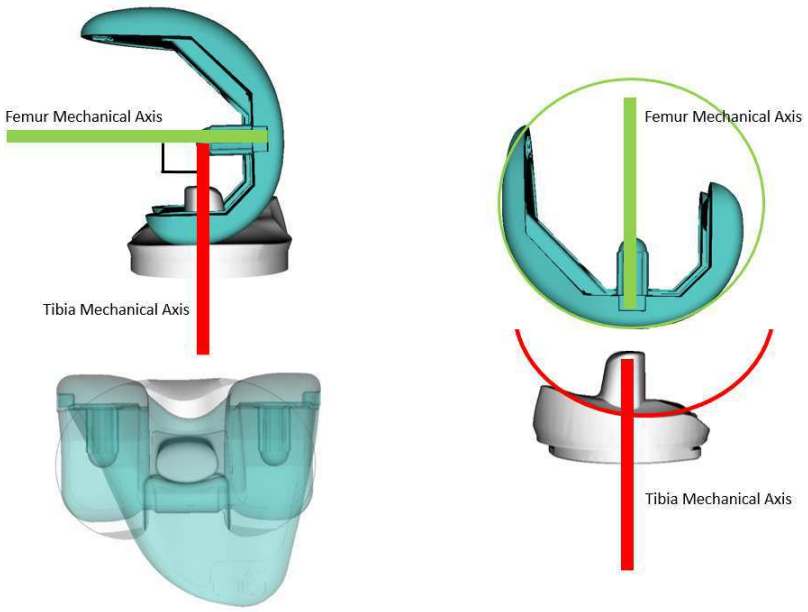

Figure 4.4 – *On the left, femur and tibia components coupling in flexion at 90°. On the right, Extension femur and tibia components coupling (ball and socket) at 90°.*

There are some orientation parameters that may be changed during the surgery to assure a correct positioning of the artificial components (Figure 4.5):

1) the varus-valgus femur cutting plane orientation on the frontal plane (from -3º to 3º , with a step of 1º)
2) the varus-valgus tibia cutting plane orientation on the frontal plane (from -3º to 3º , with a step of 1º)
3) the external rotation femur condyle cutting plane orientation on the frontal plane (from 0º to 6º, with a step of 1º)
4) the posterior slope tibial cutting plane orientation on the sagittal plane (from 3º to 5º, with a step of 1º)

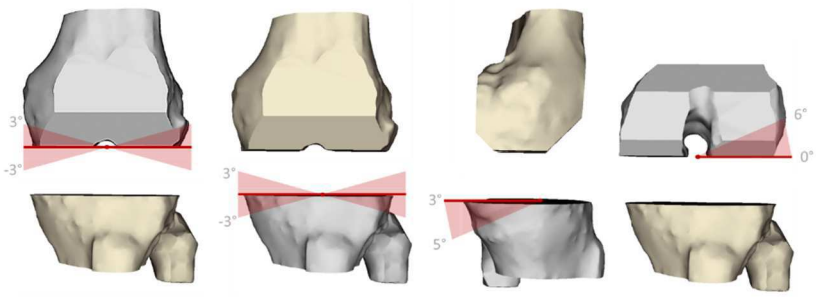

Figure 4.5 - *from left to right: varus-valgus femur, varus-valgus tibia, posterior slope tibia, external rotation femur*

The $\boldsymbol{l_0}$ of the ligaments has been calculated from the CT images of each patient for the preoperative images acquired from the fully extended knee. Since the prosthetic model used in this study was no cruciate retaining, only the LCL and the MCL were analysed. Their lengths were calculated as the geometric distance between two points representing their origins and insertions on the bones. For the MCL, the wrapping around the femur and tibia surfaces has been accounted for by adding a midpoint between the femoral and tibial attachments. In particular, the midpoint was calculated as

$$MidPoint = (Mid_X, Mid_Y, Mid_Z)$$

$$Mid_X = \frac{(MCLfem_X - (MCLtib_X)}{2}$$

$$Mid_y = TMR_y$$

$$Mid_Z = \frac{(MCLfem_Z - (MCLtib_Z)}{2}$$

where

- $MCLfem_x$ is the x coordinate of the MCL femoral attachment
- $MCLtib_x$ is the x coordinate of the MCL tibial attachment
- TMR_Y is the y coordinate of the TMR bony landmark (Chapter 3)
- $MCLfem_z$ is the z coordinate of the MCL femoral attachment
- $MCLtib_z$ is the z coordinate of the MCL tibial attachment

The y coordinate of the TMR represented the medio-lateral distance that allowed to push the midpoint to the edge of the tibial plate to realize the wrapping around the knee joint. The TMR landmark was used in this procedure according to the Table 3.2 in the Chapter 3, where it showed that it is one of the most repeatable bony landmark for the virtual palpation.

The collateral lateral ligaments origin and insertions were obtained using the procedure described in Chapter 3 (Ascani et al., 2015).

The postoperative lengths of the collateral knee ligaments ($\boldsymbol{l_{ext}}$ and $\boldsymbol{l_{ext}}$) were then estimated using the new configurations of the femur and tibia in the extended and flexed positions (Figure 4.4). These values were used to calculate the percentage of elongation ($\boldsymbol{l_{ext\%}}$ and $\boldsymbol{l_{flex\%}}$) for each ligament with respect to the $\boldsymbol{l_0}$ using the following formulas:

$$\boldsymbol{l_{ext\%} = \frac{l_{ext} - l_0}{l_0} \cdot 100}$$

$$l_{flex\%} = \frac{l_{flex} - l_0}{l_0} \cdot 100$$

The output of the model is represented by the percentage elongation of the knee ligaments in the postoperative positions, however to compute the balancing of the soft tissue, a warning threshold was defined to judge wheatear the elongation was correct or not. The definition of the threshold was defined considering the ultimate failure strain of the knee ligaments that has been extensively tackled in Chapter 2. Since, as reported in the literature, many studies suggested that any stretch beyond 17 % (ref) might start to damage the tissue, it can be presumed that this is also the region where pain start to appear. To prevent the pain and any possible damage that might occur, the threshold was fixed to the 10% of the l_0, considering any elongations beyond that value as a failure for the balancing of the knee ligaments (Figure 4.5).

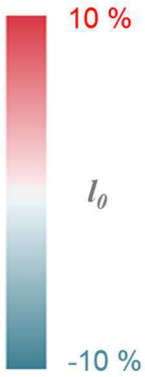

Figure 4.6 - *The 10% of the preoperative length was considered as the upper limit of elongation for the model output*

Using the above data and procedures a geometric model was developed for each patient of the dataset to estimate the ligaments extension of the knee collateral ligaments after a TKR. Identical geometric models were also developed on the dataset using MRI images to assess if the procedure has the same level of accuracy that can be reached using MRI images where the ligaments are rather visible (Mohana-Borges et al., 2005). The whole process to generate one geometric model starting from the CT scan takes on average 30/40 mins.

The preoperative length of the ligaments depends obviously from the position of the origin and insertion on the femur and the tibia in the preoperative extended position. Therefore, the sensitivity study concerns the variation of the positions of the ligaments origin and insertion.

The estimate of the positions of ligament origins and insertions affect the estimate of the length of a ligament. For each case, we have a measure of the error in the estimate of these points by comparing CT and MRI based predictions. We might consider the standard deviation (SD) of the error found for each origin and insertion point as the expected possible variation of the position of a ligament's attachment. The value of this SD for a given subject might be inputted in a sensitivity analysis as a reasonable error in the estimate of the LCL and MCL attachment points to have an indicator of how this would reflect on the ligament length estimate.

Patient	*Bone*	*Average (mm)*	*SD (mm)*
1	Femur	2.5	2.9
	Tibia	4.4	4.3
2	Femur	1.3	2.2
	Tibia	2.6	1.8
3	Femur	3.9	2.8
	Tibia	2.5	5.1
4	Femur	3.1	3.9
	Tibia	/	/
5	Femur	0.4	0.7
	Tibia	2.8	5.6
6	Femur	1.3	2.6
	Tibia	2.7	3.1

Table 4.1 – *Mean distance between the origin and insertion of the ligaments predicted using the CT scan and those estimated on the MRI images*

The mean in the Table 4.1 has been calculated, for each case and bone, as the average of the distances between the origin and insertion of the ligaments predicted using the CT scan and those estimated on the MRI images. The range within the model could predict the position is given by the $\pm SD$ on the plane tangent to the bone (Figure 4.7).

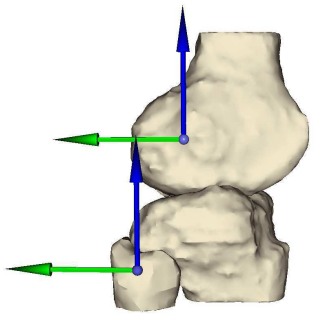

Figure 4.7 – *ZY-Plane tangent to the bone*

Using the standard deviation values of the Table 4.1 the sensitivity study has been performed applying the ± SD to the Z and Y coordinates, respectively, of the position predicted by the model for each ligament origin and insertion of the dataset. Consequently, five different positions have been calculated for each insertion obtaining 25 preoperative lengths for each ligament (Figure 4.8).

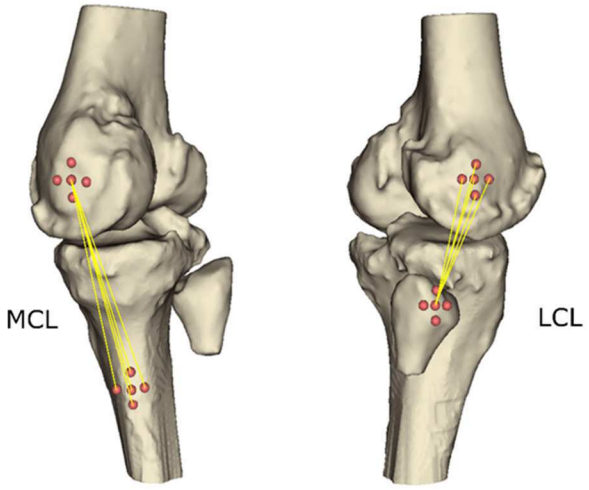

Figure 4.8 – *Sensitivity study of the MCL (up) and LCL (down) in the preoperative extension, postoperative extension and postoperative flexion*

The knee joint is surrounded by a large variety of structures and fibres that go under the name of soft tissue. Although the ligaments are inevitably the first structures of the knee soft tissue involved in TKR surgery, there are many structures such as muscles, tendons, skin, synovial membranes that may be damaged as well. For this reason, a geometric multifiber model of the lower limb has been developed in NMSBuilder choosing a random patient of the dataset (Figure 4.8). The model included: the major flexor and extensor of the knee, the knee collateral ligaments (MCL, LCL), the patellar tendon, and four skin bundles (sANT, sPOST, sLAT, sMED), along with the bones of the lower limb (Table 4.2).

Muscle	**Origin**	**Via Point 1**	**Via Point 2**	**Insertion**
Gracilis	Pelvis	\	Tibia	Tibia
Rectus Femoris	Pelvis	\	\	Patella
Sartorius	Pelvis	Femur	Tibia	Tibia
Semimembranosus	Pelvis	\	\	Tibia
Semitendinosus	Pelvis	\	Tibia	Tibia
Tensor Fasciae Latae	Pelvis	Femur	Femur	Tibia
Vastus Intermedialis	Patella	\	\	Femur
Vastus Lateral	Patella	\	\	Femur

Vastus Medial	Patella	\	\	Femur
Gastrocnemius Medial	Femur	\	\	Calcaneus
Gastrocnemius Lateral	Femur	\	\	Calcaneus
Ligament				
LCL	Femur	\	\	Fibula
MCL	Femur	\	Tibia	Tibia
Patellar Tendon	Patella	\	\	Tibia
Skin Bundle				
Anterior bundle 1	Pelvis	Femur	\	Ankle
Posterior bundle 1	Pelvis	Femur	\	Ankle
Lateral Bundle 1	Pelvis	Femur	\	Ankle
Medial bundle 1	Pelvis	Femur	\	Ankle

Table 4.2 - *Soft tissue elements included in the Multifiber model*

The origins and insertions of muscles and ligaments have been registered using a reference atlas available in the literature (Delp et al., 1990) with the same procedure extensively described in the previous chapter. The VIA points of muscles and ligament were also included in the Registration Atlas to perform the wrapping of the fibres around the bones. The four skin bundles were estimated by observing the axial plane images of the MRI of pelvis, femur, and ankle (Figure 4.9).

Since some orientation parameters can be changed during the surgery to assure a correct ligament balancing, a sensitivity analysis has been performed to investigate what structures are more stressed varying those parameters one at the time. In addition to the orientation parameters, the variation of the gap between the femoral and tibial distal cut planes (from 18 mm to 28 mm, with a step of 2 mm) could be adjusted to assure a correct ligament balancing.

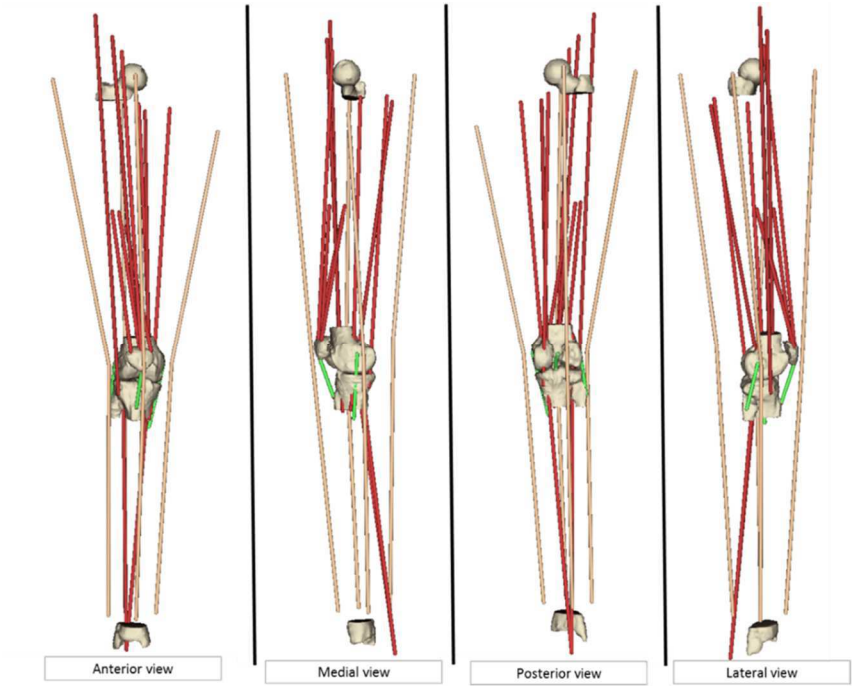

Figure 4.9 – *Multifiber Model*

4.3 Results

The results of the multifiber model showed the percentage variation of the length by varying step-by-step each orientation preplanning parameter, additionally for each orientation preplanning parameter the gap between the femoral and tibial distal cut planes was varied between 18 mm to 28 mm (with a step of 2 mm). The Figure 4.10 showed the max variations of the preplanning orientation parameters, obtained imposing a gap of 28 mm between the femoral and tibial cut planes.

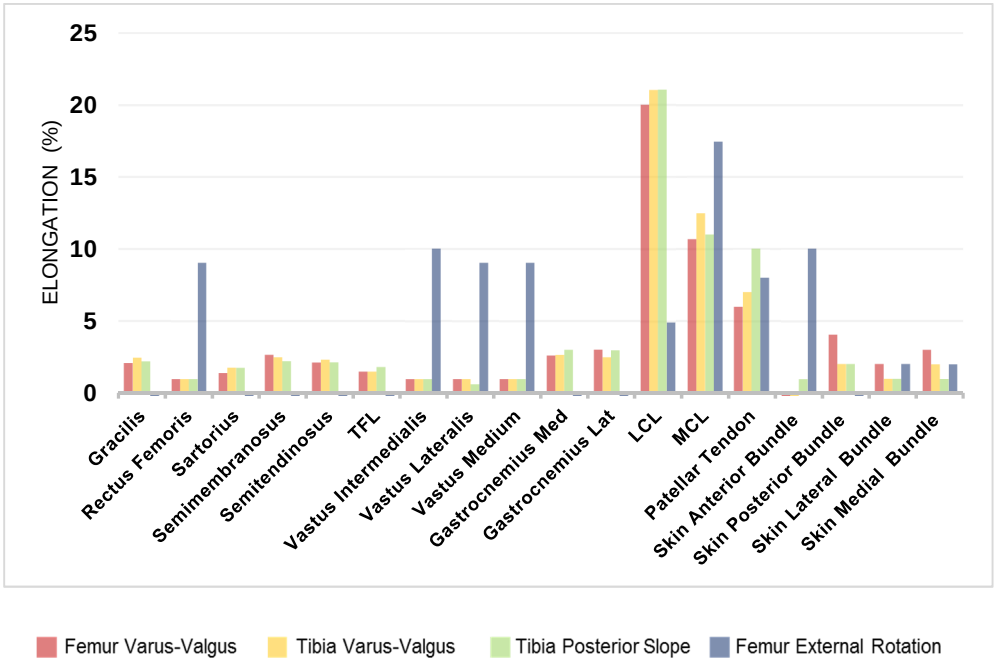

Figure 4.10 – *Results sensitivity study considering a gap between the femoral and tibial bone cuts of 28mm*

The results clearly showed that the most stressed structures among the multifiber model structures are the knee ligaments and the patellar tendon. The femur external rotation preplanning parameter shows that the elongations are uniformly higher in all the fibres included in the study, even if the most stretched fibre is the LCL. This multi-fibre modelling approach confirmed that the analysis of soft tissue balancing can be limited to the investigation of the ligaments, which ultimately also represent the most stressed structures in TKR surgery.

The values predicted by the models created using the dataset, revealed that the preoperative lengths of the MCL and LCL ligaments were not preserved after the surgery in both extended (0 deg) and flexed (90 deg) position (Table 4.3). By that it can be assumed that the prosthetic implant didn't preserve the correct kinematic of the knee where the elongations of the ligaments are rather isometric during the entire range of motion. In the postoperative extended position, the lengths of the ligaments were similar to the preoperative data, 0.6 ± 3.5 mm and -0.2 ± 2.0 mm (mean ± SD) for the LCL and MCL, respectively. In the postoperative flexed position, the LCL decreased significantly of -3.1 ± 3.0 mm, while the MCL did not differ from the preoperative length (0.6 ± 4.4).

	$\mathbf{l_0}$ *(mm)*		$\mathbf{l_{ext}}$ *(mm)*		$\mathbf{l_{flex}}$ *(mm)*	
	LCL	*MCL*	*LCL*	*MCL*	*LCL*	*MCL*
Patient 1	**61.0**	**109.1**	**64.8**	**107.3**	**53.9**	**110.9**
Patient 2	**52.6**	**82.3**	**54.8**	**81.5**	**51.2**	**79.6**
Patient 3	**69.5**	**111.8**	**71.6**	**113.6**	**67.5**	**120.1**
Patient 4	**53.2**	**96.1**	**55.3**	**93.1**	**50.2**	**91.7**
Patient 5	**62.2**	**104.2**	**56.4**	**106.1**	**54.0**	**103.8**
Patient 6	**71.0**	**101.7**	**70.3**	**102.4**	**74.1**	**102.9**

Table 4.3 *–Length of MCL and LCL for the preoperative position; postoperative length of the MCL and LCL in extended (0 deg) and flexed (90 deg) position*

The focus of the study was to determine the balancing of the knee ligaments by using a threshold to highlight when the elongation was bigger than the 10% of the l_0. The results in the Table 4.4 showed the LCL is the most affected: in extension the ligament is considerably taut (-9% – 6%) except for the patient 5 (-9 % of laxity). In flexion the length of LCL ligament decreased significantly showing a slack of -5.5 ± 5.8% (-12% – 4%). The MCL did not differ significantly from l_0, ranging from -3% up to 2% in the extend position, and from -5 % up to 7% in flexion position. The prediction of the model on the dataset did not detect any warning elongation beyond the 10% of the preoperative length.

		EXTENSION		***FLEXION***	
		CT (%)	*MRI (%)*	*CT (%)*	*MRI (%)*
Patient 1	*LCL*	**6**	**6**	**-12**	**-13**
	MCL	**-2**	**-2**	**2**	**2**
Patient 2	*LCL*	**4**	**5**	**-3**	**-3**
	MCL	**-1**	**-1**	**-3**	**-4**
Patient 3	*LCL*	**3**	**4**	**-3**	**-9**
	MCL	**2**	**2**	**7**	**8**
Patient 4	*LCL*	**4**	**4**	**-6**	**-6**
	MCL	**-3**	**-3**	**-5**	**-7**
Patient 5	*LCL*	**-9**	**-9**	**-13**	**-16**
	MCL	**2**	**2**	**0**	**0**
Patient 6	*LCL*	**-1**	**-1**	**4**	**5**
	MCL	**1**	**1**	**1**	**1**

Table 4.4 – *Postoperative percentage elongation of the MCL and LCL in extended (0 deg) and flexed (90 deg) position*

The table 4.4 also showed the comparison between the results of the models' prediction based on CT scan and the same values obtained using MRI images. The results revealed that there are not statistical differences ($p>0.05$) between the outputs obtained with MRI and CT.

The results, as shown in Table 4.5, indicated that the variation of the preoperative lengths l_0 does not influence significantly the output of the model, in terms of percentage elongation under/over the 10%. The only case in which there are some remarkable differences is the MCL ligament of the patient 3 in flexion position after surgery. Although the sensitivity analysis reveals that for this specific patient there is just a 16 % of possibility that the model gives a wrong warning about the elongation of the ligaments, the values are very close to the warning threshold (10 %). Nevertheless, the stretching values of this specific ligament appear to be pretty high after surgery (7 %), consequently this might be a doubtful case which likely could require some additional investigations in terms of preplanning parameters. The LCL ligament of the patient 1 revealed that there is the 4% of possibility that the model could predict a wrong output. All the remaining cases show that the model is robust and the output is not influenced by the changing of the preoperative length l_0.

			STRETCHING (%)																								
Patient	LIGAMENT	Knee Position	S1	S2	S3	S4	S5	S6	S7	S8	S9	S10	S11	S12	S13	S14	S15	S16	S17	S18	S19	S20	S21	S22	S23	S24	S25
1	LCL	Ext	6	4	8	6	6	8	6	10	8	8	4	3	6	4	5	6	4	8	6	6	6	4	8	6	6
		Flex	-1	-1	-2	-1	-1	-1	-1	-2	-1	-1	-1	0	-1	-1	-1	-1	-1	-1	-1	-1	-1	-1	-2	-1	-1
	MCL	Ext	-1	-1	-2	-1	-1	-1	-1	-2	-1	-1	-1	0	-1	-1	-1	-1	-1	-1	-1	-1	-1	-1	-2	-1	-1
		Flex	4	4	5	4	4	4	4	5	4	4	4	4	4	4	4	4	4	5	4	4	4	4	5	4	4
2	LCL	Ext	4	4	5	4	4	4	4	5	4	4	4	4	4	4	4	4	4	5	4	4	4	4	5	4	4
		Flex	-1	-1	-1	-1	-1	-1	-1	-1	-1	-1	-1	-1	0	-1	0	-1	-1	-1	-1	-1	-1	-1	-1	-1	-1
	MCL	Ext	-1	-1	-1	-1	-1	-1	-1	-1	-1	-1	-1	-1	0	-1	0	-1	-1	-1	-1	-1	-1	-1	-1	-1	-1
		Flex	-3	-3	-3	-3	-3	-6	-6	-6	-6	-6	0	0	1	1	0	-5	-5	5	-5	-5	0	0	0	-1	0
3	LCL	Ext	3	2	5	3	3	4	2	5	4	4	2	1	4	2	2	3	2	5	3	3	3	1	5	3	3
		Flex	2	2	2	2	2	2	2	1	2	1	2	2	2	2	2	2	2	2	2	2	2	2	2	2	2
	MCL	Ext	2	2	2	2	2	2	2	1	2	1	2	2	2	2	2	2	2	2	2	2	2	2	2	2	2
		Flex	7	7	8	8	7	5	5	5	5	5	9	9	10	10	9	5	5	5	5	5	9	9	10	10	9
4	LCL	Ext	4	4	4	4	4	4	4	5	4	4	4	3	4	4	4	4	4	4	4	4	4	4	4	4	4
		Flex	-3	-3	-3	-3	-3	-3	-3	-3	-3	-3	-3	-3	-3	-3	-3	-3	-3	-3	-3	-3	-3	-3	-3	-3	-3
	MCL	Ext	-3	-3	-3	-3	-3	-3	-3	-3	-3	-3	-3	-3	-3	-3	-3	-3	-3	-3	-3	-3	-3	-3	-3	-3	-3
		Flex	-5	-5	-4	-5	-4	-7	-7	-7	-7	-7	-2	-2	-2	-2	-2	-7	-7	-7	-7	-7	-2	-2	-2	-2	-2
5	LCL	Ext	-9	-7	-8	11	-8	-9	-10	-8	-7	-8	-9	-10	-8	-11	-8	-9	-10	-8	-11	-8	-10	-10	-8	-11	-8
		Flex	3	2	3	3	3	3	2	3	3	3	3	2	3	3	3	3	2	3	3	3	3	2	3	3	3
	MCL	Ext	3	2	3	3	3	3	2	3	3	3	3	2	3	3	3	3	2	3	3	3	3	2	3	3	3
		Flex	1	0	1	1	0	0	-1	0	0	0	1	1	2	2	1	0	-1	1	0	0	1	1	2	1	1
6	LCL	Ext	-1	-1	-1	-1	-1	-1	4	4	-1	1	-1	-1	-1	-1	-1	-1	-1	-1	-1	-1	-1	-1	-1	-1	-1
		Flex	1	1	1	1	1	1	1	0	1	1	1	1	1	1	1	1	1	1	1	1	1	1	1	1	1
	MCL	Ext	1	1	1	1	1	1	1	0	1	1	1	1	1	1	1	1	1	1	1	1	1	1	1	1	1
		Flex	1	1	1	1	1	-2	-2	-2	-2	-2	4	4	4	4	4	-1	-1	-1	-1	-1	4	3	4	4	3

Elongation <10% Elongation >10%

Table 4.5 – *Results of the sensitivity study*

4.4 Discussion

A non-optimal balancing of the knee ligaments is associated with numerous complications after TKR surgery (Stambough et al., 2014). Since a preferred outcome in TKR is the restoration of the preoperative length of the knee ligaments, the purpose of this study was to present a procedure to estimate the postoperative length of the MCL and LCL of TKR patients in two static positions: extension (0º) and flexion (90 º).

The sensitivity analysis of the multifiber model showed that the soft tissue balancing analysis might be limited to study only the ligaments, which ultimately represents the most damaged structures during the TKR surgery. Therefore, it might be considered reasonable the development of a model that takes into account only the elongation of the ligaments of the knee after the surgery.

Reported results showed changes of the length in the postoperative positions: the MCL was comparable to the preoperative length in extension and flexion whereas the LCL was significantly slacker in flexion. The findings revealed that the preoperative length of the knee ligaments was not preserved after the TKR due to the new position of the femur and tibia. Nevertheless, all the estimated post-operative elongations were below the warning threshold, implying that, as described in Paragraph 2.3, the MCL and LCL ligaments should not undergo irreversible structural damages due to the postoperative overstretching.

The analysis of the sensitivity to the l_0 allowed to quantify a crucial aspect of the methodology (Hefzy et al., 1989) and showed that the model output is not significantly sensitive to the preoperative length variation, at least when this is made to vary within the limits established in Chapter 3. In fact, even when some variations were observed, the elongation was always under/over the 10% of the preoperative length, suggesting that no planning changes would happen as a result of the origin or insertion misidentification (Table 4.5).

The length of MCL did not change significantly in the postoperative positions and this concurs with previous studies in literature (Jeffcote et al., 2007; König et al., 2011; Thompson et al., 2011) such as the work of Ghosh et al. (2012) where experimental data showed that the largest difference from the preoperative data was 2.9 mm at 110º of flexion. They also presented that after TKR the LCL was significantly slacker (4 ± 6.2 mm) as the knee flexed, confirming our findings where the LCL was found slacker of 6

% (3.1 ± 3.0 mm) of the preoperative length. Although the average values measured on the dataset were in accord with the literature, our findings reveal significantly difference between the TKR patients, confirming the importance of having a subject specific modelling approach of the knee in order to estimate the soft tissue balancing (Morrison, 1970).

The MCL and LCL appeared to be slack for most of the investigated patients and positions, with values of laxity up to 6 mm (LCL in flexion). To restore the preoperative tension of the ligament, the preoperative surgical parameters should be set considering the soft tissue balancing to avoid overly-tight or overly-loose of the fibres. However, Kuster et al. (2004) have demonstrated that patients were more satisfied with a laxer knee, allowing for a bigger range of movement during low impact activity such as walking. Reported results suggest that for all the patients included in this study a successful surgery, allowing for an ideal elongation (lower than 10%) and an acceptable range of motion (ligaments are rather loose after TKR), might be achieved. Further follow up studies are needed to validate this assumption.

The generalization of the results of this study is possible under certain limitations. First, the collateral ligaments were represented as a one bundle fibre. The use of a high number of bundles to describe the ligaments is widely adopted in literature, in particular in studies focusing on different bundles behaviour (Bergamini et al., 2011; Hosseini et al., 2014; Liu et al., 2011). However, the identification of multiple bundles using the CT scan, where they are hardly visible, would have introduced additional errors. A second limitation of the present work is that the model included only two static positions, 0º and 90 º, which are the only two positions of interest for the soft tissue balancing in the Medacta preoperative planning framework. Ghosh et al. (2012), in fact, have demonstrated that the largest elongation was found between 110º and 80º. These angles, however, will be dealt with in the following chapter, where a quasi-static model will be presented.

The industrial and clinical relevance of this work is related to the importance gained by the TKR preoperative planning surgical procedure in the last few years (Maniar and Singhi, 2014), aiming to customise the geometry of the cutting blocks to the specific anatomy of the patients. The procedure developed in this study is currently being further engineered and will be implemented in the Medacta International SA planning framework. In particular, the output of the model will be shown to the surgeon to warn

them whenever the elongation of the ligaments exceeds the 10% of the preoperative length (Figure 4.11).

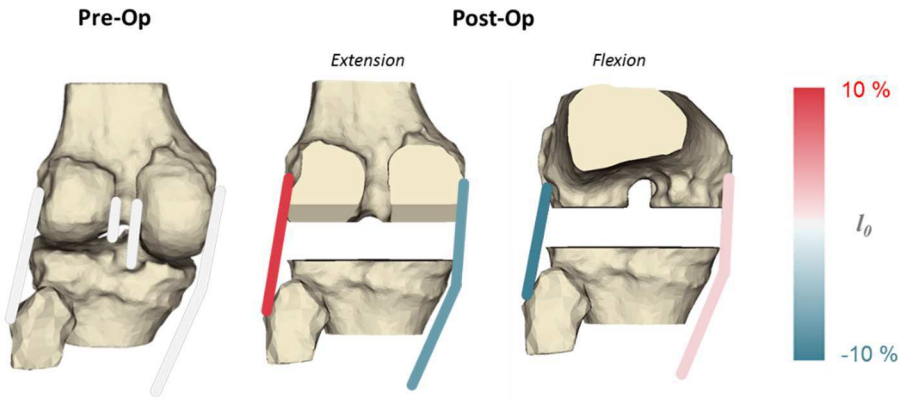

Figure 4.11 – *Soft tissue balancing for the TKR preoperative planning surgical procedure*

The automatic generation of the geometric models is an important aspect to consider for the implementation in an industrial framework. As addressed in the material and method paragraph, to create one single subject specific geometric model can take slightly less than one hour. The timing is partially justified by a certain amount of manual operations that cannot be easily replaced by automatic scripts. The manual operations that are time consuming are the segmentation of the DICOM images (CT or MRI) and virtual palpation of bony landmarks. The automatic segmentation is rather simple to achieve using one of the software available in the market that includes this feature, on the other hand an automatic virtual palpation tool is more challenging to develop. Certainly this tool must be developed and validated for two important reasons: a) to reduce the time and consequently the cost of the whole methodology b) to eliminate the operator dependence related issues.

References

Amin, A., Al-Taiar, A., Sanghrajka, A.P., Kang, N., Scott, G., 2008. The early radiological follow-up of a medial rotational design of total knee arthroplasty. Knee 15, 222–226. doi:10.1016/j.knee.2008.01.004

Ascani, D., Mazzà, C., De Lollis, A., Bernardoni, M., Viceconti, M., 2015. A procedure to estimate the origins and the insertions of the knee ligaments from computed tomography images. J. Biomech. 48, 233–7. doi:10.1016/j.jbiomech.2014.11.041

Babazadeh, S., Stoney, J.D., Lim, K., Choong, P.F.M., 2009. The relevance of ligament balancing in total knee arthroplasty: how important is it? A systematic review of the literature. Orthop. Rev. (Pavia). 1, e26. doi:10.4081/or.2009.e26

Bergamini, E., Pillet, H., Hausselle, J., Thoreux, P., Guerard, S., Camomilla, V., Cappozzo, A., Skalli, W., 2011. Tibio-femoral joint constraints for bone pose estimation during movement using multi-body optimization. Gait Posture 33, 706–711. doi:10.1016/j.gaitpost.2011.03.006

Brooks, P., 2009. Seven cuts to the perfect total knee. Orthopedics 32. doi:10.3928/01477447-20090728-27

Delp, S.L., Loan, J.P., Hoy, M.G., Zajac, F.E., 1990. An interactive Graphics-Based Model of the Lower Extremity to Study Orthopaedic Surgical Procedures. IEEE Trans. Biomed. Eng. 37, 757–767. doi:10.1109/10.102791

Ghosh, K.M., Merican, A.M., Iranpour, F., Deehan, D.J., Amis, A.A., 2012. Length-change patterns of the collateral ligaments after total knee arthroplasty. Knee Surgery, Sport. Traumatol. Arthrosc. 20, 1349–1356. doi:10.1007/s00167-011-1824-2

Harfe, D.T., Chuinard, C.R., Espinoza, L.M., Thomas, K.A., Solomonow, M., 1998. Elongation patterns of the collateral ligaments of the human knee. Clin. Biomech. 13, 163–175. doi:10.1016/S0268-0033(97)00043-0

Heesterbeek, P.J.C., Keijsers, N.L.W., Wymenga, A.B., 2010. Ligament releases do not lead to increased postoperative varus-valgus laxity in flexion and extension: A prospective clinical study in 49 TKR patients. Knee Surgery, Sport. Traumatol. Arthrosc. 18, 187–193. doi:10.1007/s00167-009-0972-0

Heesterbeek, P.J.C., Verdonschot, N., Wymenga, A.B., 2008. In vivo knee laxity in flexion and extension: A radiographic study in 30 older healthy subjects. Knee 15, 45–49. doi:10.1016/j.knee.2007.09.007

Hefzy, M.S., Grood, E.S., Noyes, F.R., 1989. Factors affecting the region of most isometric femoral attachments. Part II: The anterior cruciate ligament. Am. J. Sports Med. 17, 208–216. doi:10.1177/036354658901700210

Hosseini, A., Qi, W., Tsai, T.Y., Liu, Y., Rubash, H., Li, G., 2014. In vivo length change patterns

of the medial and lateral collateral ligaments along the flexion path of the knee. Knee Surgery, Sport. Traumatol. Arthrosc. 23, 3055–3061. doi:10.1007/s00167-014-3306-9

Jeffcote, B., Nicholls, R., Schirm, A., Kuster, M.S., 2007. The variation in medial and lateral collateral ligament strain and tibiofemoral forces following changes in the flexion and extension gaps in total knee replacement. A laboratory experiment using cadaver knees. J. Bone Joint Surg. Br. 89, 1528–1533. doi:10.1302/0301-620X.89B11.18834

König, C., Matziolis, G., Sharenkov, A., Taylor, W.R., Perka, C., Duda, G.N., Heller, M.O., 2011. Collateral ligament length change patterns after joint line elevation may not explain midflexion instability following TKA. Med. Eng. Phys. 33, 1303–1308. doi:10.1016/j.medengphy.2011.06.008

Kuster, M.S., Bitschnau, B., Votruba, T., 2004. Influence of collateral ligament laxity on patient satisfaction after total knee arthroplasty: a comparative bilateral study. Arch. Orthop. Trauma Surg. 124, 415–417. doi:10.1007/s00402-004-0700-7

Liu, F., Gadikota, H.R., Kozánek, M., Hosseini, A., Yue, B., Gill, T.J., Rubash, H.E., Li, G., 2011. In vivo length patterns of the medial collateral ligament during the stance phase of gait. Knee Surgery, Sport. Traumatol. Arthrosc. 19, 719–727. doi:10.1007/s00167-010-1336-5

Luo, C.F., 2004. Reference axes for reconstruction of the knee. Knee. doi:10.1016/j.knee.2004.03.003

Maniar, R.N., Singhi, T., 2014. Patient specific implants: scope for the future. Curr. Rev. Musculoskelet. Med. 7, 125–30. doi:10.1007/s12178-014-9214-2

Mohana-Borges, A.V.R., Resnick, D., Chung, C.B., 2005. Magnetic resonance imaging of knee instability. Semin. Musculoskelet. Radiol. 9, 17–33. doi:10.1055/s-2005-867102

Morrison, J.B., 1970. The mechanics of the knee joint in relation to normal walking. J. Biomech. 3, 51–61. doi:10.1016/0021-9290(70)90050-3

Most, E., Li, G., Schule, S., Sultan, P.G., Park, S.E., Zayontz, S., Rubash, H.E., 2003. The Kinematics of Fixed- and Mobile-Bearing Total Knee Arthroplasty. Clin. Orthop. Relat. Res. 416, 197–207. doi:10.1097/01.blo.0000092999.90435.d1

Mulhall, K.J., Ghomrawi, H.M., Scully, S., Callaghan, J.J., Saleh, K.J., 2006. Current etiologies and modes of failure in total knee arthroplasty revision. Clin. Orthop. Relat. Res. 446, 45–50. doi:10.1097/01.blo.0000214421.21712.62

Ng, F.-Y., Jiang, X.-F., Zhou, W.-Z., Chiu, K.-Y., Yan, C.-H., Fok, M.W.M., 2013. The accuracy of sizing of the femoral component in total knee replacement. Knee Surg. Sports Traumatol. Arthrosc. 21, 2309–13. doi:10.1007/s00167-012-2108-1

Park, S.E., DeFrate, L.E., Suggs, J.F., Gill, T.J., Rubash, H.E., Li, G., 2006. Erratum to “The change in length of the medial and lateral collateral ligaments during in vivo knee flexion”. Knee 13, 77–82. doi:10.1016/j.knee.2004.12.012

Parratte, S., Pagnano, M.W., Trousdale, R.T., Berry, D.J., 2010. Effect of postoperative

mechanical axis alignment on the fifteen-year survival of modern, cemented total knee replacements. J. Bone Joint Surg. Am. 92, 2143–2149. doi:10.2106/JBJS.J.00937

Sikorski, J.M., 2008. Alignment in total knee replacement. J. Bone Joint Surg. Br. 90, 1121–1127. doi:10.1302/0301-620X.90B9.20793

Stambough, J.B., Clohisy, J.C., Barrack, R.L., Nunley, R.M., Keeney, J.A., 2014. Increased risk of failure following revision total knee replacement in patients aged 55 years and younger. Bone Jt. J. 96–B, 1657–1662. doi:10.1302/0301-620X.96B12.34486

Sugita, T., Amis, A.A., 2001. Anatomic and biomechanical study of the lateral collateral and popliteofibular ligaments. Am. J. Sports Med. 29, 466–472.

Thompson, J. a, Hast, M.W., Granger, J.F., Piazza, S.J., Siston, R. a, 2011. Biomechanical effects of total knee arthroplasty component malrotation: a computational simulation. J. Orthop. Res. 29, 969–75. doi:10.1002/jor.21344

Victor, J., Wong, P., Witvrouw, E., Sloten, J. Vander, Bellemans, J., 2009. How isometric are the medial patellofemoral, superficial medial collateral, and lateral collateral ligaments of the knee? Am. J. Sports Med. 37, 2028–2036. doi:10.1177/0363546509337407

Walker, P.S., Sussman-Fort, J.M., Yildirim, G., Boyer, J., 2009. Design Features of Total Knees for Achieving Normal Knee Motion Characteristics. J. Arthroplasty 24, 475–483. doi:10.1016/j.arth.2007.11.002

Walker, P.S., Yildirim, G., Arno, S., Heller, Y., 2010. Future directions in knee replacement. Proc. Inst. Mech. Eng. H. 224, 393–414. doi:10.1243/09544119JEIM655

Wang, C.-J., Walker, P.S., Wolf, B., 1973. The effects of flexion and rotation on the length patterns of the ligaments of the knee. J. Biomech. 6, 587–596. doi:10.1016/0021-9290(73)90016-X

Chapter 5

A Subject-Specific Quasi-Static Knee Model to compute the soft tissue balance in TKR Surgery

The aim of this chapter is to create a quasi-static TKR knee model to estimate the postoperative elongation of the ligaments. A quasi-static approach takes into account the forces developed by the contact between the bodies and different anatomical structures surrounding the knee (ligaments, tendons, muscles), exploring the configuration near the equilibrium, where velocities and acceleration are close to zero. In this chapter two quasi-static models will be presented and their outputs will be compared in terms of changes in the estimates ligament elongations. Since a quasi-static knee modelling approach allows to estimate the length of the knee ligaments for any given knee flexion angles, the result will show if intermediate positions might change significantly the output of the model. The comparison with the results of the geometric model, presented in Chapter 4, will confirm if the postoperative length of the knee ligaments after TKR surgery can be reduced to the observation of two static position (0° - 90°) without including the forces developed by the contact and the anatomical structures of the knee.

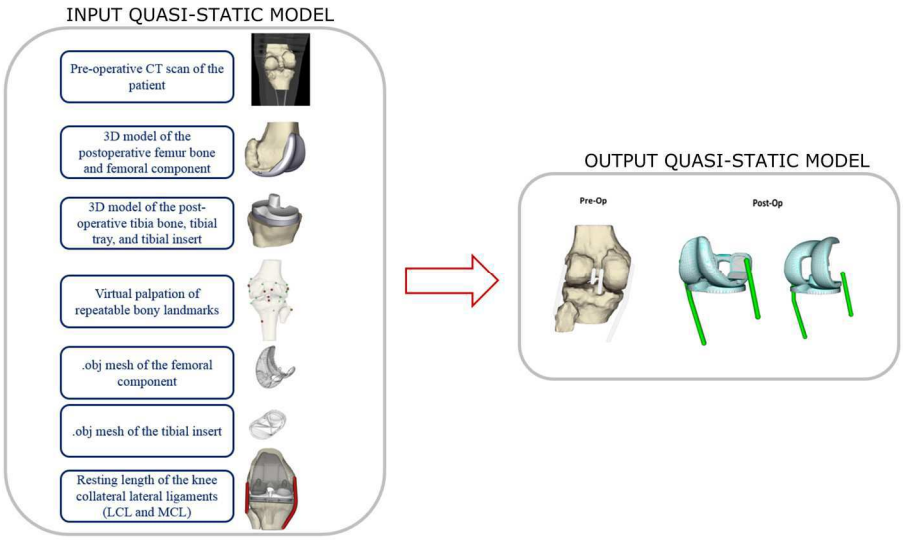

Figure 5.1 – *Input and output parameters of the quasi-static model*

5.1 Introduction

The objective of this study is to investigate the elongation of a TKR patient ligaments under quasi-static conditions and to compare relevant results to those obtained with the geometric model. The quasi-static analysis (Blankevoort et al., 1991; Pandy and Sasaki, 1998; J Wismans et al., 1980) entailed accounting for: a) the contact between the tibia and the femur and between the patella and the femur; b) the ligament forces; c) the muscle forces.

Contact mechanics between articular surfaces can be modelled using different methodologies. The most used method assumes that the contacting bodies are rigid and the contact surfaces are approximated with mathematical functions that describe known geometrical shapes, such as planes or spheres. More complex models employ 2D (Abdel-Rahman and Hefzy, 1993; Moeinzadeh et al., 1983) or 3D (Blankevoort et al., 1991; J. Wismans et al., 1980) polynomial functions to better fit the articular surface curvatures. An alternative approach assumes instead, that the contact forces are mostly developed by the deformations of the contacting bodies included in the model. These methods can be implemented adopting different numerical and analytical solution, among them there is the Hertzian theory (Hertz, 1881; Johnson, 1985) that calculates accurately deformations and contact forces but it is limited to simple geometries. Other technique are the elastic foundation model (Blankevoort et al., 1991; Hunt and Crossley, 1975) and the finite element method (FEM), which allow to process more complex objects. The FEM represents the most accurate method to estimate the deformations and the contact forces (Halloran et al., 2005), however it is computationally expensive. Therefore, the elastic foundation model assuming that the contacting bodies can be considered rigid but for layer of elastic materials at the articular surfaces, is often considered as a “lighter” alternative to the FEM. For this purpose, Li et al. (1997) have demonstrated that there were small changes in the results using the two methodologies to predict the contact pressure of a simple model composed by a cylinder and a half pipe. On the other hand, Halloran et al. (2005) compared the two techniques to measure the knee contact forces, finding that the contact areas were the same but the elastic foundation overestimated the loading peak by 15 %. In conclusion the elastic foundation is not accurate as the FEM, especially to estimate pressure distribution between complex geometries, however the computational efficiency (98% less computational time) makes this methodology

particularly relevant for preoperative planning framework for orthopaedic surgery because it allows to explore different positions within the range of motion.

The knee ligaments, which are passive structures, are usually modelled as one or more bundles that connects the origin and insertion points (J. Wismans et al., 1980). The non-linear behaviour of the ligaments is taken into account using non-linear springs that produce forces in accord the typical non-linear force-displacement curve (Figure 2.11, chapter 2) (Woo et al., 1999). Several studies in literature (Blankevoort et al., 1991; Kwak et al., 2000; Pandy et al., 1997) have used quasi-static models to investigate how the elongation of the knee ligaments is dependant by the flexion angle, which is needed for the current work. Pandy et al. (1997) investigated the ligaments function using a three dimensional model of the intact knee. The ligament elongation was analysed during anterior-posterior draw, axial rotation, and isometric contractions of the extensor and flexor muscles. The results showed that the ligaments elongation depended strictly by the flexion angle. The subject specific modelling of the knee ligaments requires some *in vivo* measurements such as the reference length or the stiffness. The reference length, as defined by Blankevoort et at. (1991), is the length of the ligaments in the reference position of the knee (typically extension). The stiffness, defined as the slope in the force deformation curve, has been determined experimentally (Woo et al., 1986) through tensile tests that showed that the stiffness is different among different types of ligaments.

The muscle forces have been included in quasi-static models to investigate how different level of muscular activations influenced the ligaments elongation (Pandy et al., 1997; Tumer and Engin, 1993). The muscles are usually modelled as musculotendinous actuators with a contractile muscle-fibre and compliant tendons in series (Zajac, 1989), which can be activated selectively during a quasi-static simulation.

In conclusion the total forced included in the models are:

- gravity
- forces developed by the ligaments
- forces developed by the contact between the femoral component and the tibial insert
- forces developed by the muscle actuator
- external forces (as replacement of the missing parts of the body)

The equilibrium of the quasi-static model of the knee joint is calculated by balancing the forces and moments acting in the model developed by the contact, the ligaments, and the muscle forces, for any given position of the joint.

In the first part of the paper the model included the two collateral ligaments in two postoperative positions, extension (0°) and flexion (0°). In the second part the model was modified adding the patella, the patellar tendon, and the rectus femoris allowing a sensitivity analysis of the ligaments length with respect to different level of muscle activations and knee joint angles (0°, 30°, 60°, 90°).

The specific aims of this study are:

a) to create a subject specific quasi static TKR tibio-femoral (TKR TF) model to estimate the postoperative length of the knee collateral ligaments at 0° and 90° of flexion;
b) to create a subject specific quasi static TKR patella-femur (TKR PF) model that includes the patella and the rectus femoris muscle, to estimate the postoperative length of the knee collateral ligaments at 0°, 30°, 60° and 90° of flexion;
c) to compare the results with the static model outputs (Chapter 4).

5.2 Materials and Methods

Experimental data. The dataset used in this study has been provided by Medacta International SA (Castel S. Pietro, Switzerland). It consists of six set of images obtained from six different patients (64 ± 5 years) who have undergone a Total Knee Replacement. Each patient's dataset includes CT and MRI of pathological knee that underwent surgery. The prosthetic model, used for the surgery, is a GMK revision posterior stabilized (PS) model no cruciate retaining (Medacta International SA), the tibial tray provides a pivot between the medial and the lateral compartment which limits the femoral component slope. The geometric stereolithography (STL) describing the 3D geometries of the prostheses were obtained from the CT images for the femoral component, tibial base plate, and the patella insert, along with the preoperative bone geometries of femur, tibia, fibula, partial talus, and partial calcaneus.

OpenSim, the open-source dynamic solver software developed by Stanford University (Delp et al., 2007) was used for the construction of the musculoskeletal models and the execution of the quasi-static analysis. This software allowed to perform a quasi-static analysis of rigid bodies, setting the forces acting on them and their inertial properties. Furthermore, NMSBuilder (SCS srl, Italy) has been used to visualise the 3D geometries and estimate the origins and the insertions of muscles and ligaments using a previously validated procedure (Ascani et al., 2015).

The preoperative length of the ligaments has been obtained from the MRI images of the preoperative images acquired from the fully extended knee. Since the prosthetic model used in this paper was no cruciate retaining, only the collateral lateral ligaments (LCL and MCL) were analysed. Their lengths were calculated as the geometric distance between two points representing their origins and insertions on the bones. For the MCL the wrapping around the femur and tibia surfaces has been accounted for by adding a midpoint between the femoral and tibial attachments as described in the previous chapter. The bones have been cut and positioned using the same procedure showed in the 4.2.1 paragraph.

TKR TF Model

The STLs of the femur and tibia were imported, and following the procedure developed in our previous work (Ascani et al., 2015) the origins and the insertions of the knee ligaments have been obtained from the CT scan. Since the prosthetic model used in this study is posterior stabilized, it was able to calculate the transformation matrices for the postoperative flexion position (90°) along with the postoperative extension position (0°). Therefore, for each patient two dynamic simulations were executed in two different position of the femoral component (Figure 5.2).

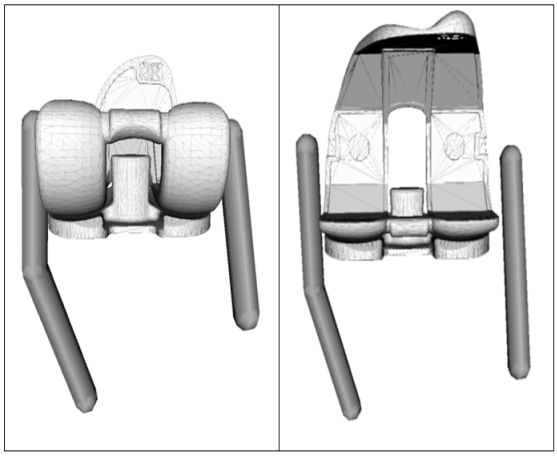

Figure 5.2 - *TKR TF model*

The new postoperative positions of the rigid bodies have been then used in Opensim to build the musculoskeletal models. The dynamic model comprises the femoral component, the tibial insert, and the two collateral ligaments (MCL and LCL).

The two rigid bodies were linked by a kinematic joint, which defines how the femur component moves respect to the grounded tibial insert. A 6 degrees of freedom joint was used to simulate the rotational and translational femur movements over the tibial insert. The center of rotation of the femoral component is the geometrical centroid of the polygonal mesh. In the TKR TF model most of the structures that wrap the joint such as the patella, the muscles, and the remaining soft tissue are not included. Consequently, the femur component, not having any constraints, kept bouncing and oscillating over the tibial insert not achieving a settled position. Therefore, to simulate the missing structure that act as constraint for the femoral component, translational and rotational springs were added on the centre of rotation. The forces developed by those springs account for the external forces applied to the model and the stiffness parameters were chosen considering

the range of motion allowed by the prosthetic implant. Since in this model the tibial insert is fixed and the femoral component is moving on the 6 degrees of freedom, many studies in literature have analysed the displacement of this prosthetic model in fixed positions. The external forces were applied only in selected directions:

- Medial-lateral direction
- Anterior-posterior direction
- Intra-extra rotation

The posterior stabilized prosthetic model is highly constrained and it allows: a translation in the medio-lateral direction of 2-3 mm, antero-posterior translation of 4-5 mm, an intra-extra rotation of 7°-10°. These values, that come from ex-vivo experiments found in the literature, were discussed and agreed by Medacta International SA which have conducted as well this kinematic test on cadavers. Consequently, the forces developed by the external forces maintained the prosthetic implant within the chosen range of motion.

The contact between the femoral component and the tibial insert has been modelled starting from the Elastic Foundation theory (Johnson, 1985), according to which the contacting solids are considered as rigid bodies except for a thin layer of elastic material of thickness h at the surfaces (Blankevoort et al., 1991; D'Lima et al., 2007; Johnson, 1985). The surfaces of each of the components of the implant that are in mutual contact have been approximated with a triangular mesh, created with the open source MeshLab software (http://meshlab.sourceforge.net/). The area A of the triangles was kept uniform and a spring was placed at the centroid of each triangle in the mesh. The force exerted by each spring along its displacement direction given by

$$F = k \cdot A \cdot x \cdot (1 + c \cdot v)$$

where:

k = stiffness of the springs

A = area of each triangle

x = displacement distance

c = dissipation coefficient of the springs

v = dx/dt

As a result, a "bed of springs" on the surface (Johnson, 1985) of each body was obtained, which was used to represent the push-back forces generated during the contact.

The layer of springs has a known thickness and it is present on both contacting surfaces, each spring is independent from the others. Each springs had a stiffness *k*,

$$k = \frac{(1-p)\cdot E}{(1+p)\cdot(1-2p)\cdot h}$$

Where:

E = Young's modulus

p = Poisson's ratio

h = thickness

The assumption of isolated springs gives an important advantage eliminating the integral nature of contact problems, this allows to analyse complex contacting surfaces and non-homogenous materials. The femoral and tibial components *.obj* meshes have been modelled with 4000 and 2000 triangles, respectively. The number of triangles has been chosen to have the area of the triangles on both surface, averagely. The material properties provided by Medacta allowed obtaining the body mass and the inertial tensors having considered the prosthetic components as homogenous rigid bodies. The elastic foundation model parameters needed to define the contact in Opensim were the stiffness, coefficient of dissipation, coefficient of static friction, coefficient of dynamic friction, and the coefficient of viscous friction. The values used to run the simulation can be found in the model parameters section (Page xxx) and they were calculated using a simplified model composed by a sphere and a cup with the same material properties of the prosthetic implant. This allowed to understand the sensitivity of the simulation algorithm with respect to the variation of these parameters, and they were set to have an interpenetration of the two surfaces less than 1 mm.

The method for modelling the ligaments is the force displacement curve that was first introduced by Blankevoort *et al.* (1991). The lateral collateral (LCL) and the medial collateral (MCL) ligaments were both modelled as one bundle element, the non-linear behaviour has been represented using one dimensional non-linear springs and non-linear splines which take the toe region into account. The ligaments' stiffness parameters (k), shown in the model parameters section, is taken from the literature (Marra et al., 2014) while the non-linear behaviour of the ligaments are described by the equation 1 and 2 (Blankevoort and Huiskes, 1996):

$$1) \qquad f = \begin{cases} 0 & \varepsilon > 0 \\ \frac{1}{4}k\varepsilon^2/\varepsilon_l & 0 \le \varepsilon \le 2\varepsilon_l \\ k(\varepsilon - \varepsilon_l) & \varepsilon > 2\varepsilon_l \end{cases}$$

$$2) \qquad \varepsilon = \left(\frac{l - l_0}{l_0}\right)$$

Where:

f = the tensile force of the ligament

k = the ligament stiffness

ε = the strain of the ligament

$2\varepsilon_l$ = the level at which the ligament moves from the non-linear region (toe region) to the linear region of the force-displacement curve.

The strain is obtained from the length l of the ligament and the resting length l_0. Two different non-linear curves, which attempts to simulate the non-linear behaviour of the ligaments, have been obtained from the literature (Arnold et al., 2010) for the MCL and LCL. The resting length, defined as the length of the ligament at which there is no strain, is a patient specific parameter calculated by the following formula:

$$l_r = \frac{l_0}{\varepsilon_r + 1}$$

where l_0 is the preoperative length of the ligaments and ε_r is the reference strain and the values is taken from the literature (Blankevoort et al., 1991).

The forces took into account in this dynamic configuration were:

1) gravity
2) forces developed by the ligaments
3) forces developed by the contact between the femoral component and the tibial insert
4) External forces

Forward dynamic simulations of the models were generated using the previously described musculoskeletal model to analyse the elongation of the collateral ligaments. The equations of motion were solved using the Simbody libraries (Sherman et al., 2011), included in Opensim, which consist of conventional error controlled, variable step integrators through time with a specified accuracy and include a variety of explicit Runge-Kutta methods, well-posed for biomechanical real time simulation (Hairer and Wanner,

1991). A convergence threshold has been then calculated, considering the linear and angular acceleration of the femoral component. In fact each dynamic simulation reached the convergence when the translational and angular accelerations of the femoral component were less than a threshold (0,001 m/s^2 and 0,001 deg/s^2 in our simulation). The simulation time was less than 10 minutes on 3.20 GHz Intel ® Xeon® personal computer. All the parameters are available in the model parameters section.

TKR PF Model

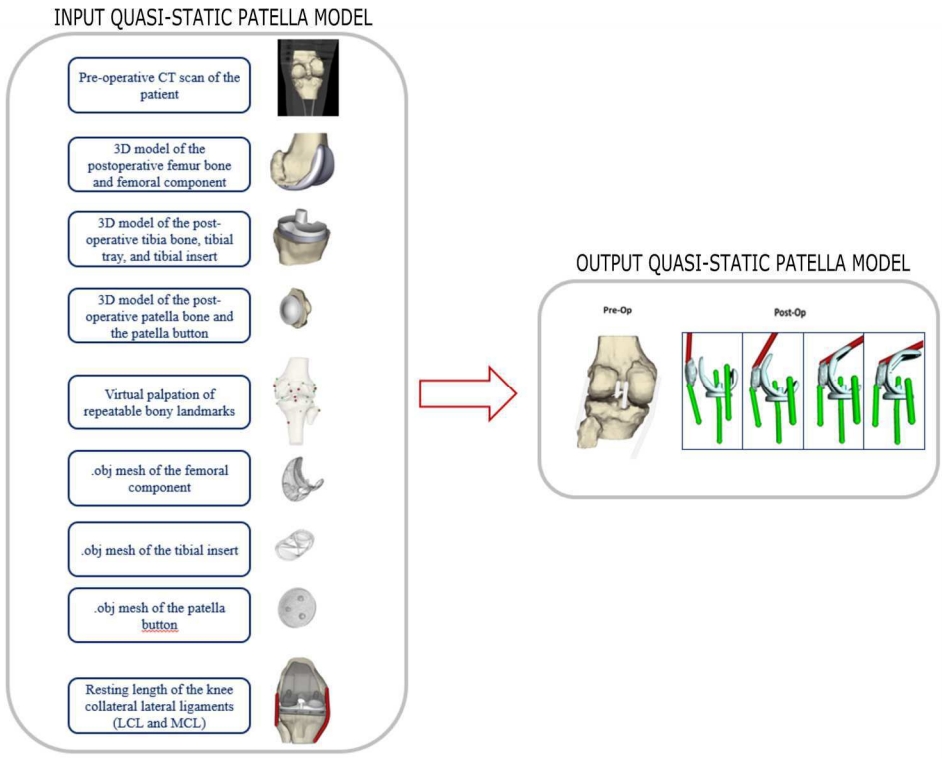

Figure 5.3 – *Input and output parameters of the quasi-static model with patella*

The second patient-specific model has been developed for each patient in NMS Builder adding the patella, the patellar tendon and the rectus femoris muscle which is one of the major extensor of the knee. Starting from the model previously created, the patella was imported and the origin and the insertions of the patellar tendon and the rectus femoris were registered. Although the same procedure was used (Ascani et al., 2015) to map those points, the atlas used in the registration procedure was inevitably extended adding the origins and the insertions of the patellar tendon and the rectus femoris muscle, using the "model of the lower limb for analysis of human movement" (Arnold et al., 2010). Since this model included new origins and insertions on the pelvis and the patella, also the expansion of the reference landmark cloud was necessary for the registration

procedure (Van Sint Jan, 2007). The new added landmarks were localised on the proximal area of the femur and the patella, since the origins and the insertions of the patella and the rectus femoris are localised in those areas. The new landmarks are: *CHF* (center of the femur head), *FCH1* (femur head top), *FCH2* (femur head anterior), *FCH3* (femur head bottom – next to femoral neck), *FCH4* (femur head posterior), *FCH5* (femur head lateral – above the femoral neck), *FCH6* (femur head medial), *PLE* (patella lateral edge), *PCE* (patella center edge), *PME* (patella medial edge), *PAX* (patella apex) (Van Sint Jan, 2007).

In addition to the positions of the femoral component obtained previously, two new angular positions at 30° and 60° degrees have been estimated in NMS Builder considering the radius of the femoral component for the lateral and medial compartment.

The TKR PF model is therefore composed by: the femoral component, the tibial insert, the patella insert, the patella, the rectus femoris muscle, and the two cruciate ligaments (MCL and LCL).

The patella and the patellar insert rigid bodies were linked by a weld joint, while the patellar insert was connected to the femoral component using the 6 degrees of freedom customized joint. The center of rotation of this joint was calculated as the geometrical center of the patellar insert mesh.

In addition to the constraints implemented previously, a spring along the axial direction of the femur was added in the 30°, 60°, and 90° of flexion positions (Figure 5.2). This constraint simulated the presence of the hip joint, in particular the displacement of the head of the femur inside the hip joint during the excitations of knee extensor muscles, which push back the femur into the acetabulum (Kapandji, 1974 – The Physiology of the Joints. Vol 2: Lower Limb). Considering the pelvis fixed, the movement of the femur inside the acetabulum is dictated by the thickness of the cartilage which averagely range from 2,5 mm to 2,8 mm (Kurrat and Oberländer, 1978; Lattanzi et al., 2014; Mechlenburg et al., 2007). Therefore, the spring placed along the axial direction of the femur simulated the femoral component movement by having a maximum displacement of *3* mm, the stiffness *k* of the spring has been calculated taking into account the push back forces of the patella during the contraction of the rectus femoris muscle, and the forces developed by the contact between the patella insert and femoral component (Figure 5.4).

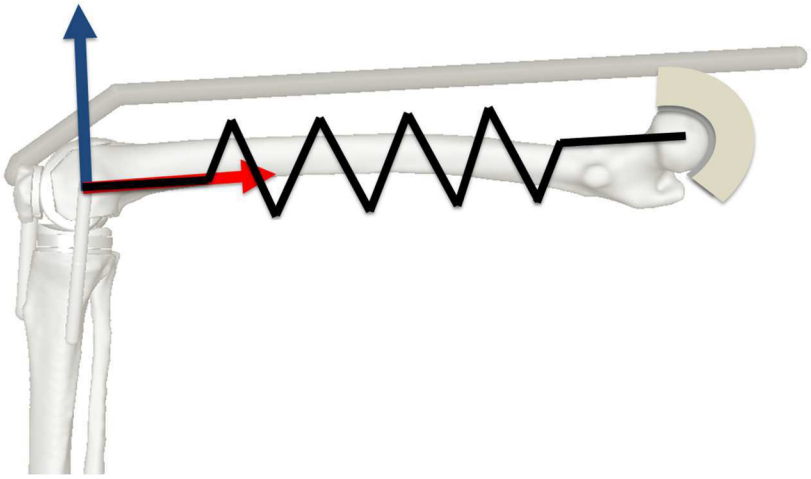

Figure 5.4 – *Knee joint modelling*

The contact between the patellar insert and the femoral component has been modelled following the same methodology and the same parameters of the previous model, based on the elastic foundation theory (Johnson, 1985), modelling the patellar insert with 1000 triangles.

The presence of an actuator such as a muscle in this model, allowed performing further investigation to observe how eventually the elongation of the knee collateral ligaments may be affected considering different level of excitation of the rectus femoris muscle (Seth et al., 2011). The muscles in Opensim are musculotendinous actuators, following Zajac (1989) to describe the active and passive force-length, force-velocity, and tendon force-strain curves, a dimensionless Hill-type muscle model needed the following parameters to be identified:

1) Maximum isometric force $(\boldsymbol{F^m_{ISO}})$
2) Tendon slack length $(\boldsymbol{l^t_s})$
3) Optimal fiber length $(\boldsymbol{l^m_0})$
4) Pennation angle at optimal fiber length $(\boldsymbol{\alpha_0})$
5) Maximum contraction velocity $(\boldsymbol{v_{max}})$

These parameters were taken from the work of Arnold et al. (2010) which is available at www.simtk.org and can be freely examined and analysed in OpenSim. The only subject specific parameters identified on the subjects were the origin and the insertions of the rectus femoris muscle.

The forces considered in this dynamic configuration were

1) gravity
2) forces developed by the two ligaments
3) forces developed by the contact between the femoral component and the tibial insert
4) forces developed by the contact between the patella insert and the femoral component
5) External Forces

Forward dynamic simulations of the TKR knee were generated using the previously described procedure to analyse the elongation of the collateral ligaments. The dynamic simulations reached the convergence when the translational and angular accelerations of the femoral component were less than a set threshold (0,001 m/s^2 and 0,001 deg/s^2 in our simulation). The simulation time for a single dynamic simulation was about 3 hours on 3.20 GHz Intel ® Xeon® personal computer. For each patient a total of sixteen forward dynamic simulations have been executed, and all the parameters are available in the model parameters section.

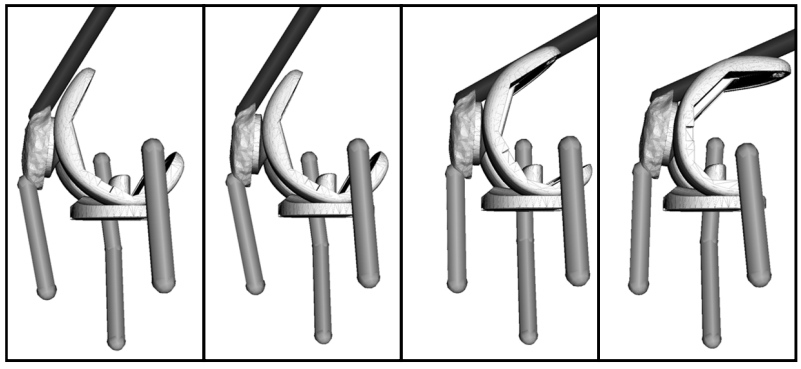

Figure 5.5 – *TKR PF model*

The criteria to evaluate the ligament balancing was based on defining a threshold as the maximum acceptable elongation before irreversible structural damages might occur. Although there are many works that have studied the ultimate strain of the knee ligaments, finding that the value is around the *17%* of the preoperative length (see Chapter 2). However, in order to avoid any possible damages, the 10% of the preoperative length was considered as the upper limit of elongation for the models' output. Therefore, our

models will suggest to the clinicians to impose a tension until the 10% of the preoperative length to perform a correct ligament balancing of the knee without provoking any irreversible damages.

Model Parameters

Material properties of the femoral and tibia component:

Implant Component	**Femoral component**	**Tibial baseplate**
Material	Co-Cr-Mo ISO 5832-4 (steel)	UHMWPE ISO 5834-2 (plastic)
Elastic Modulus *(MPa)*	2.08 E+11	7.2 E+9
Poisson's Ratio	0.3	0.45
Mass Density *(Kg/m^3)*	8280	944

Table 5.1 – *Material Properties*

Translation and rotational spring parameters:

k_{TX} (N/m)	800
Coefficient of dissipation - c_{TX}	0.8
k_{TY} (N/m)	800
Coefficient of dissipation - c_{TY}	0.8
k_{RZ} (N/m)	400
Coefficient of dissipation – c_{RZ}	0.8

Table 5.2 – *Translation and rotational spring parameters*

The Elastic Foundation Model parameters:

Stiffness (N/m)	90000000
Coefficient of dissipation	0.9
Coefficient of static friction	0.01
Coefficient of dynamic friction	0.001
Coefficient of viscous friction	0

Table 5.3 – *Elastic Foundation Model parameters*

Ligaments modelling parameters (Blankevoort et al., 1991):

Ligament	**Stiffness (N)**	ε_r
MCL	2000	0.04
LCL	2750	0.02
PT	∞	-

Table 5.4 – *Ligaments modelling parameters*

5.3 Results

All the models developed in this dissertation were evaluated by their ability to predict the elongation of the ligaments after a TKR surgery. Matching all the results allowed the evaluation of the most suitable model to be incorporated in a simulation framework to compute the TKR soft tissue balance.

TKR TF Model

The forward dynamic simulations performed for the TKR musculoskeletal model produced in output the elongation of the ligaments whenever the convergence threshold was achieved by the OpenSim dynamic solver (Figures 5.5 and 5.6). In addition to the previous results, it is also relevant to make a comparison with the same findings obtained by the geometric model. The figures below show that the length of the LCL and MCL obtained by the two models are very similar in both position (t=0.247, $p<0.05$), and the difference is never bigger than 1 mm. To notice that in the flexion position the models predict the same elongation in the majority of the cases.

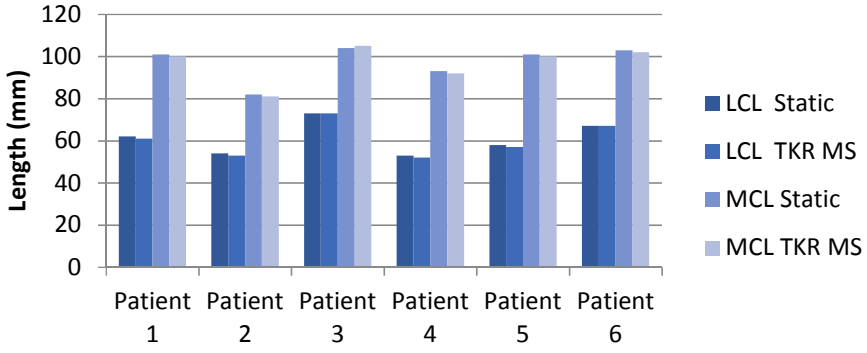

Figure 5.5 – *TKR TF Ligaments length in extension position*

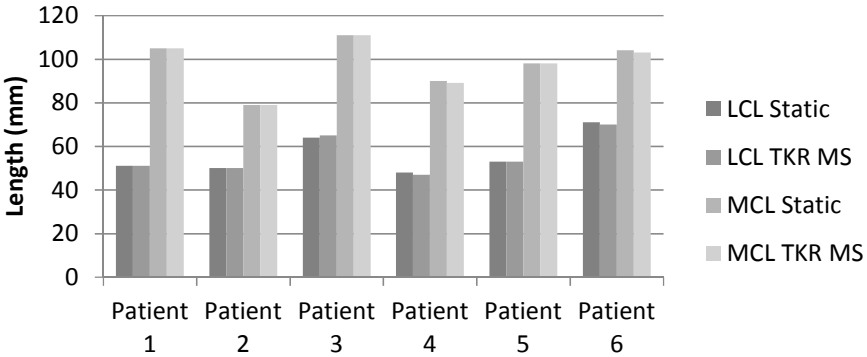

Figure 5.6 – *TKR TF Ligaments length in flexion position*

Furthermore, the percentage of elongation with respect to the preoperative length (preoperative position) has been calculated to observe if the length was under the 10% of their preoperative length (Tables 5.7 and 5.8). As shown in the tables below, although the lengths of the LCL and MCL ligaments are different from the preoperative length, the percentage of elongation remains under the 10% confirming the results of the geometric model.

Case	**LCL *(%)***	**MCL *(%)***
1	6	-2
2	5	-1
3	4	2
4	4	-3
5	-9	2
6	-1	1

Table 5.7 – *TKR TF Ligaments percentage elongation in extension position*

Case	**LCL *(%)***	**MCL *(%)***
1	-13	2
2	-3	4
3	-9	8
4	-6	-7
5	-16	0
6	5	1

Table 5.8 – *TKR TF Ligaments percentage elongation in flexion position*

TKR PF Model

The forward dynamics simulations performed on the models were longer than the previous ones, given the increased complexity of the TKR PF model. The results reveal that the rectus femoris excitations don't affect the ligaments elongation (Figure 5.9 and 5.10), contrarily the flexion angles of the femoral component dictates the changing in length of the collateral ligaments. The maximum difference found, considering different muscular excitation at the same flexion angle is about *1* mm. Moreover, the table below suggests that the LCL ligament, except for the patient 6, has a decrease in length of 10 % (range from *-16º to -5º*) from 0° to 90°. On the contrary, the MCL ligament showed a different result: half of the dataset decreased their length of *-3 %* from 0 to 90 degrees, the second half increased the elongation of *3%*. It can conceivably be said that the LCL

is more affected than the MCL ligament changing the angle of flexion from the fully extended position to the flexion position. This model confirms that the percentage of elongation on the preoperative length is still under the *10%*, confirming strongly the findings obtained with the two previous models.

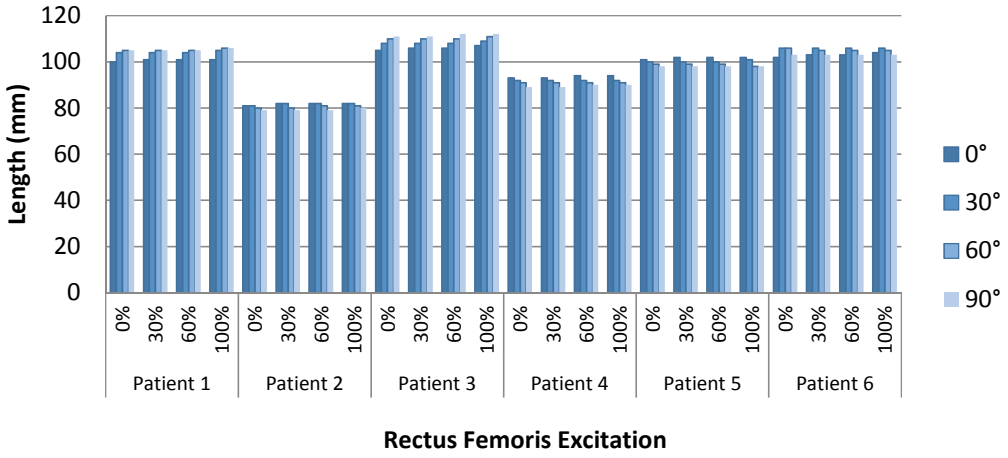

Figure 5.9 – *TKR PF forward dynamics simulation results of MCL*

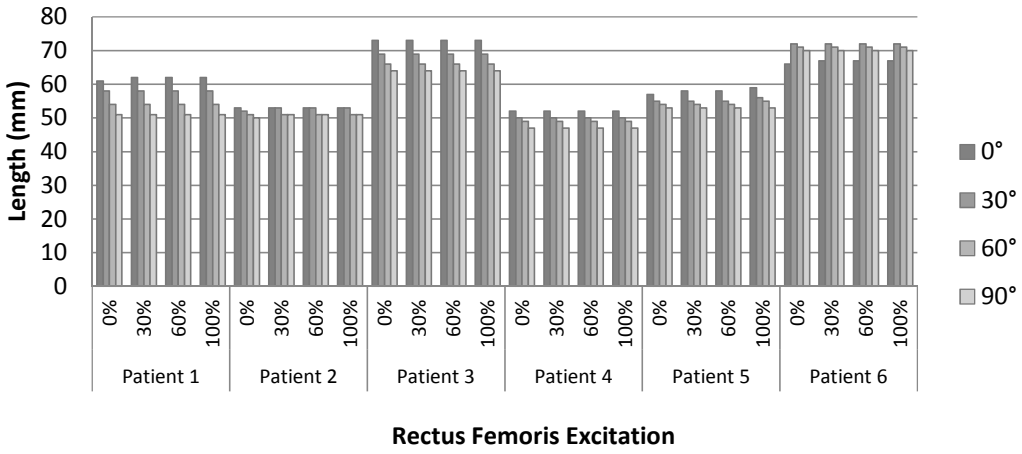

Figure 5.10 – *TKR PF forward dynamics simulation results of LCL*

The TKR P results have been successively compared with the geometric model (Tables 5.11 and 5.12), showing no significant differences (t=0.247, $p<0.05$) between the outputs. The maximum difference is still 1 mm and it doesn't affect the prediction based on the 10% threshold as stated before.

		Femoral Component Flexion (°)							
		0		30		60		90	
	Rectus Femoris Excitation (%)	*TKR PF (mm)*	*GEOM (mm)*	*TKR PF (mm)*	*GEOM (mm)*	*TKR PF (mm)*	*GEOM (mm)*	*TKR PF (mm)*	*GEOM (mm)*
P1	*0*	100	101	104	105	105	106	105	105
P2	*0*	81	82	81	82	80	81	79	79
P3	*0*	105	105	108	109	110	110	111	111
P4	*0*	93	93	92	93	91	92	89	90
P5	*0*	101	101	100	100	99	99	98	98
P6	*0*	102	103	106	106	106	106	103	104

Table 5.11 – *Comparison between the forward dynamic simulation results of TKR PF with no muscular activation and the Static model for the MCL ligament*

		Femoral Component Flexion (°)							
		0		30		60		90	
	Rectus Femoris Excitation (%)	*TKR PF (mm)*	*GEOM (mm)*	*TKR PF (mm)*	*GEOM (mm)*	*TKR PF (mm)*	*GEOM (mm)*	*TKR PF (mm)*	*GEOM (mm)*
P1	*0*	61	62	58	59	54	55	51	51
P2	*0*	53	54	52	53	51	52	50	50
P3	*0*	73	73	69	69	66	66	64	65
P4	*0*	52	53	50	51	49	50	47	48
P5	*0*	57	58	55	55	54	54	53	53
P6	*0*	66	68	72	72	71	71	70	71

Table 5.12 – *Comparison between the forward dynamic simulation results of TKR PF with no muscular activation and the Static model for the LCL ligament*

5.4 Discussion

The first goal of this paper is to develop a patient-specific musculoskeletal modelling framework based on CT, to estimate the outcome of a TKR surgery in terms of ligaments elongation. Two models, obtained increasing the complexity, have been proposed to compute the ligaments balancing after TKR surgery.

The geometric model (Chapter 4) has been developed including the femur, the tibia, the fibula and the two collateral ligaments of the knee (LCL and MCL), calculating the outcome of the surgery in terms of ligament balancing with the knee fully extended and at ninety degrees of flexion. The TKR TF dynamic model, instead, allowed obtaining the length of the LCL and MCL ligaments taking into account the contact between the femoral and tibial insert component, the forced developed by the ligaments, and the gravity. This version attempted to investigate the elongation of the ligaments when the forces are applied to two static positions: extension and flexion. The contacting model implemented, the elastic foundation (Johnson, 1985), is simple and versatile and makes the model ideal for incorporation into a multi- body dynamic simulation framework (Seth et al., 2011).

Afterward the TKR PF dynamic model has been developed to assess whether a more complex representation of the model substantially alters the model predictions. Further, two different positions were added (30° and 60°), and a sensitivity analysis has been performed to investigate how different intensity of muscle excitation may affect significantly the output of the model. The results of the TKR PF model revealed that the rectus femoris excitations don't affect the elongation of the ligaments, on the contrary the flexion angle of the femoral component changes consistently the output of the model. Nonetheless our findings revealed that the elongations of the ligaments measured at the two intermediate positions (30° and 60°) don't vary dramatically, as matter of fact they follow the flexion and extension positions trend. Therefore, this model clearly confirms that the evaluation of the ligaments balancing reduces to the flexion and extension positions. It can be said that the two positions geometrically defined in the geometric model can be used to analyse the elongation of the ligaments and then choosing the preoperative planning parameters to obtain an optimal soft tissue balancing.

The max difference between the models' prediction is equal to 1 mm, and more importantly all the models predicted an elongation under the 10% of the preoperative length, which represent the upper limit of elongation before irreversible damages may occur to the ligament (Butler et al., 1986; Woo et al., 1986, 2006). This finding stated that

the differences between the outputs of the models don't affect the ligament balancing in terms of examining the elongation under the 10% on the preoperative length, which ultimately represent the most functional information for the clinicians.

It may be conceivably said that, although there are substantial dissimilarities between the three models, the results clearly showed no significant differences in terms of ligaments elongation after the TKR surgery. Hence, concerning the computational cost, the static model may be considered as a robust choice to be incorporated in a simulation framework. The matrices operations which composes the static model procedure is certainly faster and lighter than solving dynamic differential equations.

This study includes some limitations that are worth discussing. First, we modelled the patellar tendon as a rigid link between the patella the tibia, so this may have been slightly change the position of the patella during the forward dynamics simulation (Sheehan and Drace, 2000). However, a different modelling of the patellar ligament may be the matter for further investigation. A second limitation is that in the TKR PF model only one extensor of the knee was included to perturb the ligaments elongation, however Pandy et al. (1997) demonstrated that the ligament elongation is largely governed by the geometry of the muscles passing through the knee joint. Further investigations, in the next chapter, will consider all the extensor and flexor muscles acting on the knee joint to estimate the ligaments elongation. Another limitation of this study is that this quasi-static approach is valid for this specific prosthetic model, it is unlikely to apply the same procedure for different prosthetic designs with less constraints. In fact, modifying the shape of the contacting surface the elongation of the ligaments would change a lot since is dictated by the kinematics imposed by the design.

The level of agreement of our results suggests that the TKR static model is a patient-specific musculoskeletal modelling framework based on computed tomography (CT) that reliably estimates the outcome of a TKR surgery in terms of ligaments elongation.

The automatic generation of the quasi-static models is an important aspect to consider, to create a single subject specific quasi-static model and execute the simulation can take up to 6 hours. The timing is partially justified by the computational time to compute the quasi static analysis with Opensim which takes one average 2 hours for each position analysed.

References

Arnold, E.M., Ward, S.R., Lieber, R.L., Delp, S.L., 2010. A model of the lower limb for analysis of human movement. Ann. Biomed. Eng. 38, 269–279.

Ascani, D., Mazzà, C., De Lollis, A., Bernardoni, M., Viceconti, M., 2015. A procedure to estimate the origins and the insertions of the knee ligaments from computed tomography images. J. Biomech. 48, 233–7.

Blankevoort, L., Huiskes, R., 1996. Validation of a three-dimensional model of the knee. J. Biomech. 29, 955–961.

Blankevoort, L., Kuiper, J.H., Huiskes, R., Grootenboer, H.J., 1991. Articular contact in a three-dimensional model of the knee. J. Biomech. 24, 1019–1031.

Butler, D.L., Kay, M.D., Stouffer, D.C., 1986. Comparison of material properties in fascicle-bone units from human patellar tendon and knee ligaments. J. Biomech. 19, 425–432.

D'Lima, D.D., Patil, S., Steklov, N., Colwell, C.W., 2007. An ABJS Best Paper: Dynamic intraoperative ligament balancing for total knee arthroplasty. Clin. Orthop. Relat. Res. 463, 208–212.

Delp, S.L., Anderson, F.C., Arnold, A.S., Loan, P., Habib, A., John, C.T., Guendelman, E., Thelen, D.G., 2007. OpenSim: Open-source software to create and analyze dynamic simulations of movement. IEEE Trans. Biomed. Eng. 54, 1940–1950.

Hairer, E., Wanner, G., 1991. Solving ordinary differential equations II: Stiff and differential-algebraic problems, SpringerVerlag.

Halloran, J.P., Easley, S.K., Petrella, A.J., Rullkoetter, P.J., 2005. Comparison of deformable and elastic foundation finite element simulations for predicting knee replacement mechanics. J. Biomech. Eng. 127, 813–818.

Hertz, H., 1881. On the contact of elastic solids. J. reine angew. Math 92, 156–171.

Hunt, K.H., Crossley, F.R.E., 1975. Coefficient of Restitution Interpreted as Damping in Vibroimpact. J. Appl. Mech. 42, 440.

Johnson, K.L., 1985. Contact Mechanics, Journal of the American Chemical Society.

Kurrat, H.J., Oberländer, W., 1978. The thickness of the cartilage in the hip joint. J. Anat. 126, 145–155.

Kwak, S.D., Blankevoort, L., Ateshian, G. a., 2000. A Mathematical Formulation for 3D Quasi-Static Multibody Models of Diarthrodial Joints. Comput. Methods Biomech. Biomed. Engin. 3, 41–64.

Lattanzi, R., Petchprapa, C., Ascani, D., Babb, J.S., Chu, D., Davidovitch, R.I., Youm, T., Meislin, R.J., Recht, M.P., 2014. Detection of cartilage damage in femoroacetabular impingement with standardized dGEMRIC at 3T. Osteoarthr. Cartil. 22, 447–456.

Li, G., Sakamoto, M., Chao, E.Y., 1997. A comparison of different methods in predicting static pressure distribution in articulating joints. J. Biomech. 30, 635–8.

Marra, M. a, Vanheule, V., Fluit, R., Koopman, B.H.F.J.M., Rasmussen, J., Verdonschot, N.J.J., Andersen, M.S., 2014. A Subject-Specific Musculoskeletal Modeling Framework to Predict in Vivo Mechanics of Total Knee Arthroplasty. J. Biomech. Eng. 137, 1–12.

Mechlenburg, I., Nyengaard, J.R., Gelineck, J., Soballe, K., 2007. Cartilage thickness in the hip joint measured by MRI and stereology--a methodological study. Osteoarthritis Cartilage 15, 366–371.

Pandy, M.G., Sasaki, K., 1998. A Three-Dimensional Musculoskeletal Model of the Human Knee Joint. Part 2: Analysis of Ligament Function. Comput. Methods Biomech. Biomed. Engin. 1, 265–283.

Pandy, M.G., Sasaki, K., Kim, S., 1997. A Three-Dimensional Musculoskeletal Model of the Human Knee Joint. Part 1: Theoretical Construction. Comput. Methods Biomech. Biomed. Engin. 1, 87–108.

Seth, A., Sherman, M., Reinbolt, J.A., Delp, S.L., 2011. OpenSim: A musculoskeletal modeling and simulation framework for in silico investigations and exchange. In: Procedia IUTAM. pp. 212–232.

Sheehan, F.T., Drace, J.E., 2000. Human patellar tendon strain. A noninvasive, in vivo study. Clin. Orthop. Relat. Res. 201–207.

Sherman, M.A., Seth, A., Delp, S.L., 2011. Simbody: Multibody dynamics for biomedical research. In: Procedia IUTAM. pp. 241–261.

Tumer, S.T., Engin, A.E., 1993. Three-body segment dynamic model of the human knee. J Biomech Eng 115, 350–356.

Van Sint Jan, S., 2007. Color atlas of skeletal landmark definitions: guidelines for reproducible manual and virtual palpations. CHURCILL LIVINGSTONE Elsevier, Philiadelphia (PA), USA.

Wismans, J., Veldpaus, F., Janssen, J., Huson, a, Struben, P., 1980. A Three-Dimensional Mathematical of the Knee-Joint. J. Biomech. 13, 677–685.

Wismans, J., Veldpaus, F., Janssen, J., Huson, A., Struben, P., 1980. A three-dimensional mathematical model of the knee-joint. J. Biomech. 13.

Woo, S.L., Debski, R.E., Withrow, J.D., Janaushek, M. a, 1999. Biomechanics of knee ligaments. Am. J. Sports Med. 27, 533–543.

Woo, S.L., Orlando, C.A., Gomez, M.A., Frank, C.B., Akeson, W.H., 1986. Tensile properties of the medial collateral ligament as a function of age. J Orthop Res 4, 133–141.

Woo, S.L.Y., Abramowitch, S.D., Kilger, R., Liang, R., 2006. Biomechanics of knee ligaments: Injury, healing, and repair. J. Biomech.

Zajac, F.E., 1989. Muscle and tendon: properties, models, scaling, and application to biomechanics and motor control. Crit. Rev. Biomed. Eng. 17, 359–411.

Chapter 6

A subject-specific dynamic musculoskeletal modelling framework to compute the knee soft tissue balancing for TKR surgery

This chapter aims to create a subject specific dynamic musculoskeletal model using the experimental data of the "Grand Challenge Competition to Predict In Vivo Knee Loads" (Fregly et al., 2012). The postoperative elongations of the knee ligaments are analysed by varying step-by-step each preoperative surgical parameters during a normal walking trial. The simulation of the gait task might allow to explore different surgical treatment that preserve the correct tissue balancing of the patient. The breakthrough of this approach is the development of an Orthopaedic Lifestyle Simulator, a surgical planning software that can help the surgeon to optimize the balancing of soft tissue, forecasting the type of physical activities that the patient is likely to return after the operation.

6.1 Introduction

An active life style after a TKR surgery has become a necessary requirement, especially for young patients, which now account for the 45% of the operated population (Baker et al., 2012). Unlike the medical literature, which indicates a successful rate of 95 % (Culliford et al., 2015) after ten years, more than 40% of the patients are not satisfied with their life style (Mannion et al., 2009). This fact might be related to the surgical procedure that is tuned on an elderly population that primarily concern stability over mobility. Thus, younger patients that have higher expectations in term of active life style, are not satisfied and more prone to revision surgeries (Heck et al., 1998). Although new prosthetic designs have been developed to meet these new demands (Jones and Huo, 2006), it has been demonstrated that an excessive physical activity is the second leading factor to revision surgery within the first two years after the operation (Heck et al., 1998).

Many studies in literature have demonstrated that most of the complications after a TKR surgery might be caused in the first place by a non-optimal balancing of the knee

ligaments (Dennis et al., 2010; Fehring et al., 2001). In fact, the knee ligaments, among the various soft tissues that surround the knee, play a central role in the stability and the function of the knee joint (Babazadeh et al., 2009). In this regard the best practice is intraoperative ligament balancing, based on passive functional tests, hardly representative of daily life.

The prediction of the postoperative knee ligaments elongation toward different daily life activities might represent an optimal solution to perform a correct balancing of the knee soft tissue. For instance, this might be very relevant for the creation of the subject specific cutting guides which define the new position of the tibia respect to the femur and consequently the postoperative elongation of the knee ligaments.

The creation of a patient specific musculoskeletal (MSK) modelling framework, to compute the knee soft tissue balancing toward different dynamic activities, seems to be a viable solution. In particular, the subject specific MSK model might represent a powerful tool for the surgeon that will explore how different prosthetic design or preoperative planning parameters will affect the soft tissue during a selected physical activity that belong to the patient's life-style.

The utility of MSK models in the clinic is very promising, however their limited application is represented by the impossibility of routinely validating the results, measuring forces within the human body. Small but comprehensive datasets made available in vivo measurements obtained from instrumented prostheses (Bergmann et al., 2007; D'Lima et al., 2012; Fregly et al., 2012; Westerhoff et al., 2009). Among them there is the free access database "orthoload" (www.orthoload.com) (Bergmann, 2008) which made available the contact forces of hip, shoulder, knee, and vertebral body, obtained by patients instrumented with telemetric prosthesis. A more complete dataset has been released by the "Grand Challenge Competition to Predict In Vivo Loads" which provides the knee contact forces, motion capture data, ground reaction forces, EMG, fluoroscopy, and pre and post-operative computed tomography (CT) images. The availability of these *in vivo* measurements are invaluable workbenches for validation of new modelling approaches, and in concert with the availability of software such NMSBuilder and OpenSim, allowed the research community to create and validate MSK models able to predict contact forces, individual muscle forces, and ligaments forces.

Kim et al. (Kim et al., 2009) created a MSK model to predict the leg muscle forces and validated the results using *in vivo* measurements of the knee contact forces from an instrumented prosthesis. The whole body was composed by 8 body segments linked by a

total of 21 degrees of freedom articulated linkage actuated by 58 muscle actuators and the knee ligaments (LCL, MCL, and popliteo-fibular ligament), the knee was a modelled as a hinge joint. The muscles and ligament forces were then used as input for a separated 3D quasi static knee model to estimate the lateral and medial knee contact forces. The 3D quasi static knee was a 6-deegrees-of-freedom joint and Hertzian contact theory was employed to calculate the interpenetration between the femoral and tibial components.

Thelen et al. (2014) developed a MSK model for the co-simulation of neuromuscular dynamics a knee joint mechanics during human walking. The contact between the femoral and the tibial surface has been modelled using the elastic foundation theory and the model was based on forward dynamic analysis. A computed muscle control algorithm (CMC) was used to modulate the muscle excitations to track measured joint angle trajectories during overground walking. In the investigation seventeen knee ligaments bundles were included in the model and the forces during the gait cycle were measured.

Marra et al. (2014) proposed a MSK modelling framework which comprehended two separate knee models: 1) one employing the traditional hinge joint solved using an inverse dynamic 2) another using an 11 degrees of freedom knee model solved with a force dependent kinematics (FDK) technique. The knee ligaments were modelled as non-linear multi-bundles springs and the attachments were determined following the description found in the literature, forces were then measured during one normal gait and one right-turn trial. The KCF were predicted by both hinge and FDK knee models with a root mean square error (RMSE) and a coefficient of determination (R^2) smaller than 0.3 body weight (BW) and equal to 0.9 in the gait trial simulation and smaller than 0.4 BW and larger than 0.8 in the right-turn trial simulation, respectively.

Kia et al. (Kia et al., 2014a) developed a full body MS model to evaluate six muscles driven forward dynamic simulations of walking. The model was built scaling on the lower limb of the subject a generic model based on anthropometric database available in literature (Obergefell and Rizer, 1996). The knee was modelled as a tri-axis hinge joint constrained by a combination of passive torsional spring-damper and restricted anatomical range of motion to limit the movement. The medial and lateral collateral ligaments are modelled as three bundles fibre finding a peak of 200 N at the end of the swing phase.

None of the above studies have investigated how the presence of the prosthetic implants affect the knee soft tissue balancing during a dynamic task such as walking.

Further, often the authors adopted methods for tuning the model parameters specifically aiming at optimizing the comparison with the experimental data. This approach seems likely to be difficult to reproduce and be adopted by an industrial patient-specific modelling frameworks.

The specific aims of this study is a subject specific MSK modelling framework to compute the soft tissue balancing in TKR patients, through a sensitivity analysis of the preoperative planning parameters during normal walking.

6.2 Materials and Methods

Experimental Data

The experimental data used in this chapter was entirely taken from the literature using the third "Grand Challenge Competition to Predict In Vivo Knee Loads" data (Fregly et al., 2012) available on the SimTk.org website (https://simtk.otg/home/kneeloads). The knee grand challenge competition represents one of the most complete dataset for human movement and imaging data for a patient with a knee instrumented prosthesis implanted. The motivation to make publicly available this dataset is to engage the biomechanical researchers in validating the models using the experimental knee joint contact forces (KCF). The engagement is realized under the form of a challenge in which the participants can predict the KCF and the most accurate prediction will win the competition. In particular, the participants have to send the prediction without knowing the experimental data (*blinded prediction*), after the release of the tibiofemoral forces they can improve the models and send a second prediction (*unblinded prediction*). So far, six dataset have been released and between them there are some differences in terms of data available. Among them we used for this study the third grand knee challenge because the kind of data available were more relevant to the specific aim of this study. In particular the presence of the preoperative MRI images allowed to validate the knee ligaments origins and insertions, the accuracy of this step is crucial for the purpose of this study.

The data available for this challenge were obtained from a female subject who have undergone to a posterior cruciate-retaining total knee replacement surgery of her left knee (female, height=167 cm, BW = 78.4 Kg, instrumented knee side = left). The prosthetic implant used in this study was different from the previous used in the geometric

and quasi-static models.

The dataset included:

a. *Geometry data* – The geometric stereolithography (STL) of the femoral component, tibial tray and insert, patellar button, along with the post-operative bone geometries of hemi pelvis, femur, patella, tibia, fibula, calcaneus, and talus.

b. *CT data* – The post-operative CT scan of the whole leg (pelvis to calcaneus), the pre-operative CT scan of the knee (distal femur, proximal tibia, proximal fibula, and patella)

c. *MRI data* – The MRI images of the preoperative knee region (distal femur, proximal tibia, proximal fibula, and patella).

d. *Motion data* – The experimental data collected in the gait laboratory includes the gait trials of the subject for different gait pattern. Every gait experimental pattern comprehends the trajectories of motion capture markers, ground reaction forces, and EMG signals of 15 lower extremity muscles on the leg with the instrumented prosthesis. Further the static trials, the calibration trials, the joint trials, and the maximum isometric EMG for the normalization of the EMG signal were available to construct the model. All the gait trials were performed over ground and on an instrumented tread mill.

e. *Strength data* – The strength data were acquired testing the instrumented knee of the patient with a BIODEX isokinetic dynamometer. The biodex trials were performed to calculate the patient specific maximum joint moments.

f. *eTibia data* – the data from the instrumented prosthesis was recorded and synchronized with the EMG signal for every gait, static, or calibration trial. The dataset included the forces (*Fx, Fy, Fz*) and the momentum (*Tx, Ty, Tz*) measured by the load cells over the trials. The medial and collateral forces can be calculated using the data measured through this regression equation:

g.

$$F_{medial} = 0.942 * Fx + 0.497 * Fz + 0.0184*Ty$$

$$F_{lateral} = -0.942 * Fx + 0.503 * Fz - 0.0184*Ty$$

The *eTibia* (D'Lima et al., 2005) instrumented prosthesis implant is a

custom tibial tray which embedded 4 axial load cells placed on the four corners of the metallic tray (Figure 6.1). The force transducers can measure the total tibiofemoral force or the medial and lateral distribution, allowing the calculation of the center of pressure and the mediolateral and anteroposterior moment. The eTibia sensors include also a micro-transmitter that connects the load cells with the transmitting antenna for the telemetric transmission of the force data. An external receiver connected to a PC manages the streaming, the visualization, and storage of the data (D'Lima et al., 2005).

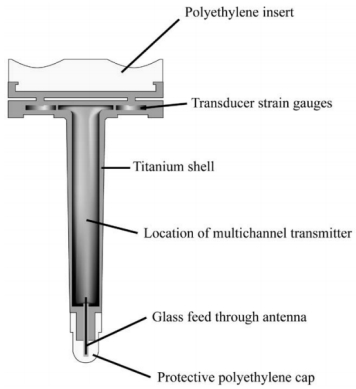

Figure 6.1 – *eTibia instrumented implant. The load cells are placed on the tibial tray whilst the antenna is located at the bottom, protected by a plastic tip*

All the measurements were given in two different datasets, one containing the raw data and a second with the data filtered, resampled, and synchronized using a common goniometer or the EMG muscle signal.

6.22 Subject specific musculoskeletal modelling framework for tissue balancing

The construction and the validation of the subject specific musculoskeletal (MS) model required the following steps (Figure 6.2):

a. Creation of the subject specific geometric model
b. Definition of the joints
c. Muscles origins and insertions
d. Knee ligaments origins and insertions
e. Identification of the subject specific muscles parameters
f. Inverse kinematics and Inverse dynamic
g. Static Optimization
h. Validation of knee joint contact forces (KCF)
i. Sensitivity analysis of the surgical variables for the soft tissue balancing

The framework is rather cumbersome and the complexity increases substantially throughout the process. Despite that, using this data a number of subject specific models have been previously proposed and validated in literature (Guess et al., 2010; Manal and Buchanan, 2013; Marra et al., 2014) until the step *h*. The proposed solutions, however, often adopted modelling approaches or criteria for tuning the model parameters specifically aiming at optimizing the comparison with the experimental data, turned out to be difficult to reproduce and be adopted by others as generic modelling frameworks. Therefore, in this study we introduced a reproducible procedure for subject specific musculoskeletal modelling based on freely available tools and on a limited number of operator dependent choices for the identification of critical model parameters, including joint axes, muscle origins and insertions, tendon slack and optimal fiber lengths.

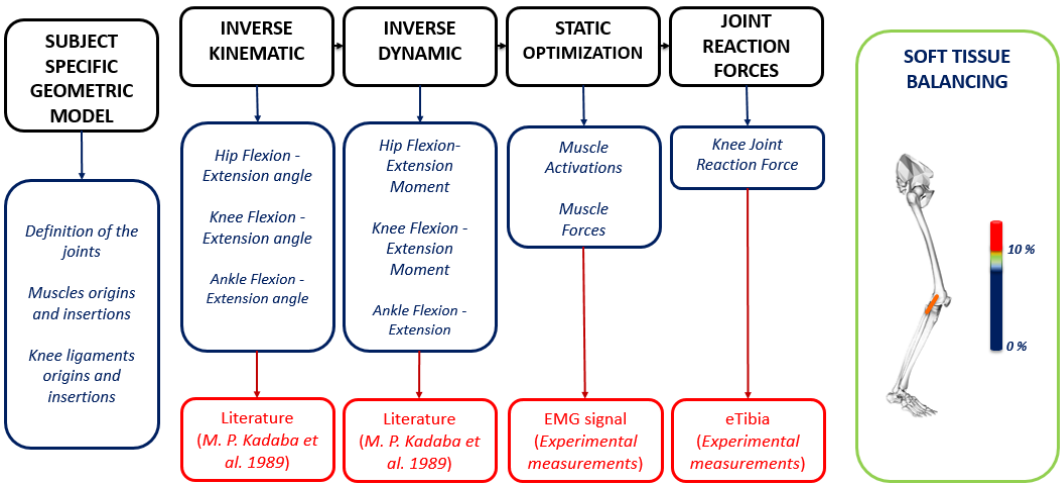

Figure 6.2 – *Subject specific musculoskeletal modelling framework to compute the soft tissue balancing*

a) Creation of the subject specific geometric model

A musculoskeletal model of the lower limb was created from the data made available for the 3rd Grand Challenge competition (Figure 6.3), a 5-body model (pelvis, femur, patella, shank, foot) has been created aligning the STL geometries (STL_3) provided by the dataset, and registering the missing body segments (metatarsal and toes). The developed model consisted of five groups that comprehend the bones geometries and the artificial implants:

- PELVIS
- FEMUR (Femur and Femoral component)
- PATELLA (Patella and patellar button)
- SHANK (Tibia, fibula, tibial insert, and tibial tray)

- FOOT

The alignment procedure was performed using NMSBuilder (SCS srl, Italy) where the STL_3 were registered onto the STL segmented directly from the CT images. That allowed to add to the aligned geometries also the soft tissue of the patient. The surface registration operations were performed in NMS Builder using a feature called "registration surface" that employs algorithms based on the iterative closest point (ICP) technique (Besl and McKay, 1992). The ICP technique minimizes the difference between two rigid clouds of points and it results very accurate when the two points clouds have the same shape (Du et al., 2010). By this means in our procedure we registered bones geometries of the same subject achieving an excellent match, however, this technique may likely not be appropriate for registration of bones geometries of different subjects because the introduction of scaling factors employs an affine transformation.

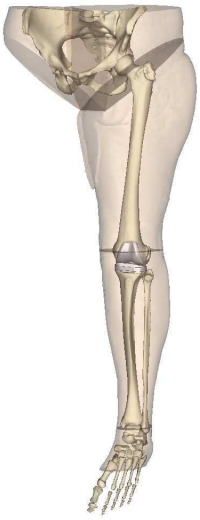

Figure 6.3 – *Geometrical lower limb musculoskeletal model*

The missing body segments of the foot (metatarsal and toes) were replaced using generic bone geometries available in literature (Delp et al., 1990). The body segments' inertial properties (White et al., 1987) were calculated accounting for different tissue densities using the function available in NMSBuilder (Table 6.1).

Group	Body	Density (Kg/mm^3)
PELVIS	Pelvis bone	1.42 e-06
	Pelvis Soft Tissue	1.02 e-06
FEMUR	Femur bone	1.42 e-06
	Femoral component	8.28 e-06
	Femoral Soft Tissue	1.02 e-06
	Patella bone	1.42 e-06

PATELLA	Patella button	9.44 e-07
SHANK	Tibia bone	1.42 e-06
	Fibula bone	1.42 e-06
	Tibial Insert	9.44 e-07
	Tibial Tray	8.28e-06
	Shank soft tissue	1.02e-06
FOOT	Foot bone	1.42 e-06
	Foot soft Tissue	1.02e-06

Table 6.1 – *Body segments' inertial properties* (White et al., 1987)

b) Definitions of the joints

The definition of the centre and rotation axes of the lower limb joints were accomplished fitting known geometries to the anatomical sites (Figure 6.4). This operation has been executed automatically through a Matlab script that allowed a least square fitting of a sphere to the femoral head and two cylinders to the femoral component, and talus trochlea. The posterior condyles of the femoral component can be approximated with a cylinder, the script allowed to calculate a cylinder with a radius comparable to the prosthetic implant and to minimize the distance between them. This operation, that identified the axis of rotation of the knee joint, was validated measuring the Hausdorff distance (Dubuisson and Jain, 1994) that was less than 1 mm. Hence, the hip joint was defined as a ball socket joint with three rotational degrees of freedom, where the centre of rotation is the centre of the sphere fitted. The three degrees of freedom of the joint describe the physiologic hip movements such: the flexion/extension, adduction/abduction, and rotation. The knee joint was modelled as a hinge joint with one rotational degree of freedom (sagittal plane), the cylinder fitted on the implant defined the axes of ration of the knee angle. The femoral component is a double radii prosthetic implant, meaning that one portion of the contact surface can be approximated with a single radius. It can be said that, during walking the portion of femoral component surface that is more in contact with the tibial insert, defining consequently the motion, is the posterior part. Therefore, the cylinder was fitted considering the curvature of the posterior portion to define the axis of the knee flexion-extension angle.

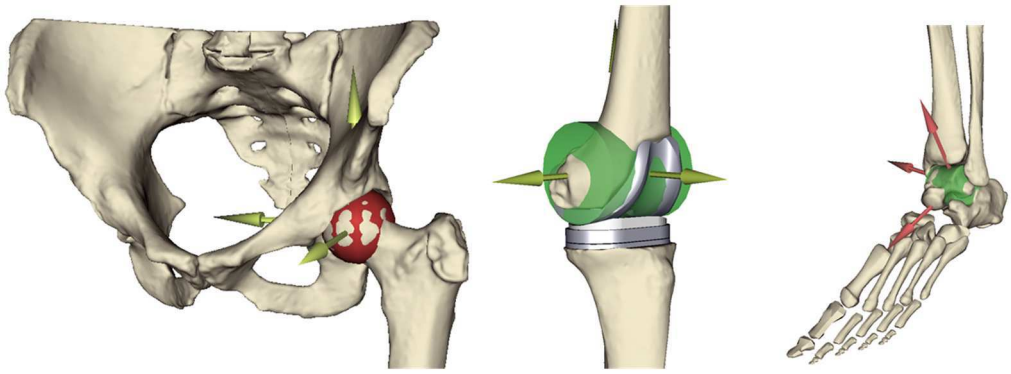

Figure 6.4 – *The definition of the body joints: ball socket (hip) and hinge (knee and ankle)*

The patella-femoral joint was modelled with a custom joint where the frontal and transversal rotations were neglected to describe the movement of the patella on the femur. The motion path was accurately described considering the congruency of the patella button with the surface of the femoral component, which can be described as an arc of circle. The motion of the joint then was defined using a spline where the four degrees of freedom were coupled with the knee joint angle. The four degrees of freedom are: the three translational degrees of freedom and the rotation on the sagittal plane. This constraint allowed having a correct movement of the patella entirely dependent by the knee flexion-extension angle; the talus trochlea joint was defined as a hinge joint in the same manner, fitting a cylinder to the bone and describing the rotation axes of the ankle flexion-extension. It is important to point out that the operation to place and size the fitting geometries was completely automatic and not operator-dependant. The LSGE Matlab library (http://www.eurometros.org) was used for fitting the cylinders to the bone geometries. This freeware library was assessed and verified against *ad hoc* generated test cases before its inclusion in the modelling pipeline.

c) Muscle origins and insertions

The muscles origins and insertions were obtained in NMSBuilder through an affine transformation that registered a reference atlas of muscles attachments (Delp et al., 1990) onto the patient bone geometries using reproducible and easily identifiable reference points (Van Sint Jan, 2007). The registration procedure took also into account the wrapping of the muscles around the bones, registering the necessary via points to define the correct path of the muscles. The accuracy of the muscles' path is crucial in the MS model because the distance of the muscle's line of action to the joint's center of rotation

defines the muscle moment arms. By that means, the definition of an inaccurate path could neglect the muscle contribution in the generation of the joint torque.

The registration method used in this chapter follows the procedure outlined in the Chapter 3: a reference landmarks cloud (C_R), containing the knee ligaments attachments, was registered trough an affine transformation to a subject-specific landmark cloud (Cs) that includes reproducible and repeatable bony landmarks. In this section the C_R contains the muscle origins and insertions, the Cs was appropriately extended to the whole lower limb using the same descriptive guidelines for the virtual palpation used in the Chapter 3 (Van Sint Jan, 2007). Thus, a landmark cloud of palpable and repeatable bony landmarks was created, for each body segment. The obtained model included 43 Hill-type musculotendon units acting across the hip, knee, and ankle joints. The patella body was articulated with the femoral component body as reported in DeMers et al. (2014) defining a coupled knee mechanism with 1 degree of freedom (Figure 6.5). The movement of the patella was determined by prescribed functions dependent by the knee flexion angle. The quadriceps muscles were wrapped around the patella and attached to the tibia in the patellar ligament insertion. Mechanically, the quadriceps muscle forces were transmitted along the line of action of the patellar ligament and the patella body worked as frictionless pulley during the knee flexion. This mechanism allowed to estimate the correct knee contact forces (Lerner et al., 2015).

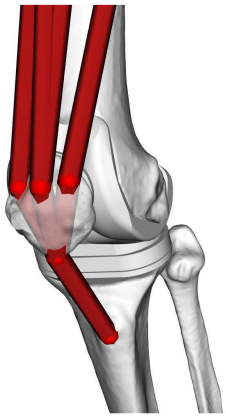

Figure 6.5 – *The musculoskeletal model was modified to transmit the forces of the quadriceps through the patella to the tibia*

d) Knee ligaments origins and insertions

The collateral lateral knee ligaments (LCL and MCL) were added to the lower limb model. The estimation of the ligaments origins and insertions were computed on the preoperative CT scan of the subject available in the dataset, following the procedure outlined in the Ascani et al. (Ascani et al., 2015) study. The affine registration allowed

the registration of the ligaments' attachments on the patient's bone geometries along with a medial point that permits the wrapping of the MCL around the femur and tibia, imitating the anatomical path on the bone surface. Hence, the LCL was represented as a straight line whilst the MCL is composed by two connected line segments. Although it has been demonstrated that the procedure is robust enough to have the same level of accuracy reachable using MRI images, the values were verified using preoperative MRI images available in the dataset. Also the path of the MCL was carefully checked on the images were the soft tissue is rather visible (Figure 6.6). The operation of virtual palpation, affine registration, and MRI validation were entirely performed in NMSBuilder.

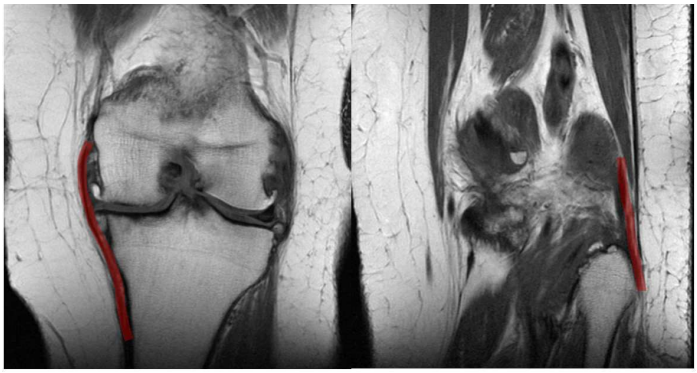

Figure 6.6 – *MRI knee ligaments preoperative position*

The knee ligaments were both modelled as one bundle element, the non-linear behaviour has been represented using one dimensional non-linear springs and non-linear splines which take the toe region into account. The non-linear behaviour of the ligaments are described by the equation 1 and 2 (Blankevoort and Huiskes, 1996):

$$f = \begin{cases} 0 & \varepsilon > 0 \\ \frac{1}{4} k\varepsilon^2/\varepsilon_l & 0 \leq \varepsilon \leq 2\varepsilon_l \\ k(\varepsilon - \varepsilon_l) & \varepsilon > 2\varepsilon_l \end{cases}$$

where

$$\varepsilon = \left(\frac{l - l_0}{l_0}\right)$$

f = the tensile force of the ligament

k = the ligament stiffness

ε = the strain of the ligament

ε_l = the level at which the ligament moves from the non-linear region (toe region) to the linear region of the force-displacement curve.

The strain is obtained from the length l of the ligament and the resting length l_0. Two different non-linear curves, which attempts to simulate the non-linear behaviour of the ligaments, have been obtained from the literature for the medial collateral ligament (MCL) and the collateral lateral ligament (LCL). The resting length, defined as the length of the ligament at which there is no strain, is a patient specific parameter calculated by the following formula:

$$l_r = \frac{l_0}{\varepsilon_r + 1}$$

where l_0 is the initial length of the ligaments and ε_r is the reference strain and the values are taken from the literature (Blankevoort et al., 1991). All the parameters are shown in the table below (Table 6.2):

Ligament	**Stiffness (N)**	$\boldsymbol{\varepsilon_r}$	$\boldsymbol{l_r}$
MCL	*2000*	*0.04*	*0.09*
LCL	*2750*	*0.02*	*0.06*

Table 6.2 – *Knee ligaments' parameters used in the model*

e) Identification of the subject specific musculotendon parameters

Following Zajac (1989) to describe the active and passive force-length, force-velocity, and tendon force-strain curves, a dimensionless Hill-type muscle model needed the following parameters to be identified:

1) Maximum isometric force $(\boldsymbol{F_{ISO}^m})$
2) Tendon slack length $(\boldsymbol{l_s^t})$

3) Optimal fiber length ($\boldsymbol{l_0^m}$)
4) Pennation angle at optimal fiber length ($\boldsymbol{\alpha_0}$)
5) Maximum contraction velocity ($\boldsymbol{v_{max}}$)

The F_{ISO}^m of each muscle was estimated using the experimental Biodex strength data provided by the dataset using the following procedure. Maximum isometric forces from Delp et al (1990) were assigned to the correspondent musculotendon units of the model. The MSK model was used to replicate computationally one of the maximum voluntary isometric contractions recorded experimentally. The subject has knee at 90 degrees of flexion, whereas the hip joint was flexed of 80 degrees and the ankle joint was in neutral position. The subject was exerting maximum flexion-extension knee joint moment. From the ratio of experimental and computational knee joint moments, scaling factors for were calculated the knee extensors and flexors muscle groups and used to update the F_{ISO}^m of the muscles in order to match the experimental values (Figure 6.7).

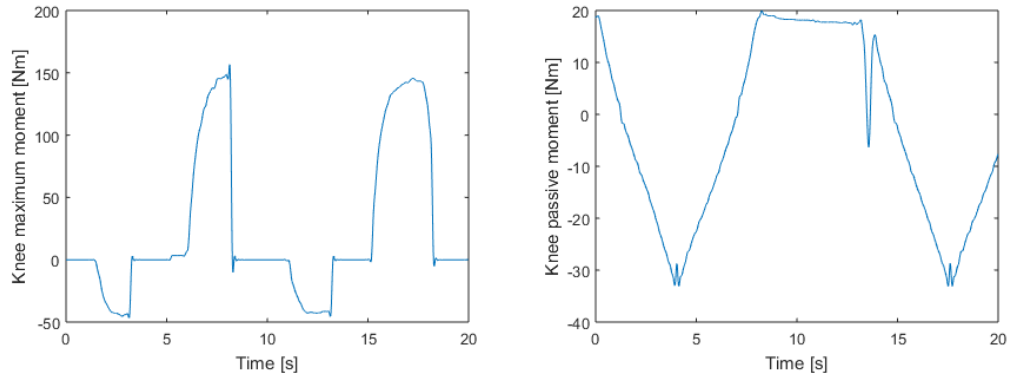

Figure 6.7 – *Knee maximum moment and knee passive moment developed by the model simulating the Biodex test. The maximum activation of the muscles with positive moment arm (agonist muscles), with respect to the direction of interest (flexion or extension) allowed the calculation of the maximum joint moment. The group of muscles with a negative moment arm (antagonist muscles) generated the maximum passive moment with respect to the direction of interest.*

The muscle parameters for the quadriceps were taken from the DeMers et al. (2014) model to take into account the new length of the fibres due to the attachment on the tibia tuberosity instead of the patella. The remaining muscle parameters were adopted from the Delp et al. (1990) model available in literature.

f) Inverse kinematics and Inverse dynamics

The standard plug-in-gait marker set in the model was edited to match the experimental marker locations from a static trial

Joint angles and moments were calculated for four gait cycles from different overground trials (*SC_ngait_og5, SC_ngait_og6, SC_ngait_og7, SC_ngait_og8*) using the OpenSim *inverse kinematics* and *inverse dynamics* tools.

The inverse kinematics (IK) tool allowed the estimation of the joints angle (hip flexion-extension, hip abduction-adduction, hip rotation, knee flexion-extension, and ankle flexion-extension) throughout the full gait cycle (heel strike – heel strike). To run the simulation, the trajectories of the experimental gait markers from the motion capture were used as input. The OpenSim solver computes for each frame of time the generalized coordinates that describe the position of the model that best matches the experimental gait markers and the virtual markers added to the model. Mathematically the IK tool solves a weighted least square problem which aim to minimize the error of the coordinate and marker in a specific time step:

$$\min_{q}\left[\sum_{i\epsilon markers} w_i\left\|x_i^{exp}-x_i(q)\right\|^2+\sum_{j\epsilon unprescribed\ ccords}\omega_j(q_j^{exp}-q_j)^2\right]$$

$$q_j = q_j^{exp}\ for\ all\ prescribed\ coordinates\ j$$

where **q** is the vector of generalized coordinates being solved for, $\boldsymbol{x_i^{exp}}$ is the experimental position of marker ***i***, $\boldsymbol{x_i(q)}$ is the position of the virtual marker on the model, $\boldsymbol{q_j^{exp}}$ is the experimental value for coordinate ***j***. The maximum error between the experimental and virtual markers during the simulation of the movement should be less than 2-4 cm, while the RMS around 2 cm (REF). If this condition is not achieved during the IK simulation, then the placement of the virtual markers on the model should be corrected until a satisfactory match is accomplished. The matching between virtual and experimental market were around 1.5 cm on average and the RMS around 2 cm.

The marker set utilized to compute the IK includes 20 markers placed on the subject's lower limb and they are reported in Figure 6.8.

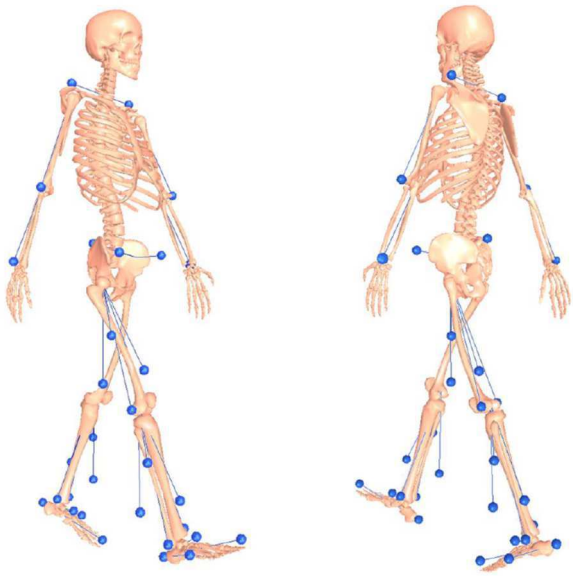

Figure 6.8 – *Marker set used for static and dynamic trials*

The inverse dynamic (ID) tool allowed to determine the moments and the forces of each joint needed to perform the motion obtained from the IK. Indeed, the motion of the model (IK) and the ground reaction forces, measured from the force plates, represented the input of the ID tool analysis. The OpenSim tool solves the classic mechanics equations of motion for the unknown joints moment and force, using the known motion of the model (IK).

$$\mathbf{M}(\mathbf{q})\ddot{\mathbf{q}} + \mathbf{C}(\mathbf{q}, \dot{\mathbf{q}}) + \mathbf{G}(\mathbf{q}) = \boldsymbol{\tau}$$

where $\boldsymbol{q}, \dot{\boldsymbol{q}}, \ddot{\boldsymbol{q}}$ are the generalized coordinated of position, velocity, and acceleration respectively. $\boldsymbol{M(q)}$ is the mass of the body segment, $\boldsymbol{C}(\boldsymbol{q}, \dot{\boldsymbol{q}})$ is the vector of the Coriolis and centrifugal forces, and $\boldsymbol{G(q)}$ is the vector of the gravitation forces. $\boldsymbol{\tau}$ is the unknown variable vector of moments and forces.

In order to replace the dynamic contribution related to the missing torso and contralateral leg, coordinate actuators acting to the 6 degrees of freedom of the pelvis respect to the ground were added to the model. This operation is fundamental to replace the missing forces on the pelvis and to ensure dynamic consistency of the system. The predictions were expressed as a fraction of the BW and resampled on a 0-100% trial duration scale with a step interval of 1% from heel strike to the subsequent heel strike. The results were assessed with data available in literature.

g) Static Optimization

The static optimization (SO) tool allowed estimating the individual muscle forces and activations on the net joints moment by minimizing the sum of muscle activations squared. This tool is an extension of the ID tool because it resolves in the same manner the equations of motion but following a specific muscle activation-to-force condition. To run the simulation, the motion of the model (IK) along with external loads (ground reaction forces, moments, and centers of pressure) were used as input.

The musculoskeletal system is an underdetermined system which has more unknown variables than equilibrium equations. Mathematically it is a redundant system excluding the possibility of having a unique solution for the muscle forces of the model. The solution employed in this study is a static optimization of the muscular forces through which the dynamic muscles forces are considered as quasi-static in each frame of time. The optimization theory also allowed solving the equation of motion using different criteria for the optimal behaviour of the recruitment strategy. Therefore, the SO tool solved for each muscle *m*, a force generator constrained by force-length-velocity properties:

$$\sum_{m=1}^{n} [a_m f(F_m^0, l_m, v_m)]\, r_{m,j} = \tau_j$$

while minimizing the objective function

$$J = \sum_{m=1}^{n} (a_m)^p$$

where *n* is the number of muscles, $a_m$is the activation level of the muscle *m*, F_m^0 is the maximum isometric force, l_m is the muscle length, v_m is the shortening velocity, $r_{m,j}$ is the moment arm about the j^{th} joint axis, τ_j generalized force acting about the j^{th} joint axis, and *p* is user defined constant.

The criterion to compute the muscle recruitment strategy was dictated by the objective function employed in the SO tool that aim to minimize the muscle activations. This strategy might be unlikely for not healthy subjects, however the OpenSim solver didn't provide the possibility to change and try different objective function.

The output of the SO analysis, which are the individual muscle forces and the activations throughout the full gait cycle, have been compared with the EMG data

available in the dataset to assess quantitatively the accuracy of the results. The accuracy of the muscular forces is crucial to determine correctly the tibiofemoral forces of the model.

h) Validation of the KCF

The joint reaction tool allowed the estimation of the KCF and moments between the femur and the tibia. To run the simulation, the following inputs were provided to the JR tool:

- Motion of the model (IK)
- External loads (ground reaction forces, moments, centre of pressure)
- Names of the joint and the body
- Muscle forces (SO)

The OpenSim joint reaction tool calculates the KCF isolating the body of the joint of interest from the kinematic chain. To calculate the joint reaction on the tibia, the solver computes the six dimensions Newton-Euler equation of motion of the tibia constructing the free body diagram in the moving space (Figure 6.9):

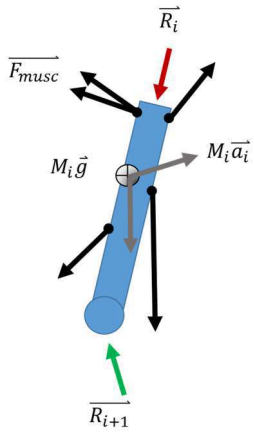

Figure 6.9 – *Joint reaction body diagram of the tibia body segment*

$$\vec{R}_i = M_i\vec{a} - \left(\sum F_{ext} + \sum F_{musc} + \sum F_{constraint} + \vec{R}_{i+1}\right)$$

where M_i is the mass of the tibia, $\vec{a}$ is the linear acceleration of the tibia including the Coriolis and gyroscopic acceleration, $\sum F_{ext}$ includes all the external forces applied to the body such as the gravity and the ground reaction forces, $\sum F_{musc}$ is the muscle forces from

the static optimization, $\vec{R}_{i+1}$ is the ankle reaction force, and $\vec{R}_i$ is the knee reaction force on the tibia. The knee joint reaction force is the unknown variable of the equation and it is then computed each frame of time.

The KCF forces predicted by the model were then compared with the experimental data. The predictions of the four walking gait trials were expressed in BW and resampled on a 0-100% of the gait cycle (heel strike to heel strike of the same foot). Difference between model prediction and experimental data were quantified in terms of magnitude, RMSE, and squared Pearson coefficient (r^2). The computed knee joint reaction forces were also compared using the magnitude and the timing of their two typical main peaks and the similarity of their shape.

i) Sensitivity analysis of the surgical variables for the soft tissue

The postoperative geometries of the bones provided by the dataset were already shaped to simulate the TKR surgery and the prosthetic implants were already placed on the subject. The surgical procedure comprised one cut on the tibia and five cuts on the femur: 1) distal cut 2) anterior and posterior cuts 3) chamfer cuts (Brooks, 2009), like extensively described in the Chapter 2. The first aim of the TKR is to place those implants perpendicular to the mechanical axis of the lower limb, which is the connecting line between the centre of the femoral head and the centre of the ankle passing through the centre of the femur and the tibial spine (Luo, 2004), considering the lower limb fully extended. In the preoperative planning of TKR there are some orientation parameters, called surgical variables, that may be changed before and eventually during the surgery to assure a correct positioning of the artificial components. These variables are (Figure 6.10):

1) the varus-valgus femur cutting plane orientation on the frontal plane (from -3° to 3°, with a step of 1°)

2) the varus-valgus tibia cutting plane orientation on the frontal plane (from -3° to 3°, with a step of 1°)

3) the external rotation femur condyle cutting plane orientation on the frontal plane (from 0° to 6°, with a step of 1°)

4) the posterior slope tibial cutting plane orientation on the sagittal plane (from 3° to 5°, with a step of 1°)

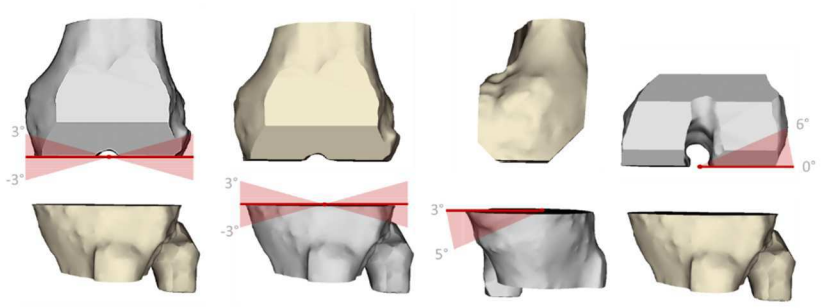

Figure 6.10 – *Surgical variables (from left): varus-valgus femur, varus-valgus tibia, tibial slope, external rotation femur*

The description of the surgical procedure employed and the intraoperative details for this subject were not provided, thus we assumed that all the surgical variables of the preoperative preplanning were in the neutral position (all the parameters set at 0° except the posterior slope at 3°) and the same condition was preserved after the surgery. Hence, the sensitivity analysis has been conducted by varying each orientation parameter throughout four normal gait cycle. Additionally, for each orientation preplanning parameter the gap between the femoral and tibial cut planes was varied between 18 mm to 28 mm (with a step of 2 mm). The changing of the surgical parameters during the walking trials allowed exploring the sensitivity of the elongation of the knee ligaments in response to the orientation of the cutting planes. For each gait cycle the maximum elongation was examined to check when the elongation exceeded the 10% of the preoperative length, which is considered the maximum acceptable elongation before irreversible structural damage occurs to the ligament. The calculation of the percentage for maximum elongation of the ligaments has been extensively exploited in the Chapter 1. The representation of the results of the sensitivity analysis was performed using a heat map for each surgical variable. Since every step of the sensitivity is composed by a curve that represents the length of the ligament over the gait cycle, only the maximum of the curve was taken into account in the representation (Figure 6.11). Therefore, the heat map intuitively showed where the ligaments might have an elongation beyond the 10% of the preoperative length.

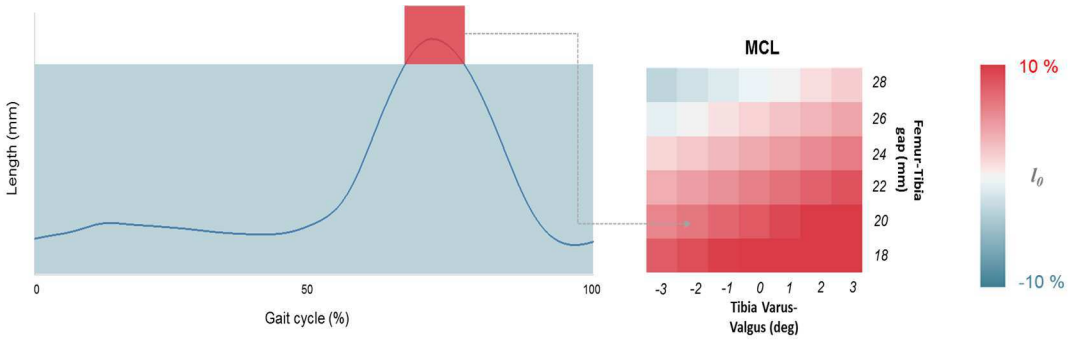

Figure 6.11 – *Example of the heat map construction. On the left the curve of the length of the MCL ligaments throughout the gait cycle with a Tibia Varus-Valgus=-2° and gap=26mm. On the right the heat map of the Tibia Varus Valgus parameter. Red colour=10% of the initial length, Blue colour=-10% of the initial length.*

In addition, the sensitivity analysis was performed on two subjects of the Medacta dataset used in the chapters for whom the subject specific origins and insertions of the ligaments were calculated and corrected using MRI images. Furthermore, a cylinder was fitted onto the femoral prosthetic implant defining the axis of rotation of the knee hinge joint. Since the sensitivity analysis relies, in our framework, only on the knee kinematics of the musculoskeletal model, the simulations were performed applying the kinematics of the knee obtained in this study to the hinge knee joint of the Medacta dataset. For one subject of the Medacta dataset, two simulations were conducted employing two different knee prosthetic implants (posterior stabilized, and sphere). Thus, this allowed the comparison of the knee soft tissue balancing between two different prosthetic designs within the same subject during the same dynamic activity.

6.3 Results

The verification of the inverse kinematics results is showed in the figures below, comparing the four gait trials of the model with the data available in the literature (Kadaba et al., 1989; Perry, 1992) for healthy subjects. The knee kinematics was also compared with data obtained from TKR patients (McClelland et al., 2011).The results are expressed throughout the 0-100% of the gait cycle, from the first heel-strike to the subsequent heel-strike. The figure below (Figure 6.12) shows that the range of motion of the knee angle spans approximately between -2° and 62° throughout the gait cycle, revealing that the

predictions of the model are in line with the kinematic data of healthy subjects. The major difference was found in the first period of the gait cycle where the patient approaches the heel-strike phase with the leg completely extended, while a healthy population revealed a flexion of 10°. Furthermore, the model kinematics resulted shifted by 5% and 11% with respect to the two healthy group, and the range of motion in the initial single stance (*0-25% of the gait cycle*) is rather low. On the other hand, the comparison with TKR patients revealed that the timing of the two curves is very similar with a difference of 3%, also the range of motion the initial single stance is comparable. The difference between the knee angles of the first heel-strike phase is smaller than the healthy population.

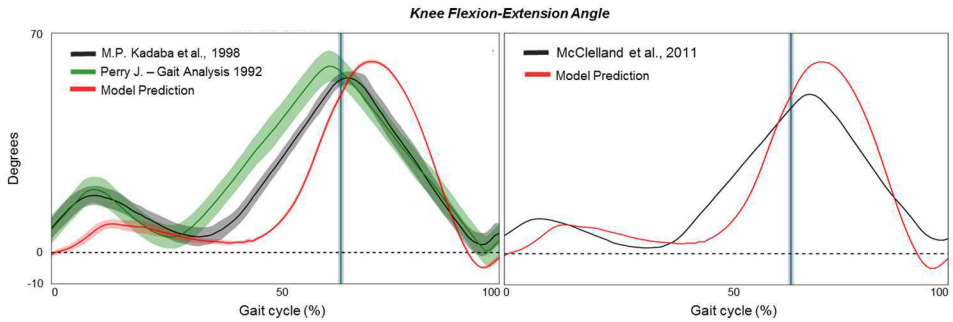

Figure 6.12 - *Knee kinematics compared with healthy subjects (Right), and TKR patient (Left)*

The hip flexion-extension angles predicted by the model showed a high correlation, the values range within the literature data with a range of motion that goes from -13° of flexion to 24° of extension (Figure 6.13). The timing of the two curves are comparable, while there is a considerable offset in the beginning and at the end of the gait cycle. The ankle flexion-extension angle showed the same range of motion of the healthy population, on the contrary a different pattern was found in the toes-off phase (*60-70% of the gait cycle*).

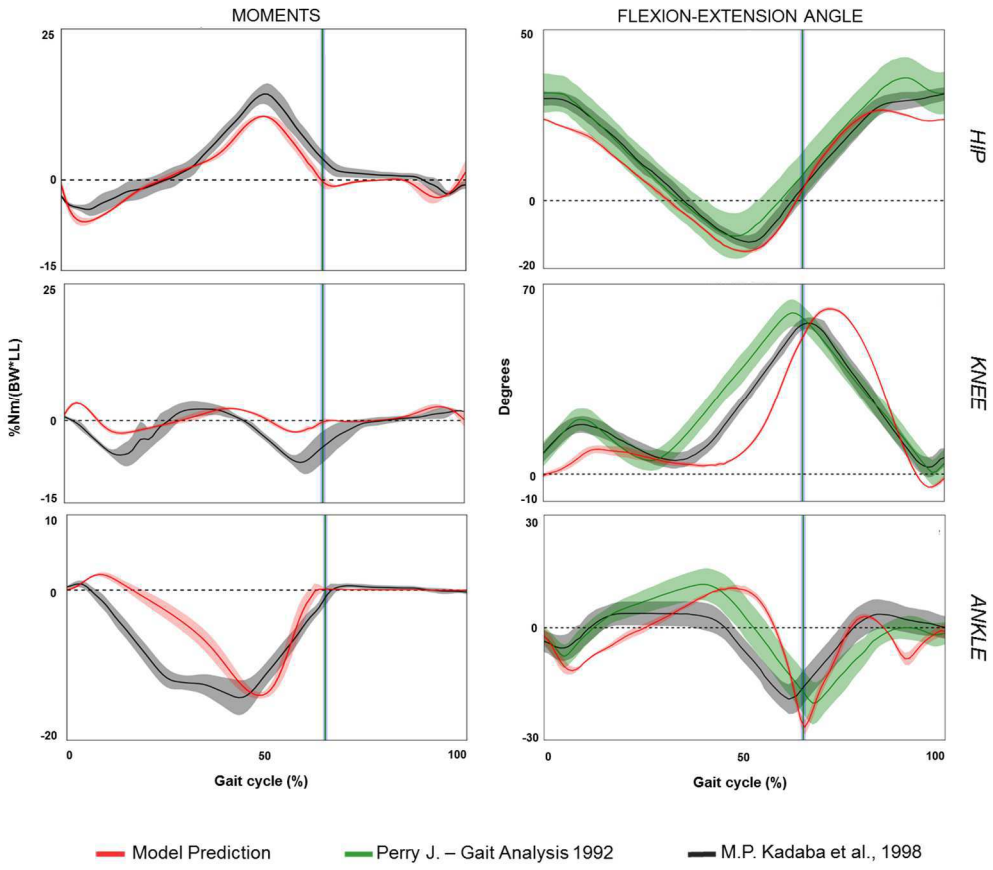

Figure 6.13 - *Knee dynamics compared with healthy subjects (Right), and knee kinematics compared with healthy subjects (Left)*

The inverse dynamics analysis showed an excellent correlation between the model and the healthy population for the hip flexion-extension moment. The knee flexion-extension moment presented a significant reduction in terms of magnitude due to the presence of the prosthetic implant in the model simulations (Figure 6.13).

The KCF predicted by the model during the walking gait trials and the experimental forces are depicted in the following figure (Figure 6.14). The model predicted the overall shape and timing of the experimental forces.

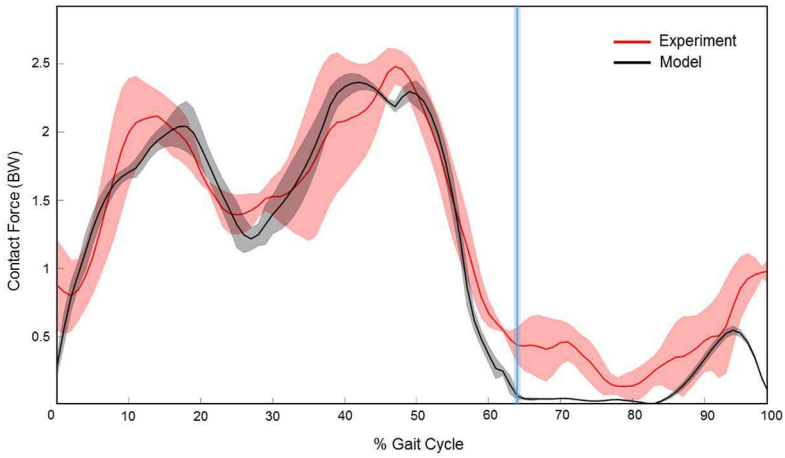

Figure 6.14 – *Total knee joint forces predicted (black) during four walking gait trials normalized on the 100% of the gait cycle. The eTibia experimental forces are showed for the same gait trials (red). The vertical blue bar represents the toe-off phase of the gait cycle (toes are leaving the ground)*

The total force measured by the instrumented prosthesis reported two peaks throughout the full gait cycle, with the first peak of 2.0 BW occurring at the beginning of the stance, and a second peak of 2.6 BW occurring toward the end of the gait cycle. The model showed an excellent accuracy showing a difference of 0.1 BW for both peaks (Table 6.3).

	Peak 1		Peak 2	
	Experiment	**Model**	**Experiment**	**Model**
Magnitude [BW]	2.0 *(0.1)*	2.1 *(0.1)*	2.6 *(0.1)*	2.5 *(0.1)*
Timing [% gait cycle]	13 *(3)*	17 *(2)*	48 *(5)*	44 *(4)*

Table 6.3*: Joint contact forces measurements in a patient with implanted instrumented prosthesis compared to predicted model from a subject specific model of the same patient.*

The timing between the two dataset was found excellent, the two peaks were shifted by less than 4 %. The computed joint contact forces were highly correlated (rho: 0.94 (0.01), $p<0.01$), with RMSE of 0.35 (0.05) BW (Figure 6.15).

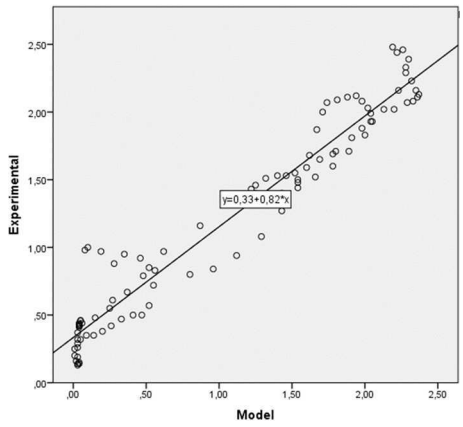

Figure 6.15: Regression line - R^2 *Linear* = 0.939

The knee ligaments forces predicted by the model are showed in figure below (Figure 6.16). The KCF results revealed a similar pattern with the values found in literature (Kia et al., 2014b; Marra et al., 2014), in particular the mean force generated by the MCL ligaments of 45 N is directly comparable with the value found by Marra et al. (2014) of 43 N throughout the walking gait cycle. The MCL ligament has a peak force of 60 N when the knee is approximately flexed of 60 degrees, and it represents the most considerable contribute. The amount of force generated by the LCL ligament is very small and remains under the 10 N during the gait cycle.

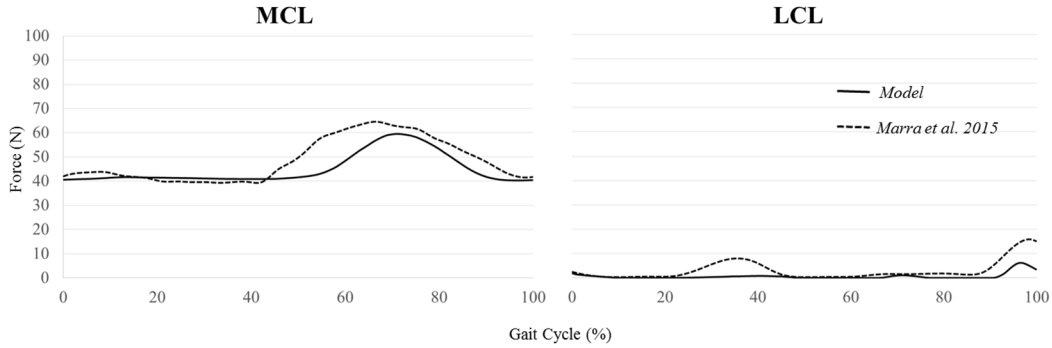

Figure 6.16 – *Ligaments Forces estimated by the model compared with the results of Marra et al. (2015)*

The length of the knee ligaments was calculated in the preoperative position finding 90.5 mm and 59.4 mm for the MCL and LCL, respectively. The length in the postoperative position was 97.3 mm (+8% longer than preoperative length) and 60.4 mm (+2% longer

than preoperative length). The gap between the femoral cut and the tibial cut in the neutral postoperative position, considered as the thickness of the prosthetic implant, was 26 mm.

The sensitivity analysis is showed in the figure (Figure 6.17), for each surgical variable the maximum elongation value during the gait cycle is reported for each gap-orientation parameter. The colour of the heat maps highlights visually when the elongation exceeded the 10% of the preoperative length.

The results showed that the collateral knee ligaments are sensitive to the femur varus-valgus parameters. The MCL ligament is rather taut and increasing the gap more than 26 mm extends the fibre up to 12% of the preoperative length. The LCL ligament seems to be less affected by this parameter especially for values of the gap above 26 mm, the maximum elongation value is 9 % and it could be reached setting a gap of 28 mm and 3 degrees of varus angle. Similar results were found for tibia varus-valgus parameter where the MCL stretches up to 13 % having 3° of valgus angle. The LCL ligaments preserves the same preoperative length, except for a larger gap and a 3° of varus angle.

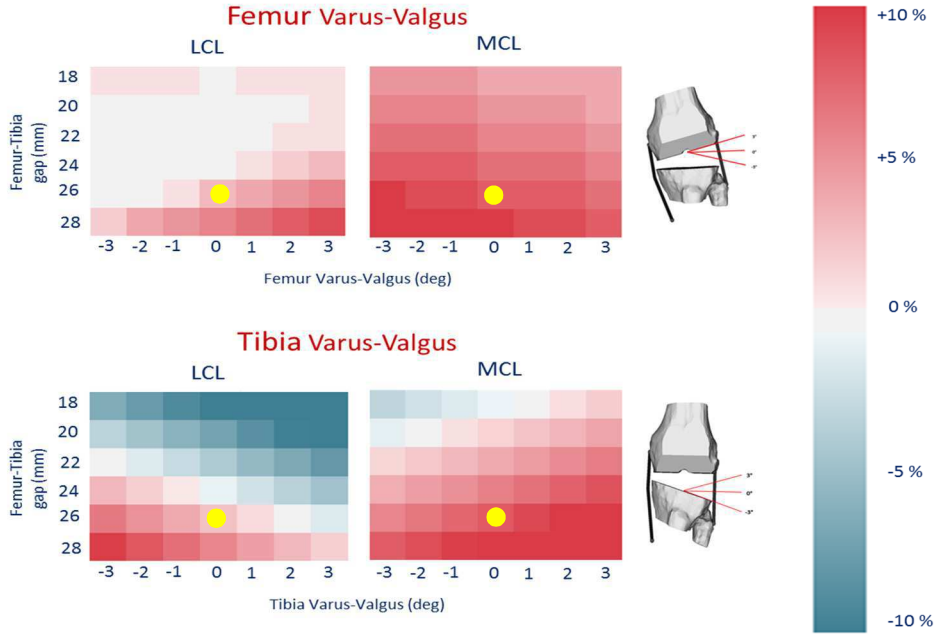

Figure 6.17 – *The figure shows the results of the Femur and Tibia varus-valgus parameters. The yellow point represents the postoperative ligament balancing imposed by surgery. The yellow dot represents the real outcome of the surgery*

The collateral knee ligaments seem to be less sensitive to the tibial slope and femoral rotation parameters. The ligaments reach values beyond the 10% of the initial length only for the MCL if a gap of 28 mm is set in the preoperative planning. However, the two

orientation parameters reveal that lower values of the gap might balance the ligaments more appropriately considering the preoperative length.

The tibia posterior slope and the femur external rotation seems to have a minor impact on the postoperative length considering the range of variation (Figure 6.18), that reach critic values only in the posterior slope for the MCL when the gap is 28 mm. The ligaments balancing appeared to be correct in this section not exceeding the 10 % of the initial length, the maximum value found was 6 % for the MCL considering the 3 degrees of natural tibial slope.

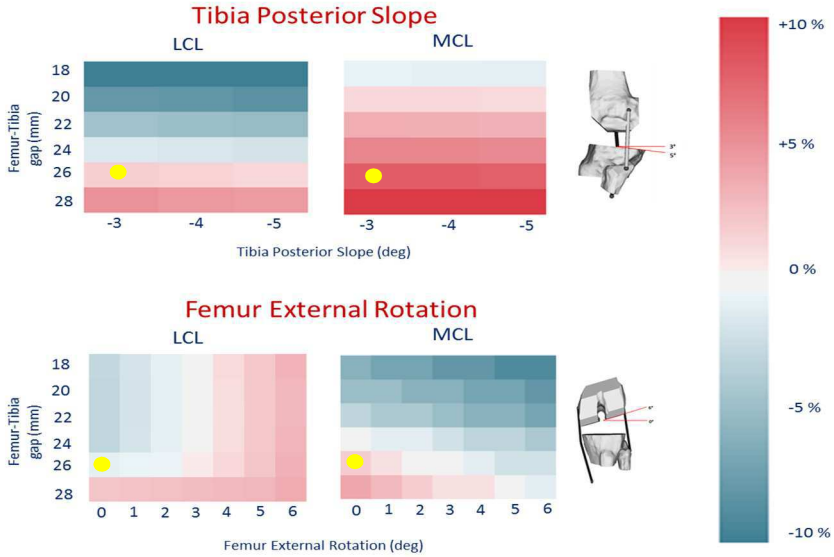

Figure 6.18 – *The figure shows the results of the Femur External Rotation and Tibia Posterior Slope parameters. The yellow point represents the postoperative ligament balancing imposed by surgery. The yellow dot represents the real outcome of the surgery*

The results showed a different postoperative outcome in the patient of the Medacta dataset, in which the simulation was performed measuring the elongation of the ligaments using two different prosthetic implant (Figure 6.19 and 6.20). The posterior stabilized implant (PS) assures a great stability to the joint providing a pivot between the knee condyles whilst the Sphere model ensures a larger range of motion and stability through a total congruency between the medial compartments. This difference has been extensively outlined in the Chapters 4 and 5. The knee soft tissue balancing appeared to be noticeably incorrect in both prosthetic models considering the sensitivity analysis of the four surgical variables. The LCL seemed to be the ligament with a major elongation (8 % with PS and 7% with Sphere) throughout the gait cycle.

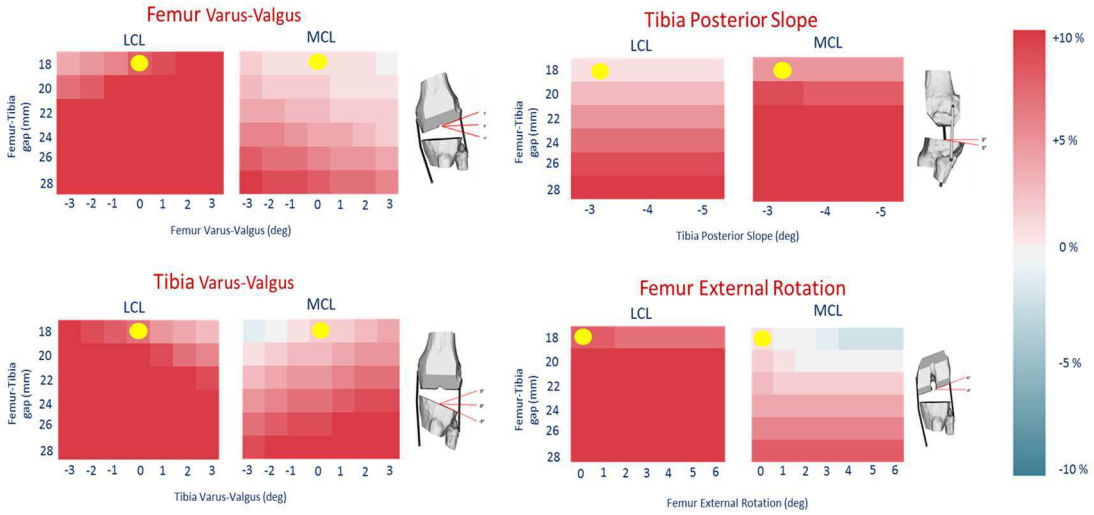

Figure 6.19 – *Patient with Posterior Stabilized Implant*

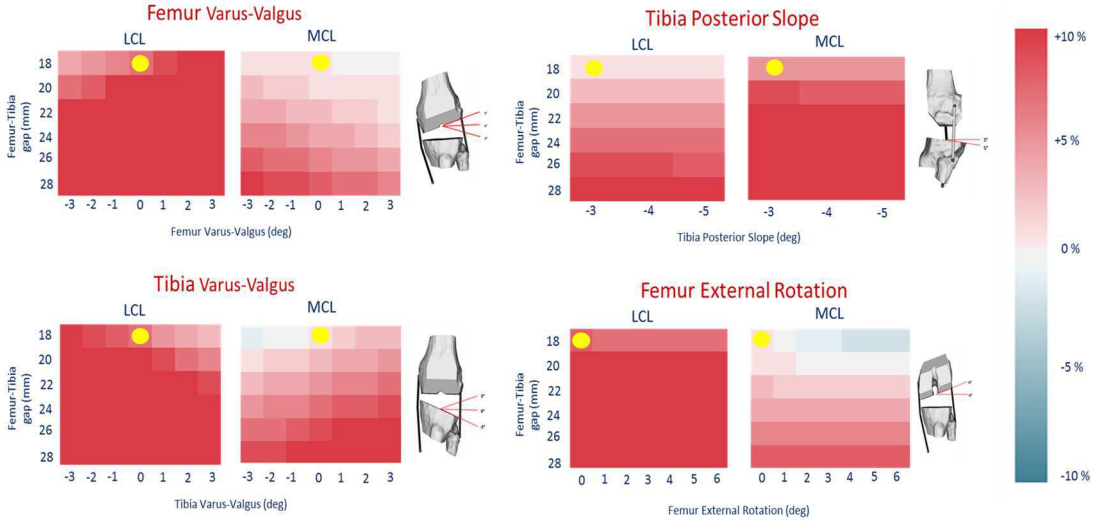

Figure 6.20 – *Patient with Sphere Implant*

To perform this sensitivity analysis on a different patient of the Medacta dataset, we applied the motion calculated on the experimental data taken form literature (Fregly et al., 2012). This might affect the accuracy of the output since the specific pathologic condition of the patient's knee can change dramatically the gait pattern (Baan et al., 2012). However, in this study the knee was modelled as one degree of freedom, therefore the knee rotation is defined by the range of motion in the sagittal plane. It can conceivably

said that this factor doesn’t influence dramatically the output of the model in terms of elongation of the ligaments under/over the 10% of the initial length.

6.5 Discussion

The first goal of this study was to develop a subject specific musculoskeletal modelling framework to compute the soft tissue balancing in TKR patients. The soft tissue balancing predictions have been performed through a sensitivity analysis of the preoperative planning parameters throughout a full normal walking gait cycle. These parameters determine the position of the artificial components of the TKR, defining the relative position of the tibia with respect to the femur and consequently the length of the knee ligaments after the surgery.

A recent study conducted by Walker et al. (2014), on a cadaveric leg implanted with an instrumented prosthesis, have demonstrated that the preoperative planning parameters have a huge impact in the definition of the knee soft tissue balancing, affecting considerably the stiffness of the knee joint. For instance, our results agree with this study confirming that the frontal varus-valgus orientation is one of the most critical variables that might overstress the tension of the ligaments after the surgery. The sensitivity analysis revealed that femur and tibial varus valgus orientation stretched the ligaments beyond the 10% of their preoperative length and this, as widely demonstrated in literature (Heesterbeek et al., 2009), may cause a premature failing of the procedure due to a limited range of motion, joint pain, or the wearing of the prosthetic implant.

The methodology suggested in this study allowed exploring through an intuitive heat map (Figure 6.15) the balancing of the ligaments once the desired preoperative planning parameters have been set. This tool is based on a warning threshold which can be described as the maximum acceptable elongation of the ligaments before irreversible structural damage might occur. The value of this threshold has been extensively described in the Chapter 2 and its value is the 10% of the preoperative length.

The level of agreement of our results showed that the TKR surgery in the analysed subject didn't take into account wisely the soft tissue balancing, not preserving the preoperative length of the knee ligaments (+8 % MCL, and +2% LCL, postoperatively). The sensitivity analysis showed that to achieve an optimal balancing, the gap between femoral and tibial cuts needs to be smaller, and the orientation of the varus-valgus frontal plane might be more varus to decrease the length of the MCL ligament.

Based on our knowledge in the literature no other studies have performed a sensitivity analysis of the preoperative planning parameters to predict the knee soft tissue balancing during a dynamic activity such as normal walking.

The creation of the musculoskeletal modelling framework is based on subject specific CT and MRI data, motion capture, and force data as input to the inverse kinematic and dynamic OpenSim tool to predict the knee joint reaction forces. The validation of the model was accomplished using the *in vivo* knee joint reaction forces provided by the "third knee grand challenge competition" (Fregly et al., 2012) along with the data described previously. Several studies have validated musculoskeletal models using *in vivo* contact forces dataset (Guess et al., 2010; Ng et al., 2012; Shelburne et al., 2005): the proposed solutions, however, often adopted modelling approaches or criteria for tuning the model parameters that, specifically aiming at optimizing the comparison with the experimental data, turned out to be difficult to reproduce and be adopted by others as generic modelling frameworks. Therefore, since the validation of the model was not the primary goal of this study, we adopted simplified joints model and reproducible procedures for subject specific musculoskeletal modelling based on freely available tools and on a limited number of operator dependent choices for the identification of critical model parameters; a least squares fitting Matlab script fitted known geometries to the anatomical sites to define univocally the joint axes, the muscles and knee ligaments origins and insertions were calculated adopting a repeatable affine registration methodology previously validated and described in Chapter 3.

Manal et al. (2014) predicted the KCF on the same dataset using an EMG driven model that allowed a tuning of the muscle parameters, founding a difference of 0.01 BW in the loading peaks and an R^2=0.92. The primary scope of the Manal's work was the validation of the KCF to participate to the challenge, thus the knee joint was modelled with a two contact point knee model (Winby et al., 2009) that allowed the estimation of the medial and lateral knee forces. Although in this study the validation of the KCF was not a primary objective, however the validity of the contact forces was necessary to have a reliable framework to perform the sensitivity analysis on the ligaments. The knee joint was modelled as an hinge joint that allowed to predict with excellent accuracy the total KCF, with a difference of 0.1 BW of the loading peaks, with a Pearson's coefficient (rho: 0.94 (0.01), $p<0.01$) and a regression coefficient ($R^2 = 0.939$) that described satisfactorily the overall trends of the curves confirming the similarity in shape and magnitude (Figure 6.13).

The prediction of muscle forces represents a challenging task because of the redundant nature of the human neural control in which the number of muscle is generally bigger than the joints degrees of freedom. Many studies have proposed optimization

theories to solve the distribution problem and simulate the loading conditions. Static optimization is usually employed to solve the indeterminate problem of equilibrating the intersegmental joint loads using a number of actuators that exceeds the joint degree of freedom (Modenese et al., 2013). Martelli et al. (2015) have proposed an alternative stochastic modelling through which the muscle forces can be selected from a space of muscle recruitment strategies that produce stable motion and variable muscle and joint forces. Individual muscle forces were calculated minimizing the sum of squared muscle activations, which is equivalent to minimize metabolic expenditure (Anderson and Pandy 2001). To enhance this technique other studies (Marra et al., 2014; Thelen et al., 2014) introduced a weighting factor in the objective function for the muscle recruitment problem. Manal et al. (2014) used an EMG driven model that aimed to minimize the difference between the knee moment estimated by the model and the knee moment computed by the inverse kinematics.

The muscle activations were not evaluated in this study, but their validity might be indirectly estimated through the evaluation of the knee contact forces that represent a direct result. Also, the common practise to evaluate the muscle activations and the muscle forces using the surface electromyography (EMG) is debatable considering that the force developed by the muscle and the EMG signal are two different phenomena governed by complex mechanism during dynamic activities (Shao et al., 2011).

The KCFs are the direct results of the muscle forces acting on the knee joint that were calculated using the static optimization algorithm. Hence, it can be hypothesized that the differences between the model and the experimental results might be due the adopted objective function, which was not representative of the compensatory strategy enrolled by the patient. In fact, examining the knee kinematics and the videos of the gait trials, it was noticed that the subject had the operated leg rather rigid throughout the gait. This is confirmed by the fact that the subject approached the force plate with a completely extended knee joint (0°), while the normal population usually have 10° of flexion in the same period (Figure 6.20).

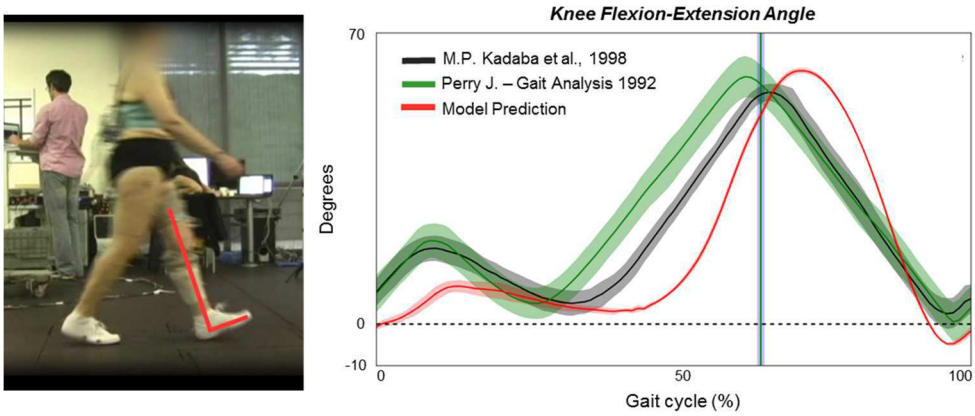

Figure 6.21 – *The figure shows the knee joint kinematics of the model compared with the healthy subjects. Our model detects accurately the knee angle in the heel-strike phase, as showed in the picture taken during the trial in the gait laboratory.*

Thus, the subject during the gait cycle might have enrolled a compensatory strategy aiming to maximize the stability of the operated leg. Many studied have demonstrated that the knee proprioception decreased after a surgery in the knee joint (Bennell et al., 2003; Corrigan et al., 1992; Knoop et al., 2011; Lephart et al., 1998), causing defects in sensory information that leaded the patients to develop compensatory pathways mechanisms. Kim et al. (2009) made the same conclusions in their study confirming that the errors between the model and the knee contact experimental data were mostly due to the objective function of the static optimization that was not representative of the recruitment strategy for task performed by the patient *in vivo*. Further studies will investigate if more appropriate objective function may improve the prediction of the knee joint reaction forces.

The prediction of the knee ligaments forces was obtained by the model for the normal walking trial. The overall predicted forces compared qualitatively well with other values found in the literature. The MCL force mean value (*47 N*) were found to be similar with the values of Marra et al. (2015) (*48 N*), the Kia et al. (Kia et al., 2014a) work showed the same pattern even though with higher peak value (*200 N*). Also, Kia et al. (2014) showed a similar pattern and mean value between MCL and LCL, on the other hand our model showed that the contribution of the LCL is less the 20 N, in agreement with the literature. Controversially, Thelen et al. (2014) showed that the LCL mean force was higher than the MCL contribution overall the gait cycle. The study conducted by Morrison (Morrison, 1970) demonstrated that the forces of the knee ligament may changes dramatically between different subject due to the specific gait, origins and insertions, and shape of the bones that defines the wrapping and the spatial geometry. This study included a subject specific characterization of the anatomical properties of the knee ligaments,

validating the findings with the use of MRI images. Most of the studies employed a scaling of generic musculoskeletal and ligament geometries to the subject to run the simulations (Kia et al., 2014a; Marra et al., 2014; Thelen et al., 2014). Although this approach is largely used because it avoids cumbersome and tedious tasks for creating subject specific models, it may be a source of error in examining the ligaments behaviour given their high specificity among different subjects' anatomy.

There are several limitations to consider in this study that are worth to discuss. Although, Marra et al. (2015) have demonstrated that there were no differences in knee contact forces using a simple hinge joint or a solution with more degree of freedom for modelling the knee joint, we believe that our model's prediction could enhance employing a more sophisticated modelling of the knee that could change the muscular activations. Another limitation is represented using this type of experimental data that are representative of a very small cohort of patients and in the limited number of prosthetic models under specific conditions.

In this chapter the sensitivity analysis was performed varying the surgical variables one at the time, the analysis of the output obtained by changing multiple parameters at the same time has not been included. This is a fundamental step to have clinical relevance in the preoperative planning, in fact the surgeon routinely change more than one parameter at the time to place the prosthetic implant on the patient. This matter has to be extensively examined in further studies.

This study demonstrated the potential of the subject-specific computational models to help the surgeon during the preoperative planning set up to perform a correct knee soft tissue balancing. Further improvements of this modelling approach, may aim to the creation of a subject specific lifestyle simulator that could disrupt the vision of undergoing to orthopaedic surgery, performed as cure for joint osteoarthritis. This simulator would predict the postoperative outcome of the TKR surgery exploring different prosthetic implants that could match the specific lifestyle activities of the patient. The subject specific model will assist the surgeon in choosing the implants that will assure the best performance for a selected task and to perform a personalized surgical procedure based on the specific patient characteristic. Their most frequent activities are analysed using highly personalized computational models and the surgeon is provided with a set of parameters that help him in planning the best intervention to maintain or restore full function.

References

Ascani, D., Mazzà, C., De Lollis, A., Bernardoni, M., Viceconti, M., 2015. A procedure to estimate the origins and the insertions of the knee ligaments from computed tomography images. J. Biomech. 48, 233–7. doi:10.1016/j.jbiomech.2014.11.041

Baan, H., Dubbeldam, R., Nene, A. V., van de Laar, M.A.F.J., 2012. Gait Analysis of the Lower Limb in Patients with Rheumatoid Arthritis: A Systematic Review. Semin. Arthritis Rheum. 41, 768–788.e8. doi:10.1016/j.semarthrit.2011.11.009

Babazadeh, S., Stoney, J.D., Lim, K., Choong, P.F.M., 2009. The relevance of ligament balancing in total knee arthroplasty: how important is it? A systematic review of the literature. Orthop. Rev. (Pavia). 1, e26. doi:10.4081/or.2009.e26

Baker, P.N., Deehan, D.J., Lees, D., Jameson, S., Avery, P.J., Gregg, P.J., Reed, M.R., 2012. The effect of surgical factors on early patient-reported outcome measures (PROMS) following total knee replacement. Bone Joint J. 94–B, 1058–1066.

Bennell, K.L., Hinman, R.S., Metcalf, B.R., Crossley, K.M., Buchbinder, R., Smith, M., McColl, G., 2003. Relationship of knee joint proprioception to pain and disability in individuals with knee osteoarthritis. J. Orthop. Res. 21, 792–797. doi:10.1016/S0736-0266(03)00054-8

Bergmann, G., 2008. Orthoload.com [WWW Document]. Charité Univ. Berlin. URL http://www.orthoload.com/?page_id=7

Bergmann, G., Graichen, F., Bender, A., Kääb, M., Rohlmann, A., Westerhoff, P., 2007. In vivo glenohumeral contact forces-Measurements in the first patient 7 months postoperatively. J. Biomech. 40, 2139–2149. doi:10.1016/j.jbiomech.2006.10.037

Besl, P.J., McKay, H.D., 1992. A method for registration of 3-D shapes. IEEE Trans. Pattern Anal. Mach. Intell. 14, 239–256. doi:10.1109/34.121791

Blankevoort, L., Huiskes, R., 1996. Validation of a three-dimensional model of the knee. J. Biomech. 29, 955–961. doi:10.1016/0021-9290(95)00149-2

Blankevoort, L., Kuiper, J.H., Huiskes, R., Grootenboer, H.J., 1991. Articular contact in a three-dimensional model of the knee. J. Biomech. 24, 1019–1031. doi:10.1016/0021-9290(91)90019-J

Brooks, P., 2009. Seven cuts to the perfect total knee. Orthopedics 32. doi:10.3928/01477447-20090728-27

Corrigan, J.P., Cashman, W.F., Brady, M.P., 1992. Proprioception in the cruciate deficient knee. J. Bone Joint Surg. Br. 74, 247–50. doi:10.1177/036354658901700101

Culliford, D., Maskell, J., Judge, A., Cooper X K, C., Prieto-Alhambra, D., Arden, N.K., 2015. Future projections of total hip and knee arthroplasty in the UK: results from the UK Clinical Practice Research Datalink. Osteoarthr. Cartil. 23, 594–600. doi:10.1016/j.joca.2014.12.022

D’Lima, D.D., Fregly, B.J., Patil, S., Steklov, N., Colwell, C.W., 2012. Knee joint forces: prediction, measurement, and significance. Proc. Inst. Mech. Eng. H. 226, 95–102. doi:10.1177/0954411911433372

D’Lima, D.D., Townsend, C.P., Arms, S.W., Morris, B. a., Colwell, C.W., 2005. An implantable telemetry device to measure intra-articular tibial forces. J. Biomech. 38, 299–304. doi:10.1016/j.jbiomech.2004.02.011

Delp, S.L., Loan, J.P., Hoy, M.G., Zajac, F.E., 1990. An interactive Graphics-Based Model of the Lower Extremity to Study Orthopaedic Surgical Procedures. IEEE Trans. Biomed. Eng. 37, 757–767. doi:10.1109/10.102791

DeMers, M.S., Pal, S., Delp, S.L., 2014. Changes in tibiofemoral forces due to variations in muscle activity during walking. J. Orthop. Res. 32, 769–776. doi:10.1002/jor.22601

Dennis, D.A., Komistek, R.D., Kim, R.H., Sharma, A., 2010. Gap balancing versus measured resection technique for total knee arthroplasty, in: Clinical Orthopaedics and Related Research. pp. 102–107. doi:10.1007/s11999-009-1112-3

Du, S., Zheng, N., Ying, S., Liu, J., 2010. Affine iterative closest point algorithm for point set registration. Pattern Recognit. Lett. 31, 791–799. doi:10.1016/j.patrec.2010.01.020

Dubuisson, M.-P., Jain, a. K., 1994. A modified Hausdorff distance for object matching. Proc. 12th Int. Conf. Pattern Recognit. 1, 566–568. doi:10.1109/ICPR.1994.576361

Fehring, T.K., Odum, S., Griffin, W.L., Mason, J.B., Nadaud, M., 2001. Early failures in total knee arthroplasty. Clin. Orthop. Relat. Res. 315–318. doi:10.1097/00003086-200111000-00041

Fregly, B.J., Besier, T.F., Lloyd, D.G., Delp, S.L., Banks, S.A., Pandy, M.G., D’Lima, D.D., 2012. Grand challenge competition to predict in vivo knee loads. J. Orthop. Res. 30, 503–13. doi:10.1002/jor.22023

Guess, T.M., Thiagarajan, G., Kia, M., Mishra, M., 2010. A subject specific multibody model of the knee with menisci. Med. Eng. Phys. 32, 505–515. doi:10.1016/j.medengphy.2010.02.020

Heck, D. a, Melfi, C. a, Mamlin, L. a, Katz, B.P., Arthur, D.S., Dittus, R.S., Freund, D. a, 1998. Revision rates after knee replacement in the United States. Med. Care 36, 661–669. doi:10.1097/00005650-199805000-00006

Heesterbeek, P.J.C., Jacobs, W.C.H., Wymenga, A.B., 2009. Effects of the balanced gap technique on femoral component rotation in TKA. Clin. Orthop. Relat. Res. 467, 1015–1022. doi:10.1007/s11999-008-0539-2

Jones, R.E., Huo, M.H., 2006. Rotating Platform Knees: An Emerging Clinical Standard. In the Affirmative. J. Arthroplasty. doi:10.1016/j.arth.2006.01.021

Kadaba, M.P., Ramakrishnan, H.K., Wootten, M.E., Gainey, J., Gorton, G., Cochran, G. V, 1989. Repeatability of kinematic, kinetic, and electromyographic data in normal adult gait. J. Orthop. Res. 7, 849–860. doi:10.1002/jor.1100070611

Kia, M., Stylianou, A.P., Guess, T.M., 2014a. Evaluation of a musculoskeletal model with prosthetic knee through six experimental gait trials. Med. Eng. Phys. 36, 335–344. doi:10.1016/j.medengphy.2013.12.007

Kia, M., Stylianou, A.P., Guess, T.M., 2014b. Evaluation of a musculoskeletal model with prosthetic knee through six experimental gait trials. Med. Eng. Phys. 36, 335–44. doi:10.1016/j.medengphy.2013.12.007

Kim, H.J., Fernandez, J.W., Akbarshahi, M., Walter, J.P., Fregly, B.J., Pandy, M.G., 2009. Evaluation of predicted knee-joint muscle forces during gait using an instrumented knee implant. J. Orthop. Res. 27, 1326–1331. doi:10.1002/jor.20876

Knoop, J., Steultjens, M.P.M., van der Leeden, M., van der Esch, M., Thorstensson, C.A., Roorda, L.D., Lems, W.F., Dekker, J., 2011. Proprioception in knee osteoarthritis: A narrative review. Osteoarthr. Cartil. doi:10.1016/j.joca.2011.01.003

Lephart, S.M., Pincivero, D.M., Rozzi, S.L., 1998. Proprioception of the ankle and knee. Sport. Med. 25, 149–155. doi:10.2165/00007256-199825030-00002

Lerner, Z.F., DeMers, M.S., Delp, S.L., Browning, R.C., 2015. How tibiofemoral alignment and contact locations affect predictions of medial and lateral tibiofemoral contact forces. J. Biomech. 48, 644–650. doi:10.1016/j.jbiomech.2014.12.049

Luo, C.F., 2004. Reference axes for reconstruction of the knee. Knee. doi:10.1016/j.knee.2004.03.003

Manal, K., Buchanan, T.S., 2013. An electromyogram-driven musculoskeletal model of the knee to predict in vivo joint contact forces during normal and novel gait patterns. J. Biomech. Eng. 135, 21014. doi:10.1115/1.4023457

Mannion, A.F., Kämpfen, S., Munzinger, U., Kramers-de Quervain, I., 2009. The role of patient expectations in predicting outcome after total knee arthroplasty. Arthritis Res. Ther. 11, R139. doi:10.1186/ar2811

Marra, M. a, Vanheule, V., Fluit, R., Koopman, B.H.F.J.M., Rasmussen, J., Verdonschot, N.J.J., Andersen, M.S., 2014. A Subject-Specific Musculoskeletal Modeling Framework to Predict in Vivo Mechanics of Total Knee Arthroplasty. J. Biomech. Eng. 137, 1–12. doi:10.1115/1.4029258

Martelli, S., Calvetti, D., Somersalo, E., Viceconti, M., 2015. Stochastic modelling of muscle recruitment during activity. Interface Focus 5, 20140094–20140094. doi:10.1098/rsfs.2014.0094

McClelland, J.A., Webster, K.E., Feller, J.A., Menz, H.B., 2011. Knee kinematics during walking at different speeds in people who have undergone total knee replacement. Knee 18, 151–155. doi:10.1016/j.knee.2010.04.005

Modenese, L., Gopalakrishnan, A., Phillips, A.T.M., 2013. Application of a falsification strategy to a musculoskeletal model of the lower limb and accuracy of the predicted hip contact force vector. J. Biomech. 46, 1193–1200. doi:10.1016/j.jbiomech.2012.11.045

Morrison, J.B., 1970. The mechanics of the knee joint in relation to normal walking. J. Biomech. 3, 51–61.

Ng, V.Y., DeClaire, J.H., Berend, K.R., Gulick, B.C., Lombardi, A. V., 2012. Improved accuracy of alignment with patient-specific positioning guides compared with manual instrumentation in TKA. Clin. Orthop. Relat. Res. 470, 99–107. doi:10.1007/s11999-011-1996-6

Obergefell, L., Rizer, A., 1996. The development of the GEBOD program. Proc. 1996 Fifteenth South. Biomed. Eng. Conf. 251–254. doi:10.1109/SBEC.1996.493162

Perry, J., 1992. Gait Analysis: Normal and Pathological Function, Journal of Pediatric Orthopaedics. doi:10.1001

Shao, Q., MacLeod, T.D., Manal, K., Buchanan, T.S., 2011. Estimation of ligament loading and anterior tibial translation in healthy and ACL-deficient knees during gait and the influence of increasing tibial slope using EMG-driven approach. Ann. Biomed. Eng. 39, 110–121. doi:10.1007/s10439-010-0131-2

Shelburne, K.B., Torry, M.R., Pandy, M.G., 2005. Muscle, ligament, and joint-contact forces at the knee during walking, in: Medicine and Science in Sports and Exercise. pp. 1948–1956. doi:10.1249/01.mss.0000180404.86078.ff

Thelen, D.G., Won Choi, K., Schmitz, A.M., 2014. Co-simulation of neuromuscular dynamics and knee mechanics during human walking. J. Biomech. Eng. 136, 21033. doi:10.1115/1.4026358

Van Sint Jan, S., 2007. Color atlas of skeletal landmark definitions: guidelines for reproducible manual and virtual palpations. CHURCILL LIVINGSTONE Elsevier, Philiadelphia (PA), USA.

Walker, P.S., Meere, P. a, Bell, C.P., 2014. Effects of surgical variables in balancing of total knee replacements using an instrumented tibial trial. Knee 21, 156–61. doi:10.1016/j.knee.2013.09.002

Westerhoff, P., Graichen, F., Bender, A., Rohlmann, A., Bergmann, G., 2009. An instrumented implant for in vivo measurement of contact forces and contact moments in the shoulder joint. Med. Eng. Phys. 31, 207–213. doi:10.1016/j.medengphy.2008.07.011

White, D.R., Woodard, H.Q., Hammond, S.M., 1987. Average soft-tissue and bone models for use in radiation dosimetry. Br. J. Radiol. 60, 907–913. doi:10.1259/0007-1285-60-717-907

Winby, C.R., Lloyd, D.G., Besier, T.F., Kirk, T.B., 2009. Muscle and external load contribution to knee joint contact loads during normal gait. J. Biomech. 42, 2294–2300. doi:10.1016/j.jbiomech.2009.06.019

Zajac, F.E., 1989. Muscle and tendon: properties, models, scaling, and application to biomechanics and motor control. Crit. Rev. Biomed. Eng. 17, 359–411.

Chapter 7

Conclusions

7.1 Summary

The dissertation attempted to address a specific research question that stems from the clinical need of having a prediction of the knee soft tissue balancing as part of the TKR preoperative planning framework (Figure 7.1) that allow to produce subject specific cutting guides.

The procedure developed in this dissertation will be added in the industrial preoperative planning tool called *MyKnee*® (Medacta International SA, Switzerland). In particular, this study is composed by the development of different knee joint models of gradual complexity that estimated the postoperative length of the collateral knee ligaments (LCL and MCL). In the course of this study it has been demonstrated that the subject specific static model of the TKR knee joint, predicted significantly similar outputs compared with the quasi-static models which are more complex and computationally heavier. In addition, the dynamic model developed in chapter 6, allowed to estimate the postoperative length of the ligaments using a subject specific MSK model of the lower limb during a dynamic task such as walking.

Throughout the dissertation, the models were evaluated by their ability to predict the elongation of the ligaments after a TKR surgery, allowing to understand how the position of the prosthetic implant might affect the knee soft tissue. Unlike the current methodology used in the preoperative planning framework to manufacture disposable cutting guides, the balancing of the ligaments can be examined according with the preoperative parameters set by the surgeon. In addition, to make the feedback more intuitive and readable, the length of the ligaments was showed using a colour scale that reflects the percentage of elongation with respect to the preoperative length. The red colour warns the surgeon that the ligament is too taut, whereas the white colour means the preoperative length has been preserved. The warning threshold used to create the colour scale is based on the 10 % of the preoperative length.

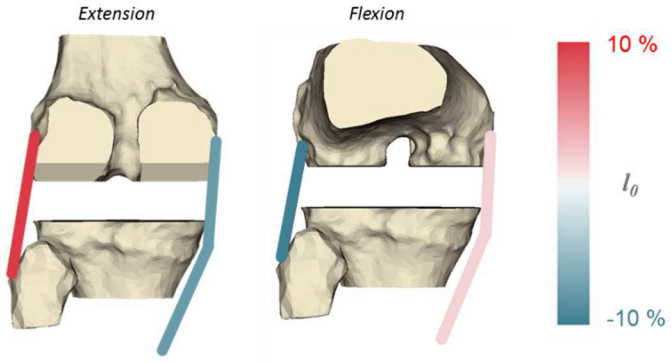

Figure 7.1 – *Optimized TKR surgery procedure that shows preoperatively the elongation of the ligaments after the surgery*

A methodology to accurately estimate the knee ligaments origin and insertion, starting from a reproducible and repeatable landmark cloud virtually palpated on CT scan, has been developed and validated thorough a comparison with the same estimations calculated from MRI, which can be considered as a reliable reference (Taylor et al., 2013). This procedure was essential to estimate the preoperative length from CT scan images, which typically are the only patient's data available to perform a subject specific preoperative planning. The preoperative length is a crucial parameter in this study since it represents one of the inputs of the models; so the robustness of this procedure was proved by the sensitivity analysis in chapter 4, which showed an absence of variation in the models' output changing the ligaments origin and insertion position within a range imposed by the SD provided by the procedure (Ascani et al., 2015).

A subject specific static models of the knee have been created to estimate the postoperative length of the sMCL and LCL of TKR patients in two static positions: extension (0º) and flexion (90 º). The results of the study revealed that the models predicted accurately the postoperative length, having compared the findings with the same results obtained using MRI images. The results showed that the preoperative length was not preserved after the TKR due to the new position of the femur and tibia. Nevertheless, all the estimated postoperative elongations were below the warning threshold, implying that the ligaments should not undergo irreversible structural damages due to the postoperative overstretching.

Subject specific quasi-static models have been developed, using the same dataset, to investigate if the forces produced by the contact between the bodies and different anatomical structures (ligaments, tendons, and muscles), might affect significantly the prediction of the model compared with the static model's outputs. The results showed

that there are not significant differences between the static and quasi-static models' output, not even when in the quasi-static model two more positions were added (30° and 60°), and a sensitivity analysis has been performed to investigate how different level of muscle excitation might affect significantly the output of the model.

The final study in this dissertation developed a new methodology to compute the knee soft tissue balancing during a dynamic physical activity such as walking. The study was inspired by the availability of experimental *in vivo* KFC data from the "Grand Challenge Competition to Predict In Vivo Knee Loads" (Fregly et al., 2012). A subject specific dynamic MSK of the lower limb was created and validated using experimental data, the collateral lateral knee ligaments were added to the model to observe the postoperative trend over the gait cycle. In particular, a sensitivity analysis was performed varying each preoperative planning parameters. The results were represented through the use of heat maps that showed the maximum elongation of the ligaments throughout the gait cycles (Figure 6.11). The heat maps intuitively revealed for each preoperative planning parameters, where the ligaments had an elongation beyond the 10% of the preoperative length, helping to choose the correct values to ensure an appropriate soft tissue balance.

7.2 Novelty and Utility of the Work

TKR surgery is currently the most popular treatment for the deterioration of the knee cartilage, which affects more than 600.000 people per year in USA (Bozic et al., 2010). Despite the improvements carried out by the surgical procedure and the availability of intraoperative medical devices, about 60.000 patients undergo to a revision surgery every year and more than 40 % have a limited life-style in terms of physical activities (Mannion et al., 2009). The reasons of the failure lies in the surgical procedure that primary benefits the alignment of the bones (Bäthis et al., 2004); the reduction of the number of revision surgeries and the return to an acceptable life-style revolve mostly on the correct balance of the soft tissues wrapping the knee (Asano et al., 2004). Among the different surgical procedures the pre-operatively planned, custom-made cutting guides were introduced in the market few years ago, this new technology is considered the most promising because it can tailor the surgical instrumentation using the specific anatomy of the patient (Hafez et al., 2006). However, this procedure does not include any information about how a given position of the femur and tibia might influence the ligaments. For this

reason, a subject specific predictive model of the knee joint was successfully used to investigate the balancing of the knee soft tissue within the preoperative planning framework that allow the manufacturing of custom made cutting guides (Figure 7.2).

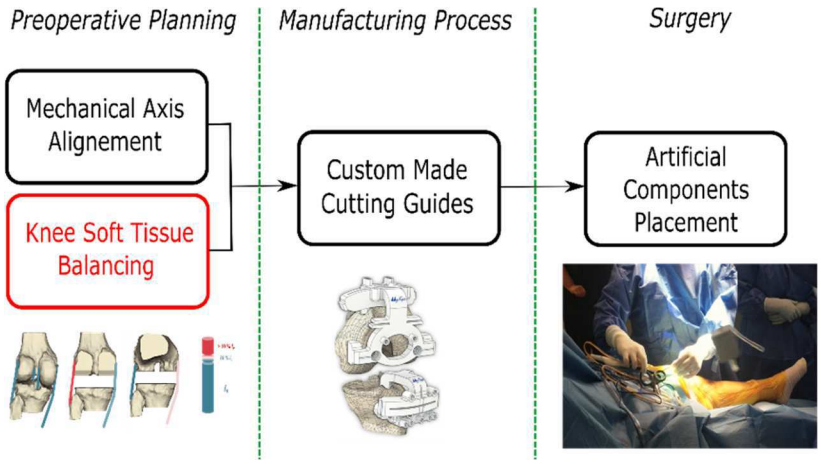

Figure 7.2 – *Optimized TKR surgery procedure that employs pre-operatively planned, custom-made cutting guides*

The last model developed in this study represents a possible future application that aim to personalize the surgery considering also the physical activity the patient is likely to return after the operation.

The potential of this new optimized TKR procedure might improve the current surgeon's criteria that are entirely based on his own experience. The use of TKR subject specific computational models might introduce standard procedures to select the most correct values of the preplanning parameters including also an optimal soft tissue balance along with the mechanical alignment (Figure 7.2).

Throughout the years, the industrial and clinical relevance gained by the TKR surgery pushed the research community to produce a large amount of work dedicated to this subject. Although the computational modelling of the TKR knee has been largely studied to answer many research questions, however to the best of my knowledge there are no studies or freely available tools in literature that allow the estimate of postoperative length of the knee ligaments after TKR surgery starting from CT scan images.

7.3 Limitations

The studies conducted in this dissertation had several limitations that have been extensively tackled through the chapters.

The main limitation is that the output of the models revolves entirely on the preoperative length of the knee ligaments, which was obtained from CT scan images and validated using MRI images. The preoperative length of the knee ligaments, following the Blankevoort et al. (1991) terminology, was defined as the length of the knee ligaments when the leg is in the reference position (fully extended). The dataset available for this dissertation did not allow to investigate the position of the patient during the CT scan, thus the procedure developed in this study assumed that the patients were in the reference position. Although it has been demonstrated that the models' output is not significantly sensitive to the changing of the preoperative length, however the accuracy of this parameter is still a problem that has to be addressed in future *in vivo* studies.

A second limitation is that the collateral ligaments (LCL and MCL) were represented as a one bundle fibre. Although the modelling of the knee ligaments using a high number of bundles is frequently adopted in literature, the identification of multiple bundles using CT scan images, where they are not visible, might have introduced more noise than information in the simulations. Also, the objective of this study was to estimate a parameter that described intuitively the overall response of the ligament rather than focusing on different bundles behaviour (Bergamini et al., 2011; Hosseini et al., 2014; Liu et al., 2011).

Although a preferred outcome after a TKR surgery is the restoration of the preoperative length of the knee ligaments, the balancing of the ligaments in this methodology was considered acceptable as the length of the ligaments did not exceed the 10 % of the preoperative length. This assumption stems from the findings of the medical literature, it has been demonstrated that an excessive stretching of the ligaments after TKR is the leading factor to revision surgery due to the wear of the plastic tibial insert, a limited range of motion, joint stiffness and pain. Nevertheless, the laxity of the ligaments after the operation is certainly an issue that needs to be taken into account to achieve an optimal ligaments balancing, even though Kuster et al. (2004) have demonstrated that TKR patients were more satisfied with a laxer knee, allowing for a bigger range of movement and absence of pain.

Another limitation is represented by the use of a small dataset that might be representative of a very small cohort of patients and the absence of a clinical follow-up that might have validated our results. Future retrospective or prospective studies will confirm the accuracy of this methodology.

7.4 Future Work

The models developed could be improved by solving some of the limitations described throughout the dissertation.

The static models have proven to estimate correctly the postoperative length of the collateral knee ligaments, for this reason it will be further engineered and included in an industrial preoperative planning software. A first study, with a selected group of surgeons, will assess the feasibility and the accuracy of the procedure performing the current available preoperative planning procedure and the optimized preoperative planning on the same patient. The surgery will be performed following the available planning, however the surgery's outcome and the intraoperative surgeon's feedback will confirm if the optimized procedure would have been more accurate. A second study, with the same group of surgeon's, will start using the optimized preoperative planning to perform the surgery to observe if there is a reduction of the intraoperative complications such as ligaments resection, re-cut of the bones, or change of the implant size. Also the overall patients' satisfaction is a crucial aspect that needs to be assessed after the operation. A statistical analysis on a large cohort of TKR patients will assess the improvements compared with the current available preoperative planned TKR surgery. Moreover, throughout this validation process, the clinicians' feedback will allow to further improve the methodology and the user interface, leading step by step to a stable version that can be implemented in the final release.

The dynamic model developed in chapter 6 might represent the core for a new technology for TKR surgery, tha can be called "Orthopaedic Lifestyle Simulator" (OLS). The OLS is a surgical planning software that can help the surgeon to optimize the balancing of soft tissue, forecasting the type of physical activities that the patient is likely to return after the operation. Demand for better musculoskeletal health services drives R&D departments of major companies to invest massively in new product development to account for the demand of these younger patients for whom generally a joint replacement is not recommended. This frequently-performed surgery is currently based

on surgeons' subjectivity even when a personalized preoperative planning is performed. The OLS disrupts the vision of undergoing to orthopaedic surgery predicting the postoperative outcome in terms of personalized life style activities. Using only a set of medical images (CT or MRI), a patient specific three dimensional model of the patient is created to assess the physical performance after the surgery. The breakthrough of this idea is the concept of tailoring the surgical procedure to the anatomy, but also the life style expectations of each patient, the surgeon will select the prosthetic implants that will assure the best performance for a selected task that belong to the specific patient's lifestyle.

References

Asano, H., Hoshino, A., Wilton, T.J., 2004. Soft-tissue tension total knee arthroplasty. J. Arthroplasty 19, 558–561. doi:10.1016/j.arth.2004.01.003

Ascani, D., Mazzà, C., De Lollis, A., Bernardoni, M., Viceconti, M., 2015. A procedure to estimate the origins and the insertions of the knee ligaments from computed tomography images. J. Biomech. 48, 233–7. doi:10.1016/j.jbiomech.2014.11.041

Bäthis, H., Perlick, L., Tingart, M., Lüring, C., Zurakowski, D., Grifka, J., 2004. Alignment in total knee arthroplasty. A comparison of computer-assisted surgery with the conventional technique. J. Bone Joint Surg. Br. 86, 682–687. doi:10.1302/0301-620X.86B5.14927

Bergamini, E., Pillet, H., Hausselle, J., Thoreux, P., Guerard, S., Camomilla, V., Cappozzo, A., Skalli, W., 2011. Tibio-femoral joint constraints for bone pose estimation during movement using multi-body optimization. Gait Posture 33, 706–711. doi:10.1016/j.gaitpost.2011.03.006

Bozic, K.J., Kurtz, S.M., Lau, E., Ong, K., Chiu, V., Vail, T.P., Rubash, H.E., Berry, D.J., 2010. The epidemiology of revision total knee arthroplasty in the United States. Clin. Orthop. Relat. Res. 468, 45–51. doi:10.1007/s11999-009-0945-0

Fregly, B.J., Besier, T.F., Lloyd, D.G., Delp, S.L., Banks, S.A., Pandy, M.G., D'Lima, D.D., 2012. Grand challenge competition to predict in vivo knee loads. J. Orthop. Res. 30, 503–13. doi:10.1002/jor.22023

Hafez, M. a, Chelule, K.L., Seedhom, B.B., Sherman, K.P., 2006. Computer-assisted total knee arthroplasty using patient-specific templating. Clin. Orthop. Relat. Res. 444, 184–192. doi:10.1097/01.blo.0000201148.06454.ef

Hosseini, A., Qi, W., Tsai, T.Y., Liu, Y., Rubash, H., Li, G., 2014. In vivo length change patterns of the medial and lateral collateral ligaments along the flexion path of the knee. Knee Surgery, Sport. Traumatol. Arthrosc. 23, 3055–3061. doi:10.1007/s00167-014-3306-9

Kuster, M.S., Bitschnau, B., Votruba, T., 2004. Influence of collateral ligament laxity on patient satisfaction after total knee arthroplasty: a comparative bilateral study. Arch. Orthop. Trauma Surg. 124, 415–417. doi:10.1007/s00402-004-0700-7

Liu, F., Gadikota, H.R., Kozánek, M., Hosseini, A., Yue, B., Gill, T.J., Rubash, H.E., Li, G., 2011. In vivo length patterns of the medial collateral ligament during the stance phase of gait. Knee Surgery, Sport. Traumatol. Arthrosc. 19, 719–727. doi:10.1007/s00167-010-1336-5

Mannion, A.F., Kämpfen, S., Munzinger, U., Kramers-de Quervain, I., 2009. The role of patient expectations in predicting outcome after total knee arthroplasty. Arthritis Res. Ther. 11, R139. doi:10.1186/ar2811

Taylor, K.A., Cutcliffe, H.C., Queen, R.M., Utturkar, G.M., Spritzer, C.E., Garrett, W.E., DeFrate, L.E.,

2013. In vivo measurement of ACL length and relative strain during walking. J. Biomech. 46, 478–483. doi:10.1016/j.jbiomech.2012.10.031